

THE ROLE OF CAPICUA IN ADULT HIPPOCAMPAL NEUROGENESIS

by

Brenna Hourigan

A thesis submitted in partial fulfillment of the requirements for the degree of
Master of Science

Department of Cell Biology

University of Alberta

©Brenna Hourigan, 2023

ABSTRACT

Adult hippocampal neurogenesis (AHN) involves generating hippocampal granule neurons and the subsequent integration of granule neurons into the hippocampus synaptic circuit. This continuous neuron generation supports ongoing learning and memory formation. Consequently, dysregulation of AHN and impairment of synaptic integration have been implicated in various neurological disorders including Alzheimer's disease, pathological aging, and stress. Thus, by studying the regulation of AHN and how granule neurons are generated, it is possible to identify therapeutic targets which can lead to more effective treatment options for these disorders. To generate functional adult-born neurons, neural progenitor cells proliferate to expand the precursor cell pool and differentiate into neurons. Newly generated cells then undergo postmitotic maturation to migrate to their final destination and develop elaborate dendritic branching, which allows them to receive input signals. Little is known about factors that regulate neuronal differentiation, migration, and dendrite maturation during adult hippocampal neurogenesis. This thesis highlights the importance of the transcriptional repressor capicua (CIC) for AHN. I show that CIC is dynamically expressed within the adult dentate gyrus of the hippocampus, where AHN occurs. The *Cre-loxP* system was utilized to generate *Emx1-Cre; Cic^{lox/lox}* mice to remove CIC from forebrain excitatory neurons, including those involved with AHN. By using the *Emx1-Cre; Cic^{lox/lox}* knockout mice line in combination with immunofluorescence studies, I show that conditionally deleting *Cic* from the mouse dentate gyrus compromises the adult neural progenitor cell pool without altering their proliferative potential. I further demonstrate that the loss of *Cic* impedes neuronal lineage development and disrupts dendritic arborization and migration of adult-born neurons. This study uncovers a previously unrecognized role of CIC in neurogenesis of the adult dentate gyrus.

PREFACE

The work presented herein represents my experiments and data analyses in collaboration with Dr. Tan laboratory members and collaborators. All procedures in mice were approved by the Animal Care and Use Committee of the University of Alberta. All methods were performed in accordance with the relevant guidelines and regulations. The study was carried out in compliance with the ARRIVE guidelines: <https://arriveguidelines.org>. The data presented in Chapter 3 is published as, “Capicua regulates the development of adult-born neurons in the hippocampus”, *Scientific Reports vol 3, issue 11(1)11725* and was conducted primarily by me and Dr. Tan laboratory technician Spencer Balay (University of Alberta, Department of Cell Biology) with collaborative efforts by Dr. Tan undergraduate students Graydon Yee and Saloni Sharma (University of Alberta, Department of Cell Biology). For figures No. #6-10, #12, #14, #16 and #17-20, I conducted the immunofluorescence staining. For figures No. #11, I conducted the immunofluorescence staining and all raw quantifications. For figures No. #13 and #15, I conducted the immunofluorescence staining and quantification analysis in #13D, E, #15B, and D-F. The unpublished Chapter 4 data presented was conducted by me in collaboration with Dr. Olivier Julien and PhD candidate Bridgette Harley (University of Alberta, Department of Biochemistry). For figures No. #22, #23, I generated the final image as described in the thesis. For figure No. #24, I conducted the immunoblotting experiment. For figures No. #25, #26 and #29, I created the final image, conducted the immunoblot experiments and quantification analysis. For No. #27, I conducted the immunostaining, and confocal. For figure No. #28, I conducted the immunostaining experiment.

ACKNOWLEDGEMENTS

I thank Dr. Sarah Hughes and Dr. Anastassia Voronova (University of Alberta) for their valuable advice, critiques, and feedback as advisory committee members. I also thank Dr. Sarah Hughes for her generous help with confocal microscopy, Dr. Oliver Julien and PhD candidate Bridgette Harley (University of Alberta) for their mass spectrometry data analysis, and Dr. Alyson Fournier (McGill University, Montreal Neurological Institute) for the CRMP4 antibody. I thank my supervisor Dr. Qiumin Tan for her enduring patience, professional wisdom, and relentless strive for scientific objectivity in every piece of data and equality in every person with research ability. I additionally thank Dr. Qiumin Tan for providing the opportunity to learn and grow in a scientifically rich research environment that I wish I had taken advantage of sooner, and more often. Finally, I want to thank my family and life partner for their unconditionally support and love, which allowed me to complete this endeavour. We acknowledge the support of the Natural Sciences and Engineering Research Council of Canada (NSERC, funding reference number RGPIN-2019-06153).

TABLE OF CONTENTS

ABSTRACT.....	II
PREFACE.....	III
ACKNOWLEDGEMENT.....	IV
TABLE OF CONTENTS.....	V
LIST OF FIGURES.....	VI
LIST OF SYMBOLS.....	VIII
CHAPTER 1: INTRODUCTION.....	01
CHAPTER 2: METHODOLOGY.....	22
CHAPTER 3: CAPICUA IS IMPORTANT FOR ADULT HIPPOCAMPAL NEUROGENESIS.....	26
CHAPTER 4: DYSREGULATION OF GENES IMPORANT FOR AXON GUIDANCE AND GROWTH IN THE <i>Emx1-Cre; Cic</i> KNOCKOUT MICE.....	59
CHAPTER 5: DISCUSSION AND FUTURE DIRECTION.....	75
BIBLIOGRAPHY.....	80

LIST OF FIGURES

Chapter 1: Introduction

- FIGURE 1:** Schematic of adult hippocampal neurogenesis in the hippocampal dentate gyrus...07
- FIGURE 2:** The hippocampal trisynaptic circuitry.....11
- FIGURE 3:** How capicua mediates repression towards gene targets.....15
- FIGURE 4:** Human orthologs of capicua transcripts and protein domain composition.....16
- FIGURE 5:** How capicua is inhibited by an RTK/MAPK pathway.....17

Chapter 3: Capicua is important for adult hippocampal neurogenesis

- FIGURE 6:** CIC expression in the adult mouse brain.....27
- FIGURE 7:** CIC expression along the neurogenic lineage in the adult dentate gyrus.....28
- FIGURE 8:** CIC is expressed at a low but detectable level in DCX⁺ cells.....30
- FIGURE 9:** Knockout efficiency of *Emx1-Cre; Cic* knockout mice.....33
- FIGURE 10:** The size of the adult subgranular zone is not significantly altered in the *Emx1-Cre; Cic* knockout mice.....34
- FIGURE 11:** *Emx1-Cre; Cic* knockout mice have a diminished pool of adult hippocampal neural progenitor cells.....35
- FIGURE 12:** Adult neural progenitor cells are reduced in the dentate gyrus of the *Emx1-Cre; Cic* knockout mice.....37
- FIGURE 13:** Impaired development of DCX⁺ cells in the *Emx1-Cre Cic* knockout mice.....41
- FIGURE 14:** Apoptotic cell death of DCX⁺ cells is unaltered in the *Emx1-Cre Cic* knockout mice.....42
- FIGURE 15:** Reduced dendritic branching and abnormal migration of DCX⁺ cells in the *Emx1-Cre Cic* knockout mice.....43
- FIGURE 16:** DCX⁺ cells in *Emx1-Cre Cic* knockout mice show morphological and migration defects.....45
- FIGURE 17:** Molecular characteristics of abnormally migrated DCX⁺ cells in the *Emx1-Cre Cic* knockout mice.....46
- FIGURE 18:** Expression pattern of NFIA during adult hippocampal neurogenesis.....49
- FIGURE 19:** Expression pattern of NFIB during adult hippocampal neurogenesis.....50
- FIGURE 20:** Upregulation of NFIB in neuroblasts of the *Emx1-Cre Cic* knockout mice.....52

FIGURE 21: NFIA levels in DCX⁺ cells are not altered in the *Emx1-Cre Cic* knockout mice.54

Chapter 4:

FIGURE 22: Heatmap of top 30 differentially expressed genes in adult *Cic^{flox/flox}* and *Emx1-cre; Cic* knockout mice.....62

FIGURE 23: Gene set enrichment analysis (GSEA) from bulk RNA sequencing data and gene ontology (GO) category terms63

FIGURE 24: Immunoblot of CIC -L and CIC-S and CRMP4 (sigma)65

FIGURE 25: Immunoblot analysis of Alyson Fournier (AF)-in house versus Sigma CRMP4 antibodies66

FIGURE 26: Immunofluorescence staining of CRMP4 in dentate gyrus of control and *Emx1-Cre; Cic^{flox/flox}* knockout mice.....68

FIGURE 27: CRMP4 expression in mossy fibers of *Cic^{flox/flox}* (control) and *Emx1-Cre; Cic^{flox/flox}* (knockout) mice.....69

FIGURE 28: Abnormal synaptic termination in CA3 hippocampal region.....70

FIGURE 29: Immunoblot analysis of phospho-Ser9 GSK3B.....72

LIST OF SYMBOLS

AHN: Adult hippocampal neurogenesis
Atxn1: Ataxin 1
AXH: Ataxin-1 and HMG-box protein 1
BrdU: Bromodeoxyuridine
CA1/3: Cornu ammonis 1/3
CALB1: Calbindin
CAMKII: Ca²⁺/calmodulin-dependent protein kinase II
cAMP: Cyclic adenosine monophosphate
CBS: Capicua binding site
CDK5: Cyclin-dependent kinase 5
CHIP-Seq: Chromatin immunoprecipitation followed by sequencing
ChR2: Channelrhodopsin 2
Cic, CIC, cic: *capicua*
CIC-L: Capicua-long isoform
CIC-S: Capicua-short isoform
CNO: Clozapine-N-oxide
CNS: Central nervous system
CREB: cAMP response element-binding protein
CRMP: Collapsin response mediator protein
CRMP4: Collapsin response mediator protein 4
DAPI: 4',6-diamidino-2-phenylindole
DCX: Doublecortin
DCX^{hi}: Doublecortin^{high expression}
DCX^{lo}: Doublecortin^{low expression}
DG: Dentate gyrus
DNMT1/3a: DNA-methyltransferase 1/3a
DREADDs: Designer receptors exclusively activated by designer drugs
DUX4: double homeobox protein 4
DYRK2: Dual tyrosine kinase 2
EdU: 5-ethynyl-2'-deoxyuridine

EGFP: Enhanced green fluorescent protein

EGFR/ERBB: Epidermal growth factor receptor

Ephrin/EphB2: Ephrin/erythropoietin-producing hepatocellular carcinoma, family member B2

ETV4/5: ETS Variant Transcription Factor 4/5

FEME: Fast endophilin-mediate endocytosis

FGF: Fibroblast growth factor

FRT: Flippase recombination target

FLP: Flippase

FZD: Frizzled

GABA: Gamma-aminobutyric acid

GFAP: Glial fibrillary acidic protein

GPCR: G-protein-coupled receptors

GCL: Granule cell layer

GSK3B: Glycogen synthase kinase-3 beta

(H3)-thymidine: Tritium thymidine

HDAC: Histone deacetylase

Hkb: huckebein

HM4Di: inhibitory human M4 muscarinic

HMG: High mobility group domain

HSPC: Hematopoietic stem and progenitor cell

IPC: Intermediate progenitor cell

LRP: Low density lipoprotein receptor-related

LTP: Long term potentiation

MAPK: Mitogen activated protein kinase

MBP: Myelin basic protein

MEF2: myocyte enhancer factor-2

Mmp: Matrix ixeuronsixeptidase

nCREB: Dominate negative CREB

NICD: Notch intracellular domain

NES, Nes: *nestin*

NS: Normalized enrichment score

NeuN: Neuronal nuclei
NFI: Nuclear factor I
NFIA: Nuclear factor 1 A-type
NFIB: Nuclear factor 1 B-type
NFIB^{hi}: Nuclear factor I B-type^{high expression}
NFIX: Nuclear factor 1 X-type
Ngn2: Neurogenin 2
NLS: Nuclear localization signal
NPC: Neural progenitor/precursor cell
NRP1/2: Neuropilin 1/2
NSE: Neuron-specific enolase
pCREB: phosphorylated CREB
OLIG2: Oligodendrocyte transcription factor 2
PEA3: Polyoma enhancer activator 3
PJA1: Praj1
PLXND1: Plexin D1
PSA-NCAM: polysialylated neuronal cell adhesion molecule
Ras/MAPK: Ras/mitogen-activated protein kinase
REST: Repressor element 1-silencing transcription factor
RGL: Radial-glia like
RTK: Receptor tyrosine kinase
Sema3A: Semaphorin 3A
SCA1: Spinocerebellar ataxia type 1
SGZ: Subgranular zone
Sin3A: Switch-independent 3
SOX2: SRY (Sex Determining Region Y) Box 2
TBR2: T-box brain protein 2
TCF/LEF: T-cell factor/lymphoid enhancer factor
***tll*:** tailless
tSNE: t-distributed stochastic neighbour embedding

CHAPTER 1: INTRODUCTION

1.1: Early research history and the adult hippocampal neurogenesis debate

1.1.1 The establishment of the neurogenesis dogma: In the early 20th century, knowledge about the central nervous system (CNS) expanded through dedicated research and deliberations among expert researchers in neurobiology. One of the founding fathers of neuroscience, Santiago Ramón y Cajal established the basis for axon growth, neuroplasticity, and the neuron doctrine [1]. By 1913, as a highly revered Noble Laureate, Cajal's viewpoints and research became a paragon to strive for, rather theories and work which still required critical assessment. When Cajal made the statement below in his post-laureate works, it was interpreted as a fact that cells in the adult human brain lacked the ability to regenerate [2].

“The functional specialization of the brain imposes on the neurons two great lacunae; proliferative inability and irreversibility of intraprotoplasmic differentiation. It is for this reason that once the development was ended, the founts of growth and regeneration of axons and dendrites dried up irrevocably. In adult centers the nerve paths are something fixed, ended, immutable. Everything may die, nothing may be regenerated. It is for the science of the future to change, if possible, this harsh decree” [2]

This thinking would remain steadfast in the scientific community for decades, until scientists started to question this dogma and technology evolved to test novel ideas.

1.1.2 Evidence for mitosis in the adult central nervous system: Throughout the 20th century, the theory that the adult CNS was non-regenerative persisted, despite the sporadic presentation of contrary evidence. In 1912, Ezra Allen published a study using 1-day to 120-day-old Wistar rats, plus a rat under 2 years of age [3]. Using thionin and eosin staining to mark condensed chromatin, Allen was able to visualize cells in the CNS undergoing mitosis [3]. Abundant mitotic cells in the cerebrum, cerebellum, and spinal cord were observed in animals between 1-4 days of age [3]. However, mitotic cells declined after 6 days of age, and by 25 days of age little to no mitotic cells were found in the cerebellum and spinal cord [3]. However, in the lateral ventricles of the cerebrum, mitotic cells continued to be observed beyond 25 days and were present in the brain of the rat over 1 year of age [3]. Allen had identified mitotic cells within the cerebrum of the adult rat brain. Unfortunately, this and other similar studies fell into obscurity, due to the technical inability to provide a cellular identity as to which cell type(s) were undergoing mitosis.

Progress regarding the identity of these cells would come about with the use of radioactive nucleotides in the development of fine resolving autoradiography [4].

1.1.3 Evidence for adult hippocampal neurogenesis revealed by radioactive nucleotide

analogs: The term "adult hippocampal neurogenesis" (AHN) was first coined by research scientist Joseph Altman, who utilized the radioactive nucleotide tritium(H3)-thymidine to garner information about the cellular origins of CNS cells undergoing mitosis [5-7]. Due to its radioactive nature, H3-thymidine, which incorporates into DNA during the S phase of the cell cycle, can be traced by autoradiography. In 1965, Joseph Altman and colleagues, injected H3-thymidine into the dentate gyrus (DG) of 4-month-old adult rats [5]. Rats were killed at different time points (four days to eight months post-injection), and the H3-thymidine incorporation traced [5]. While the highest number of mitotic cells in the DG were observed in rats four-days post injection, mitotic cells were observed in all age groups, though the total number of mitotic cells decreased as the post-injection period increased [5]. His work indicated the presence of mitotic cells in the adult hippocampal DG. While Joseph Altman is now recognized as a pioneer in AHN, at the time, his work was largely dismissed.

1.1.4 The criticisms and research limitations about adult hippocampal neurogenesis: Joseph Altman's findings were corroborated after his 1965 study by electron microscopy and further autoradiographic evidence [8-11]. Despite this, the scientific community remained skeptical about AHN. A major reason for such doubt was due to the lack of techniques that allowed researchers to unambiguously identify CNS cells. In their 1965 paper, Altman claimed that certain cells often categorized as a glia or "neuroglial" cells were miscategorized undifferentiated neural progenitors [5]. The authors based their assertion on; 1) the histological appearances of H3-thymidine labeled cells and 2) the abundance of mitotic H3-labeled cells that Altman had identified, were low in the adult brain but high in the young brain [5]. At the time, critics commented that no one could state with certainty that these were undifferentiated cells. With no ability to specifically identify these cells, Altman's findings remained underappreciated.

1.1.5 The transition from radioactive to other nucleotide analogs and adult hippocampal neurogenesis in humans:

In the 1960's, researchers began to utilize fluorescence as an alternative to radiation for detecting mitosis [12]. Instead of H3-conjugated thymine, nucleoside analogs such as Bromodeoxyuridine (BrdU) and 5-ethynyl-2'-deoxyuridine (EdU) were being used as efficient and safer alternatives, capable of integrating into DNA but lacking radiation concerns [13]. The development of antibodies also paved the way for the identification of specific cellular markers of CNS cells, creating a degree of consensus regarding the identities of previously observed mitotic cells. Using these analogs, researchers were able to validate Altman's findings. In 1996, a study by Kuhn, Dickinson-Anson, and Gage used BrdU to assess the proliferation of neural precursors across the life span of the rat [14]. Twelve-week-old Fisher 344 rats were injected with BrdU and then killed at various time points post injection (1 day to 10 weeks post injection) [14]. The researchers identified cells co-stained for BrdU and newborn neuronal markers polysialylated neuronal cell adhesion molecule (PSA-NCAM) and neuronal nuclei (NeuN) [14]. In older rats (21 months old), researchers observed a significant reduction in BrdU positive cells due to the reduction of neural progenitor production in the DG [14]. However, while substantially diminished compared to young adults, the number of BrdU cells did not drop to zero [14]. Together this suggests that there is a reduction in the birth of neurons as opposed to a lack of neuronal generation. In 1998, Eriksson and colleagues examined autopsied brain tissues from five cancer patients (average age: 64.4 ± 2.9 years) who received BrdU as a part of their treatment [15]. The researchers found BrdU⁺ cells colocalized with calbindin (CALB1), neuron specific enolase (NSE), and NeuN in the hippocampal DG, an indication of the presence of AHN in the adult human brain [15]. The advancement of technology and elegantly designed experiments conducted by dedicated researchers slowly led to AHN becoming an accepted phenomenon in the scientific community.

1.2 Contemporary research history and current questions regarding adult hippocampal neurogenesis

1.2.1 Transgenic mouse models to substantiate adult hippocampal neurogenesis: With the advancement of utilizing proteins to visualize and trace specific cell types in the CNS, rodent models began to take on a new level of application. Transgenic rodent models allowed researchers to continually expand knowledge regarding AHN. One of the earliest examples of a transgenic *in vivo* rodent model was generated in mice by ligating a 2.5 kb promoter segment of

the *nestin* (*Nes*) gene (a gene encoding a protein marker for neural stem cells) to the coding region of enhanced green fluorescent protein (EGFP) [16]. After validating EGFP expression, this *Nes:EGFP* mouse model was used to mark EGFP⁺ neural progenitor cells (NPCs) in the CNS [16]. Researchers observed EGFP⁺ cells in postnatal day 7 (P7) and adult 12-week-old *Nes:EGFP* mice [16]. Such transgenic mice have been utilized in AHN research to examine neural stem cells. For example, Filippov *et al.* classified morphological and physiological differences between the stem cells and neural progenitor cells (NPCs) of AHN [17, 18].

1.2.2 Cre-lox and FLP-FRT technologies to efficiently generate finely tuned genetically manipulated mice:

More finely tuned transgenic rodent models arose from genetic manipulations using Cre-lox and Flippase-flippase recombination targets (FLP-FRT) technologies. With FRT or lox sites flanking the gene of interest, either gene inversion or deletion can be initiated by flippase (FLP) or Cre recombinase binding to FRT or to lox sites, respectively. By selecting the promoter under which the Cre recombinase or FLP is expressed, cell type specificity and time selectivity of expression can be achieved. Researchers can remove or induce gene expression in rodent models to observe the consequences of altered gene expression on AHN. For example, previous studies reported that constitutive knockout of Presenilin-1 (*PSI*) is embryonic lethal. By crossing transgenic mice encoding lox sites flanking the *PSI* gene with transgenic mice encoding Cre recombinase under the expression of *αCAMKII*, *PSI* was successfully deleted from the forebrain of adult postmitotic neurons in the progeny [19, 20]. As *αCAMKII* is not expressed until 2-3 weeks postnatally, hence bypassing the obstacle of embryonic lethality [20]. Using this model, the researchers demonstrated that removing *PSI* from excitatory neurons lead to an accumulation of Aβ plaques and reduced newborn neurons during enriched environment-induced adult neurogenesis [19].

1.2.3 Viral-mediated genetic manipulations:

By the mid-1990s, viral-mediated genetic approaches were being explored for gene therapy and for labeling cells in CNS research. Depending on the purpose and cell types under investigation, different types of viruses could be exploited. Adenoviruses associated viruses provide an efficient transfection, but viral vectors stay episomal and are lost or diluted upon cell division. Retroviruses yield both efficient and stable infections but are limited to infecting cells undergoing replication, as they require a dispersed nuclear membrane for infection. Lentiviruses infect non-dividing cells and provide a stable infection [21, 22]. Viral-mediated gene delivery can be designed to target specific cells

within a milieu of cells for genetic manipulation. In 2001, one group used a herpes simplex virus to induce fibroblast growth factor (FGF) expression in FGF knockout neural progenitors [23]. Similarly, an oncoretrovirus was used to target neural progenitors in the adult hippocampal DG and perform lineage tracing experiments to assess the fate of transfected NPCs [24]. In this experiment, shRNA targeting disrupted-in-schizophrenia 1 (*Disc1*), a gene when mutated increases susceptibility to schizophrenia, was introduced into 10–12-week-old rats. Reductions of *Disc1* in neural progenitors led to alterations in adult born neuron maturation, including increased soma size, negatively impacted dendrite establishment, dysregulated branching complexity, ectopic positioning beyond the hippocampal DG, and accelerated maturation as indicated by reduced membrane resistance and increased synaptic integration [24].

1.2.4 Optogenetics and chemogenetics: With the establishment of viruses as vectors for genetic manipulation, the potential for other genetic manipulations exploded, including expressing channelrhodopsins and designer receptors activated exclusively by designer drugs (DREADDs) in the CNS. Utilizing light-sensitive proteins like channelrhodopsin-2 (ChR2), researchers can now perform millisecond neural circuit control and generate robust readouts of neuronal activity [25]. In 2012, Gu *et al.* injected a retrovirus encoding either ChR2-EGFP or ChIEF (a derivative of ChR2) into the CNS of rodents to trace the fate of NPCs and collected data on synaptic integration [26]. Activated by 473 nm wavelength of light, these channelrhodopsins mimicked the glutamatergic monosynaptic response, allowing the researchers to observe their synaptic formation and trace the output synaptic response [26]. Alternatively, by taking advantage of the minimally biologically activated G-protein-coupled receptors (GPCRs) DREDDs, the control of specific pathways can be fine-tuned. DREDDs are designed to be normally inactive *in vivo* but are activated upon exposure to a specific compound, such as clozapine-N-oxide (CNO). DREDDs have been used in AHN research to inhibit adult-born neurons in the adult DG. By using inhibitory human M4 muscarinic (HM4Di) to silence excitatory responses in adult-born neurons through CNO, researchers could assess how adult-born neurons affect the activity of mature granule neurons that were born developmentally [27].

1.3: The cellular process of adult hippocampal neurogenesis

1.3.1 Overview of how neurons are generated in the adult hippocampus: AHN involves generating mature glutamatergic granule neurons within the DG of the adult hippocampus (**Fig. 1**). AHN commences when DG subgranular zone (SGZ)-resident quiescent neural stem cells,

herein referred to as radial glial-like cells (RGL; type 1 cells) exit quiescence and enter the cell cycle [17, 28, 29]. RGLs may divide asymmetrically to become neural progenitor cells (NPCs) or divide symmetrically to maintain the stem cell pool. The progenitor cell phase lasts 1–3 days and serves to expand the pool of rapidly amplifying intermediate progenitor cells (IPCs; type 2a/b cells). Many IPCs are eliminated, however, within days after they exit the cell cycle, presumably through apoptosis [30]. The few cells that do survive proceed to the postmitotic maturation phase (neuroblasts; type 3), when they migrate tangentially and radially into the granule cell layer (GCL). During this postmitotic maturation phase, neuroblasts establish a polarized morphology by extending an elaborate dendritic tree toward the molecular layer and projecting an axon into the hilus, becoming an immature neuron [31, 32]. Adult-born immature neurons undergo further dendritic maturation and fine-tuning of their electrophysiological properties, ultimately becoming a mature neuron [33]. This entire process takes about 6–8 weeks in mice and encompasses six developmental milestones which can be identified based on molecular markers and cell morphology.

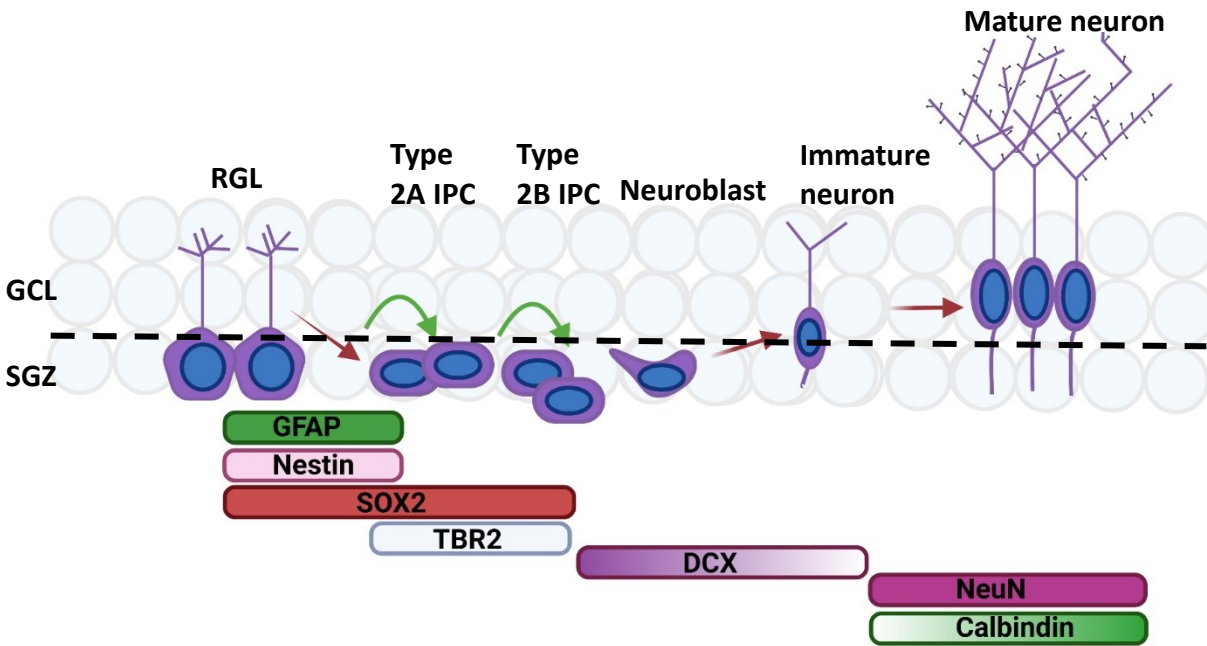


Figure 1: Schematic of adult hippocampal neurogenesis in the hippocampal dentate gyrus. AHN commences when DG SGZ quiescent radial glial-like cells exit quiescence and enter the cell cycle. RGLs divide asymmetrically to become NPCs. Cells that survive proceed to become neuroblasts and enter the postmitotic maturation phase when they migrate tangentially and radially into the GCL. During this postmitotic maturation phase, neuroblasts establish an elaborate dendritic tree toward the molecular layer and project an axon into the hilus, becoming an immature neuron. Adult-born immature neurons undergo further dendritic maturation and fine-tuning of their electrophysiological properties, ultimately becoming a mature neuron. This entire process takes about 6–8 weeks. AHN = adult hippocampal neurogenesis, DG = dentate gyrus, SGZ = subgranular zone, GCL = granular cell layer, IPC = intermediate progenitor cell, NPC = neural progenitor cell, RGL = radial glial-like cell. Figure created with BioRender.com (2023).

Type 1/Radial glial like cells: RGL cells are multipotent, quiescent stem cells with self-renewal capacity [34]. Within the DG, RGLs are localized to the SGZ, where they extend a single primary process to the granular layer of the DG. RGLs express the markers Nestin (NES), glial fibrillary acidic protein (GFAP), and SRY (Sex Determining Region Y) Box 2 (SOX2). While mostly quiescent, RGLs can enter the cell cycle and divide asymmetrically to generate one neural progenitor cell and one RGL cell or symmetrically, to produce two RGLs [35, 36]. While it is known that RGL populations originate from the dentate neuroepithelium, RGLs exhibit heterogeneity, in terms of morphology and markers [37, 38]. The proliferation of RGLs is responsive to external environmental cues, which can impact RGL proliferation capacity and multipotency [39-41]. One example is the modulation of Notch signaling pathway [42]. Notch receptors are single-pass transmembrane heterodimers that are activated upon forming a complex with Delta and Jagged, membrane-bound ligands on the neighboring cell. Ligand binding results in cleavage of the transmembrane domain, and subsequent release of the notch intracellular domain (NICD) into the cytosol. This NICD domain translocate to the nucleus and complexes with the DNA-binding protein RBPj. The NICD-RBPj complex in turn induces the expression of transcription factors involved with stem cell maintenance such as SOX2 [43-46] .

Type 2a/b intermediate neural progenitors: IPCs are short-lived, highly amplifying cells localized to the SGZ [47, 48]. They express the markers SOX2 and Eomes/T-box brain protein 2 (TBR2) [49, 50]. Much like RGL cells, these proliferating cells are sensitive to cues from the neurogenic niche due to the transduction of key signaling pathways. One such notable example is the Wnt/ β -catenin signaling pathway [51, 52]. Activation of the canonical Wnt/ β -catenin pathway entails the formation of Wnt/low-density lipoprotein receptor-related protein/fizzled (Wnt/LRP/FZD) ternary complex [53]. In consequence, β -catenin phosphorylation is inhibited, thus preventing its ubiquitination and degradation [54]. β -catenin translocate to the nucleus where it interacts with members of the T cell factor/lymphoid enhancer binding factor (TCF/LEF) transcription factors and regulating the expression of target genes [55]. During AHN, proliferating NPCs have β -catenin bound to the *Cyclin D1* promoter, but upon differentiation, β -catenin dissociates from the *Cyclin D1* promoter and binds to promoter regions of neural differentiation genes neurogenin 2 (*Ngn2*) and *Neurod1* [56, 57].

Type 3/neuroblasts: Recently neuronal fate committed cells are called neuroblasts. Early stage neuroblasts are spherical, located to the SGZ and express high levels of doublecortin (DCX)

[58]. Upon postmitotic maturation however, neuroblasts migrate to the GCL. Concomitantly, they develop a single axon oriented towards the hilus and elaborate dendrites that reach into the molecular layer [32, 59]. During this stage neuroblasts continuously receive signals that promote maturation of the neuroblast including proper migration, axon and dendrite formation, as well as integration of the adult-born neuron into the hippocampal synaptic circuit [60-62]. These signals are thought to act on transcription factors regulating genes necessary for proper maturation such as migration, dendrite and synapse development genes. For example, transcription factor myocyte enhancer factor-2 (MEF2) is regulated by neuronal activity through calcium-sensitive pathways [63-65]. MEF2 is thought to regulate dendritogenesis during AHN, possibly through the regulation of activity-regulated cytoskeletal-associated protein (Arc) and synaptic RAS GTPase-activating protein (synGAP) [63, 66, 67].

Immature neurons: Immature neurons express minimal levels of DCX as they undergo neuronal maturation. Their nuclei become larger and start to express mature neuron markers CALB1 and NeuN [14]. At this stage, immature neurons establish their position within the GCL [68, 69]. They acquire a polarized neuronal morphology, with axons extending through the hilus and toward the cornu ammonis 3 (CA3) region, while dendrites project through the hippocampal molecular layer [70-72]. As immature neurons mature, dendrites grow and branch, and spine density increases, resulting in a continuous need or “demand” for active terminals from neighbouring cells [59, 60, 69, 73-81]. The integration of new neurons results in the formation of new networks and the modification of preexisting ones. Such integration means that immature neurons are likely to be important for hippocampal function. For example, the functional implication for the synapses that form between perforant path terminals and immature neurons is that these synapses display a low threshold for the induction of long-term potentiation (LTP). Resultingly, synaptic plasticity is enhanced in the excitatory inputs to newly born neurons [82-87]. In turn, due to the enhanced synaptic plasticity these immature neurons may play a role in information process [87, 88].

Mature neurons: Mature neurons are localized to the GCL of the hippocampal DG, expressing markers such as CALB1, NeuN, and NSE. They exhibit an elaborate dendrite structure and an axon, necessary for partaking in the hippocampal circuitry. The dendrite structure is a characteristic inverted cone-shaped with dendritic arbors extends unidirectionally through the molecular layer [89-91]. These dendrites are important for establishing connections with the

multitude of participants they connect with. Mature neurons receive excitatory input from the entorhinal cortex and commissural fibers from glutamatergic mossy cells [92, 93]. They also receive inhibitory inputs from GABAergic interneurons in the entorhinal cortex and in the hilar region. Furthermore, projections from CA3 pyramidal cells and mossy cells have been observed [94, 95]. The axons and initial segments of mature neurons contact basket cells in the SGZ. Mature neurons also send their single mossy-fiber (MF) axon to the hippocampal CA3 region that targets pyramidal and GABAergic interneurons [70, 96]. Individual mossy fiber terminals are morphologically distinct depending on the nature of the target cell, but also display distinct functional features in terms of transmission and plasticity [97].

Functions of adult hippocampal neurogenesis: Early work of the hippocampal circuitry suggests that the hippocampus is a key structure for memory formation/clearance [98]. Studies in rodents with hippocampal DG lesions indicate that such lesions negatively affect memory acquisition and retrieval [99-105]. Granule neurons exhibit an unusual low firing rate, which theoretically increases the probability that granule cells will encode similar inputs [106, 107]. The hippocampal trisynaptic circuit is thought to form a part of the major pathway necessary for memory formation (**Fig. 2**). Mature granule neurons play a key role in the trisynaptic circuitry by receiving input from the entorhinal cortex (EC). The hippocampus and AHN appear to also be key players in mood regulation. Patients suffering from depression have a reduced hippocampal volume [108-110]. Moreover, studies in rodents have demonstrated that dorsal hippocampal lesions affect memory formation while ventral hippocampal lesion affects mood regulation [111-113]. Chronic antidepressant drug treatments stimulate AHN proliferation and in a chronic stress mouse model, ablating neurogenesis partially suppressed antidepressant effects [114-118]. Altogether, AHN has been implicated in properly maintaining and executing hippocampal-related functions including pattern separation, memory formation/clearance and working memory.

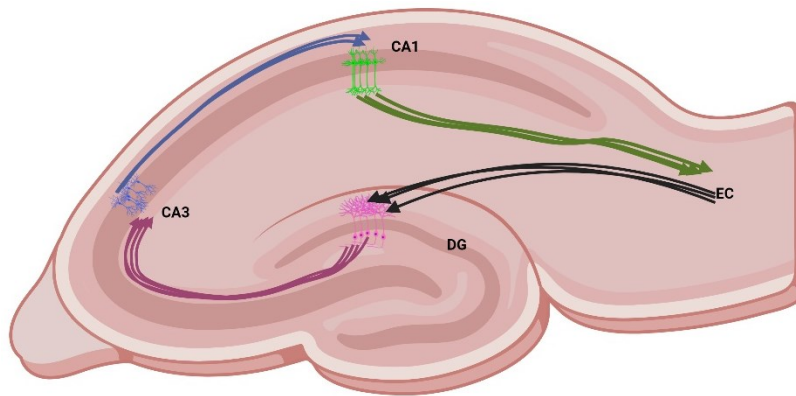


Figure 2: The hippocampal trisynaptic circuitry. The major excitatory input to the hippocampus comes from the entorhinal cortex (EC) by the perforant path (black arrows) to granule neurons (purple) in the dentate gyrus (DG). The mossy fibers (purple arrows) project to the pyramidal neurons in the cornu ammonis 3 (CA3) region. The axons from the CA3 pyramidal neurons (Schaffer collaterals) convey the processed input to the cornu ammonis 1 (CA1) pyramidal neurons (green). CA1 pyramidal neurons project to the EC. Figure created with BioRender.com (2023).

1.4 Homeostatic regulation of adult hippocampal neurogenesis by transcription factors: For mature neurons to be generated within the DG, the external environmental signals that influence gene expression need to be properly regulated in the cell to avoid aberrant lineage progression/repression. Transcription factors provide a means to do this by orchestrating transcriptional regulation during NPC proliferation, differentiation, and neuronal maturation stages of AHN. One example is *NeuroDI*, where SOX2 occupies SOX/LEF binding sites and represses the expression of *NeuroDI* [119]. Induction of neuronal differentiation by canonical Wnt signaling however, results in the replacement of SOX2 by a β -catenin-containing transcriptional activator complex and expression of *NeuroDI* [57].

1.4.1 Regulation of adult stem cell quiescence and progenitor cell proliferation by Repressor element 1-silencing transcription factor: Multiple signaling molecules, including Notch, Wnt, and Shh, have been reported to crosstalk with repressor element 1 (RE1)-silencing transcription factor (REST) in other systems, suggesting that REST may integrate diverse signaling pathways to control gene expression [120-122]. REST is expressed in stem cells and mature neurons [120]. REST acts by binding to a 21-23 bp region (RE1) in promoter regions of target genes and recruiting protein binding partners coREST, HDAC1 and mSin3a to repress its targets [120]. During AHN, REST is important for maintaining RGL quiescence and preventing precocious differentiation from type 1 to type 2 cells by repressing cell cycle and ribosome biogenesis genes [120, 123].

1.4.2 Neural differentiation by Nuclear Factor 1 X-type: NFI transcription factor nuclear factor 1 x-type (NFI-X) is highly expressed in progenitors and neuroblasts, with lower expression levels in stem cells and mature neurons [124]. When NFI-X was deleted in immature neurons during AHN, there was decreased mature granule neurons and increased oligodendrocyte progenitors, suggesting that NFI-X represses the latent oligodendrogenesis potential of AHN [124].

1.4.3 Mature neuron synaptic integration by cAMP response element-binding protein: Far less transcription factors involved with neuronal maturation have been identified, but one of the more notable examples is cAMP response element-binding protein (CREB). The activated form of CREB, phosphorylated CREB (pCREB), is present in neuroblasts and in immature neurons [125]. Studies with retrovirus injections of a dominant negative form of CREB (nCREB) show that mice injected with nCREB have immature neurons with aberrant dendrite morphology and

polarity, necessary for proper neuron maturation [125]. The precise contribution of CREB to AHN is still largely unknown. Of note, CREB is known to regulate the miR-212/132 tandem miRNAs, the deletion of which causes dendrite defects [126].

1.5: The roles of the transcriptional repressor capicua

1.5.1 Discovery of *capicua* and *Drosophila* head/tail development: In 2000, Jimenez *et al.* studied how the receptor tyrosine kinase (RTK) pathways affect development of the anterior and posterior terminals of the *Drosophila* embryo [127]. The *torso* RTK pathway in *Drosophila* had been shown to contribute to embryo development by repressing Groucho (Gro), a corepressor that mediates repression of *tailless* (*tll*) and *huckbein* (*hkb*). *Tll* and *hkb* are zygotic genes necessary for embryonic differentiation of head and tail structures. While Gro was known as a corepressor, Gro itself did not bind DNA directly, so the search was focused on finding the DNA binding factor that mediated repression. Using a P-element screen for female-sterile flies containing mutations that negatively affected *Drosophila* anterior-posterior terminal development, the researchers identified *capicua* (*cic*, Catalan for head and tail) as important for proper development of embryo terminal ends. Noting that these effects resembled gain-of-function mutations in *torso* and *torso* RTK pathway components, researchers asked whether *cic* was connected to the *torso* RTK pathway. Similar to gain-of-function mutations in *torso*, loss-of-function mutations in *cic* increased *hkb* and *tll* expression but did not affect Gro activity. Immunostaining for *cic* expression in *torso* mutants revealed ectopic accumulation of *cic* at the terminal ends of the embryo. Shortly after *capicua* was identified in *Drosophila*, its orthologs were identified in humans and mice [128, 129], and the discovery of its function in the RTK pathways paved the way for further studies dissecting the role of *cic* in mammals.

1.5.2 Regulation of *capicua*: *Capicua* encodes an evolutionary conserved high mobility group domain (HMG) box DNA binding transcriptional repressor. In *Drosophila*, *cic* was found to be connected to the epidermal growth factor receptor (EGFR) RTK signaling and further research with mice and human orthologs revealed how CIC regulates gene expression as well as how it is negatively regulated by RTK pathways [130]. CIC binds to an octameric capicua binding site (CBS) in the promoter regions of gene targets (**Fig. 3**), such as those involved in cell cycle and proliferation. CIC has two isoforms, CIC-short (CIC-S) with a molecular weight of 160 kD and CIC-long (CIC-L) with a molecular weight of 250 kD (**Fig. 4**). Both isoforms are conserved in *Drosophila*, mice and humans, with the same protein domain structures, except for that CIC-L

has an extended N-terminus region [131]. CIC is negatively regulated in the cytoplasm by RTK pathways through phosphorylation, mediated by mitogen activated phosphokinases (MAPKs) such as *rolled* in *Drosophila* and ERK in mammals. By phosphorylation of a serine residue within the nuclear localization sequence of CIC, nuclear localization is prevented (**Fig. 5**) [132]. In addition, phosphorylation of a serine residue within the DNA binding high mobility group domain (HMG) prevents CIC from binding to DNA targets. CIC can also be proteasomally degraded in the nucleus, which is mediated by nuclear E3 ligase PRAJA1 (PJA1) polyubiquitylation (**Fig. 5**)[133]. Long noncoding RNA (lncRNA)-mediated regulation of CIC expression has also been reported [134]. In peripheral blood cells from schizophrenia patients, overexpression of AC006129.1, the genomic locus of which is located close to *CIC* in chromosome 19, leads to downregulated *CIC* levels. Mechanistically, AC006129.1 recruits DNA methyltransferases 1 and 3a (DNMT1 and DNMT3a) to induce DNA methylation of *CIC* promoter region to decrease the expression of *CIC*.

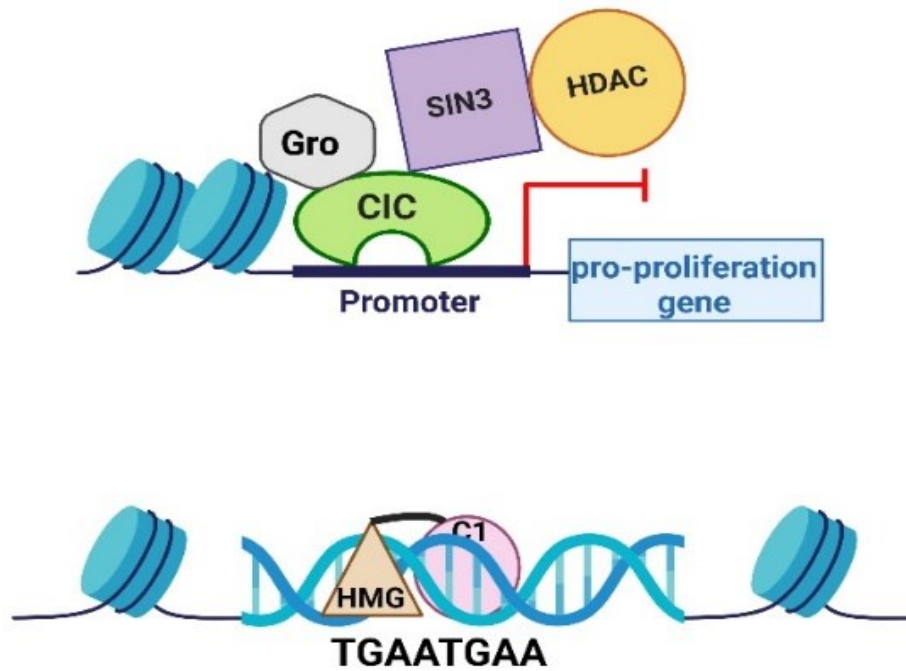


Figure 3: How capicua mediates repression of gene targets. Top panel: By binding to corepressors such as Gro, capicua is able to mediate gene repression of growth and proliferation genes through the recruitment of chromatin remodelers SIN3 and HDAC. **Bottom panel:** Capicua has two DNA binding domains; the high mobility group domain (HMG) and C1 domain that bind to the octamer consensus sequence (TGAATGAA) on complementary strands within the promoter region of targets. Figure created with BioRender.com (2023).

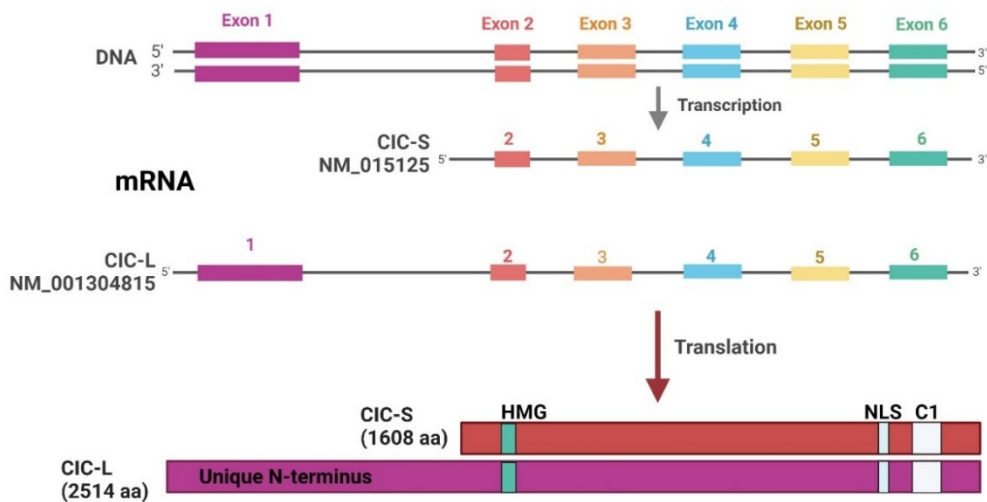


Figure 4: Capicua transcript and proteins in humans. Two *CIC* transcripts (*CIC-S* and *CIC-L*) are made from the use of alternative promoters. Both transcript isoforms are translated into *CIC* proteins. Both protein isoforms are conserved in *Drosophila*, mice and humans, with the same protein domain structures, except for that *CIC-L* has an extended N-terminus region with unknown function. HMG = high mobility group domain, NLS = nuclear localization sequence. The C1 domain is involved alongside the HMG domain to bind octameric DNA sequences that are *CIC* binding sites. Figure created with BioRender.com (2023).

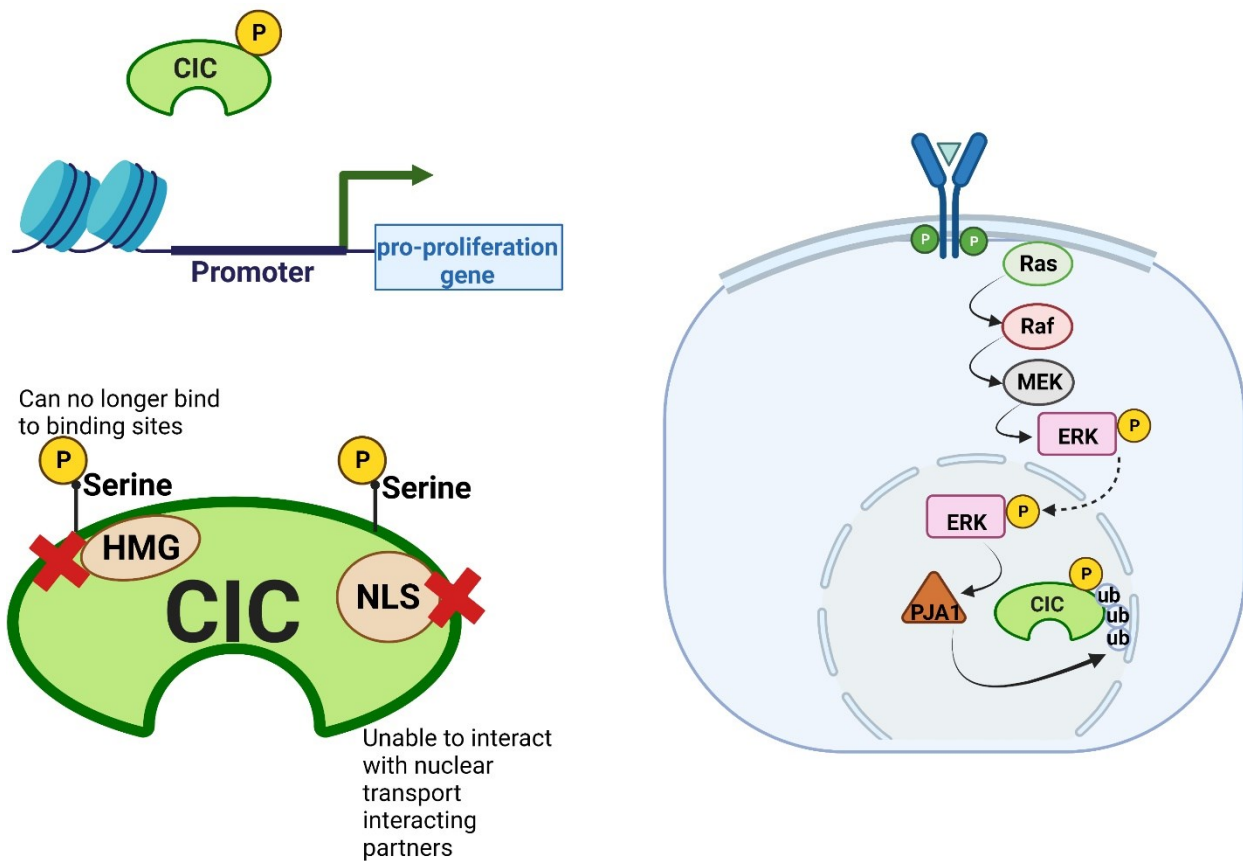


Figure 5: How capicua is inhibited by the RTK/MAPK pathway. Left panel: CIC is phosphorylated when mitogen activated protein kinases (MAPKs) are activated. Phosphorylation at two serine residues, one near the HMG domain, prevents binding of CIC to DNA targets, while the second serine residue near the nuclear localization sequence (NLS) prevents binding to nuclear transport proteins. As a result, CIC is excluded from the nucleus and/or transported out into the cytoplasm. **Right panel:** Regulation of CIC can also be mediated by degradation of CIC, involving polyubiquitination by PRAJA1 (PJA1). Figure created with BioRender.com (2023).

1.5.3 CIC and cancer: Shortly after *capicua* was identified in *Drosophila*, orthologs were identified in humans and mice [128, 129]. As such, questions began to be asked about the role of *capicua* and the conservation of role between *Drosophila* and mammals. In the mid-2000s, CIC was found to play a role in EGFR signaling in medulloblastomas and Ewing's sarcoma [128]. Such cancers form when a chromosomal breakage followed by a fusion at chromosome 4 occurs to create a CIC-DUX4 fusion protein [135]. This fusion protein was shown to be a potent transcriptional activator of pro-proliferation genes ETV1 and ETV5, encoding two members of the PEA3 transcription factor family [135]. In 2011, CIC was shown to be a major contributor to oligodendrogliomas [136]. Oligodendrogliomas were identified by loss of heterozygosity between chromosomes 1p and 19q [136]. Examining the sequences near the breakage point revealed that *CIC* was mutated in about 60% of the tumors examined and 25% of these *CIC* mutations were predicted to inactivate CIC [136]. *Cic* deletion has also been implicated in T cell lymphoblastic leukemia/ lymphoma in mice [137]. Hematopoietic specific *Cic* knockout mice (*Tek-Cre; Cic^{fllox/fllox}*) develop T cell leukemia due to Notch pathway activation and *Myc* overexpression in preleukemic hematopoietic stem and progenitor cells [137].

1.5.4 CIC and spinocerebellar ataxia type 1: Spinocerebellar ataxia type 1 (SCA1) is a neurodegenerative disorder caused by the expansion of a polyglutamate track in the protein ataxin-1 (ATXN1). CIC was found to be an interactor with ATXN1 and its paralog ataxin1-like (ATXN1L) [131]. Both CIC-S and CIC-L isoforms were shown to bind to the ataxin-1 and HMG-box protein 1 (AXH) domain in ATXN1 [138]. The AXH domain of ATXN1/ATXN1L and the highly conserved N-terminal region of CIC-S, including amino acid residues 28–48, mediate their interaction [138]. The resulting interaction is that ATXN1L plays a more pivotal role in the stabilization of CIC than ATXN1; CIC levels decreased more substantially in response to the loss of ATXN1L than to the loss of ATXN1, leading to substantial derepression of CIC target gene expression [139]. While the polyglutamate expansion in ATXN1 is necessary for SCA1 pathogenesis, the main driver of the disease is suggested to be a stabilized interaction between CIC and ATXN1, leading to gain-of-function toxicity [138]. This idea is suggested through mouse models that revealed SCA1 symptoms did not manifest in cerebellar *Atxn1/Atxn1-like* double knockout mice nor in cerebellar *Cic* knockout mice [138].

1.5.5 CIC and lung alveolarization: While gain of function of the ATXN1-CIC complex underlies the pathogenesis of SCA1, the normal physiological role of this complex remained

largely unknown. *Atxn1* and *Atxn1-like* double knockout mice presented with perinatal lethality with abnormal embryonic lung development [140]. Specifically, the alveolarization stage was impaired, generating extra air spaces in the lungs of mutant mice [140]. Transcriptomic studies of the double knockout mice revealed that genes involved in cell surface, plasma membrane and extracellular matrix were significantly changed in the knockout mice [140]. In particular, a group of matrix metalloproteinase (*Mmp*) genes, known to alter the extracellular matrix, were upregulated [140]. After observing decreased CIC levels in the *Atxn1/Atxn1l* double knockout, the authors generated *Cic* knockout mice and observed alveolarization defects comparable to that in the *Atxn1/Atxn1l* knockouts [140]. In search for molecular underpinnings, researchers identified *Etv4*, a *Cic* target gene which turns on *Mmp* gene expression, was highly upregulated in the *Cic* knockout mice [140].

1.5.6 CIC and bile acid homeostasis and T-cell development: To assess other roles of CIC in peripheral tissue, one approach taken was to assess metabolites in the serum of *Cic-L^{-/-}* mice comparison to wildtype [141]. At postnatal day 18 (P18), *Cic-L^{-/-}* mice had reduced glucose levels but increased bile acid and bilirubin [141]. By microarray analysis, in conjunction with gene ontology and pathway analysis, researchers identified drug metabolism genes as the most significantly down-regulated genes in *Cic-L^{-/-}* [141]. As the expression of genes involved in drug metabolism is regulated by several nuclear receptors and liver-enriched transcription factors, the researchers noted that hepatic levels of several liver-enriched transcription factors and nuclear receptors, including FOXA2, HNF1a, C/EBPb, and RXRa, were significantly down-regulated in the livers of *Cic-L^{-/-}* mice [141]. Thus, this data indicated that CIC deficiency may perturb bile acid homeostasis by inducing proinflammatory signaling cascades in the liver [141]. CIC has also been shown to regulate immune cell development [142, 143]. For example, the inducible whole-body *Cic* knockout mice (*UBC-cre/ERT2; Cic^{fllox/fllox}*) showed a reduction in hematopoietic stem and progenitor cell (HSPCs) in the bone marrow compared with control mice [137]. However, there was a significant expansion of the immature T-cell cells in the thymus [137]. A hematopoietic-specific *Cic* knockout mouse model, *Vav1-Cre; Cic^{fllox/fllox}*, has revealed an increase in the frequency of immature T cells with a reduction in the more mature T cells [137]. Further examination revealed that this was due to a block in the transition from the immature to mature T-cells [137]. In *Cic*-deficient T-cells, calcium influx and expression of TCR signaling pathway components was decreased, with a concurrent upregulation of genes involved in the

inactivation of MAPKs and anti-apoptotic processes [143]. The *Vav1-Cre; Cic^{fllox/fllox}* has also been shown to exhibit an autoimmunity response by tissue infiltration of macrophages and dendritic cells, and an altered T-cell composition in the spleen [144]. A third mouse model, *CD4-Cre; Cic^{fllox/fllox}*, which deletes *Cic* from CD4⁺ T-cells also have altered T-cell populations due to the increased cell differentiation via *Maf* upregulation.

1.5.8 The role of CIC in neuronal differentiation and maturation during brain

development: In 2018, Lu, Tan *et al.* studied whether the Ataxin1-CIC complex was important for development of the forebrain [145]. By using a *Cic* or *Atxn1/l* knockout mouse model, with the *Emx1-Cre* driver to delete *Cic* or *Atxn1/l* from excitatory neurons and glial cells of the forebrain, they assessed the consequences of deleting *Cic* or *Atxn1/l* [145]. Both *Cic* and *Atxn1/l* knockout mice exhibited numerous abnormalities in behavioral tests including contextual fear, open field, elevated plus maze, which assess hippocampal related functions [146]. In the cortex, reduced thickness of cortical layers 2/3 but not layers 5/6 was observed, in conjunction with cortical neurons in layers 2/3, but not in layers 5/6, exhibited reduced dendrite complexity [145]. While these results occurred in both *Cic* and *Atxn1/l* knockout mice, CIC protein levels were reduced in the *Atxn1/l*-knockout mice, but the total protein levels of ATXN1 and ATXN1L were not changed in the *Cic* knockout mice [145]. This suggested that the primary driver for these abnormalities was the loss of *Cic* [145]. Furthermore, *CIC* heterozygous loss of function mutations has been identified in humans. All affected individuals have neurodevelopmental deficits, suggesting that CIC is important for proper brain development [145]. Consistent with this idea, *Nestin-Cre; Cic* knockout mice, which removes *Cic* from neural stem cells, exhibit a reduction in neurons in the cerebral cortex layers 2/3 but not in 5/6, similar to that observed in the *Emx1-Cre; Cic^{fllox/fllox}* knockout mice [147]. In the *Nestin-Cre; Cic* knockout mice, a reduction in total neurons was accompanied by reduced neuronal differentiation. [147]. RNA sequencing and chromatin-immunoprecipitation sequencing (CHIP-seq) studies revealed that the CIC target gene *Vgf*, is upregulated in neuron progenitors in the *Cic* knockout mice [147]. Upregulation of VGF in neural progenitors is thought to impair neuronal differentiation [147]. Altogether, this indicates the importance of CIC in neuronal differentiation and maturation during postnatal development, potentially through proper positioning and dendrite development of neuronal cells. Consistent with a role in neuron differentiation and maturation, immunofluorescence staining of embryonic day 12 (E12) dorsal telencephalon brain tissue from wildtype mice show increased

Cic expression as cells progressed through the neuronal lineage, with NeuN⁺ neurons having the highest level of CIC expression, while neural progenitors and immature neurons exhibiting relatively low levels of CIC [148]. In P21 cortices of *FoxG1-Cre;Cic^{flox/flox}* knockout mice, where *Cic* is removed from forebrain neuronal and glial cells, NeuN⁺ cells were decreased but GFAP⁺ cells were increased in knockouts relative to controls [148]. During oligodendroglial lineage progression, Olig2⁺ Sox2⁺ cells and Olig2⁺ Pdgfra⁺ oligodendrocyte progenitor cells were increased, whereas CNPase⁺ immature oligodendrocytes were decrease in the *Cic* knockout mice [148]. EdU labeling and immunostaining of the proliferation marker Ki67 reveal increased neural progenitor proliferation and self-renewal in *Cic*-null NPCs [148]. Furthermore, *Cic*-null cells underwent more frequent symmetric divisions and fewer asymmetric divisions compared with control [148]. Overall, this indicates an increase of glial cell production at the expense of neural stem cell differentiation. In summary, CIC regulates neural stem cell proliferation, fate specification, as well as neuronal differentiation and maturation during brain development. Furthermore, hippocampal-related functions are abnormal in *Cic* knockout mice, and neurodevelopment deficits are present in humans haploinsufficient for *CIC*.

1.6 Rationale and research objectives: There has been an emphasis to focus on the neural stem and progenitor cell phase in AHN research. Such studies of progenitor cell maintenance have revealed that this phase is controlled by myriads of extrinsic and intrinsic signals that lead to activation of a coordinated network of transcription factors. Whether such a coordination event occurs during later phases of AHN, namely neuronal differentiation, survival, and maturation is largely unknown because these later stages have been understudied. Recent lineage tracing and single-cell transcriptomic studies demonstrate that adult and developmental DG neurogenesis are one continuous process that share a common cellular origin and conserved molecular properties [149, 150]. Moreover, many transcription factors important for embryonic cortical and hippocampal development also play a role in adult DG neurogenesis. Therefore, the approach was to ask whether the transcriptional regulator CIC, involved with neuron maturation during brain development is also required for similar processes during AHN. While CIC is important in neuronal maturation and dendrite development during early postnatal brain development, whether CIC is also required for neurons to mature during adult neurogenesis remains unknown. Therefore, I undertook a project to explore the role of CIC in the adult brain with a focus on AHN.

CHAPTER 2: METHODOLOGY

Mouse model: Generation of the *Cic^{lox}* mice has been previously described [145]. The *Cic^{lox}* mice are also available from The Jackson Laboratory (stock number: 030555). Wildtype C57BL/6J mice and *Emx1-Cre* mice [B6.129S2-*Emx1^{tm1(cre)Krl}/J*, stock number: 005628] were obtained from The Jackson Laboratory. No sex differences were observed in our studies. Both male and female mice were used for experiments. For studies involving wildtype C57BL/6J animals, animals were eight weeks of age. For EdU labelling experiments, 8-week-old mice were used. For all other experiments, 11- to 20-week-old *Emx1-Cre; Cic^{lox/lox}* mice were used, and their littermate *Cic^{lox/lox}* and *Emx1-Cre; Cic^{lox/+}* mice were used as controls.

Ethics statement: All procedures in mice were approved by the Animal Care and Use Committee of the University of Alberta. All methods were performed in accordance with the relevant guidelines and regulations. The study was carried out in compliance with the ARRIVE guidelines: <https://arriveguidelines.org>.

5-ethynyl-2'-deoxyuridine (EdU) labelling experiment in mice: EdU (Santa Cruz, sc-284628) was reconstituted in DMSO to a concentration of 100 mg/mL, aliquoted and stored at -20°C until further use. For progenitor proliferation analysis, on the day of experiment, EdU was diluted with endotoxin-free PBS to a final concentration of 5 mg/ml and injected intraperitoneally into 8-week-old mice to a final *in vivo* concentration of 50 µg/g body weight. A second dose of EdU was injected two hours after the first injection to maximize labelling efficiency. Mice were euthanized two hours or three weeks after the second injection by an intraperitoneal injection of sodium pentobarbital into the body cavity and used for brain section preparation.

Preparation of mouse brain sections: Mice were deeply anaesthetized via intraperitoneal injection of sodium pentobarbital, and transcardially perfused first with PBS then with 4% paraformaldehyde in PBS. Mouse brains were then dissected and immersed in a 4% paraformaldehyde solution overnight at 4°C to further fix the tissues, followed by submerging the brains in cryoprotective 15% and 30% sucrose, each for 24 hours. The mouse brains were cut coronally using a brain matrix and cryo-embedded using Tissue-Tek OCT compound. Coronal brain sections (40 µm-thick) were cut using a cryostat (Leica Microsystems Inc., Buffalo Grove, IL), transferred to ColorFrost Plus Microscope Slides (Fisher Scientific, 22-230-890), and air-dried for immunofluorescence staining. Excess slides were stored at -80°C. Frozen slides were

thawed at room temperature and dried for several hours to overnight before undergoing staining procedures.

EdU labelling detection: EdU detection was performed by using the Click-iT Alexa Fluor 555 dye EdU kit (Invitrogen, C10338) according to the manufacturer's protocol. Briefly, slides with brain sections were post-fixed with 4% paraformaldehyde, washed with 3% bovine serum albumin in PBS, then permeabilized with 0.5% Triton-X 100 in PBS at room temperature for 20 min. Slides were then incubated with the Click-iT reaction cocktail that contained Click-iT reaction buffer, Alexa Fluor 555 Azide, CuSO₄, and reaction buffer additive for 30 min while being protected from light. Slides were then washed once with 3% BSA in PBS and then three times with PBS before being further processed for immunofluorescence staining or counterstaining with DAPI.

Immunofluorescence staining: Immunofluorescence staining was performed as previously described with modifications [145]. Slides containing brain sections were first post-fixed in 10% neutral buffered formalin (Fisher Scientific, SF98-4) for 5–10 min, then washed three times with PBS. Antigen retrieval was performed using the Antigen Unmasking Solution (Vector Laboratories, H-3300) at 95°C for 20–60 min in a water bath with gentle shaking (60 rpm). Slides were cooled to room temperature and permeabilized with 0.3% Triton X-100 in PBS, then blocked with 5% normal donkey serum in 0.3% Triton X-100 in PBS. Slides were incubated at 4°C overnight with the primary antibodies in blocking buffer. The slides were washed three times with 0.3% Triton X-100 in PBS, then incubated with secondary antibodies in blocking buffer at room temperature for two hours. The slides were then washed twice with 0.3% Triton X-100 in PBS, and then once with PBS. Autofluorescence quenching was carried out to reduce background autofluorescence using the Vector TrueVIEW Autofluorescence Quenching Kit (Vector Laboratories, SP-8400) and all slides within one experiment were treated similarly. Slides were counterstained with DAPI and then mounted using VECTASHIELD Vibrance mounting media (Vector Laboratories, H-1700).

Antibodies: The following primary antibodies were used for immunofluorescence staining: rabbit anti-Ki67 (Abcam, ab15580, 1:1000), rabbit anti-CIC (Lu et al. 2017; 1:500), mouse anti-DCX (Santa Cruz Biotech, sc-217190; 1:25), goat anti-SOX2 (R&D Systems, AF2018; 1:500), mouse anti-NES (Abcam, ab11306; 1:200), rabbit anti-TBR2 (Abcam, 183991; 1:500), rabbit anti-CALB1 (Swant, CB38; 1:500), rabbit anti-NeuN (Abcam, ab177487; 1:500), rabbit anti-

GFAP (DAKO, Z0334; 1:2000), rabbit anti-OLIG2 (Millipore, AB9610; 1:1000), rabbit anti-NFIB (Invitrogen, PIPA552032; 1:200), rabbit anti-NFIA (Sigma, HPA006111-100UL; 1:200), and rabbit anti-CRMP4 (A gift from Dr. Alyson Fournier 1:500). The secondary antibodies used were donkey anti-rabbit Alexa Fluor 488 (Invitrogen, A21206; 1:1000), donkey anti-mouse Alexa Fluor 647 (Invitrogen, A31571; 1:1000), donkey anti-rabbit Alexa fluor 555 (1:1000) and donkey anti-goat Alexa Fluor 555 (Invitrogen, A21432; 1:1000).

Confocal microscopy and image and data analyses: Immunofluorescent images were taken using a laser-scanning confocal microscope (Zeiss LSM 700) with 20x dry or 40x oil objective lens for analysis. For each animal, tiled and z-stacked images of the dentate gyrus were acquired from at least three comparable coronal sections spanning the entire dorsal dentate gyrus and analyses were performed on images of these sections. Each data point represents the average value from multiple sections per animal. Quantifications of fluorescence intensity and cell counts were carried out using ImageJ. Cell counts for total SOX2⁺ and SOX2⁺ Ki67⁺ cells were restricted to cells within the subgranular zone of the dentate gyrus, which was defined as “a layer of cells expanding 5 μm into the hilus and 15 μm into the granular cell layer” [30]. Dendrite analyses were carried out using the Simple Neurite Tracer plugin of ImageJ. To quantify NFIA and NFIB immunofluorescence intensity and the number of cells expressing high levels of these proteins, images of single fluorescence channel were adjusted using the MaxEntropy method and an automated threshold calculated by ImageJ. The images were further subjected to Watershed binary processing to split cell clusters into individual cells. Particle analyses were then performed on the processed images, which yielded the number of cells expressing NFIA or NFIB and the mean fluorescence intensity of these cells. Final images were generated using ImageJ and Photoshop Elements.

Mouse dentate gyri dissection: Four knockout and three control mice were euthanized with intraperitoneal injection of sodium pentobarbital. After euthanasia, mice were decapitated, and brains were dissected out and place into cold, clean 1x PBS. DG microdissection was performed as described [151]. Dissected DG were placed in an Eppendorf tube, snap-frozen in liquid nitrogen immediately, and stored at -80°C until use.

Protein extraction: Dentate gyri (4 knockout, 3 control) frozen at -80°C were transferred to a 2 mL Dounce homogenizer with 500 μL of RIPA buffer (50 mM Tris HCl, pH 7.4; 150 mM NaCl; 0.1% Triton X-100; 0.1% (w/v) SDS; 0.5% (w/v) sodium deoxycholate; 1 mM EDTA) supplied

with fresh phosphatase and protease inhibitors. Tissues were homogenized with 30 strokes of pestle A and 30 strokes of pestle B. Tissue homogenate was transferred to a 1.5 mL Eppendorf tube and incubated on ice for 20 min. Samples were centrifuged at 13,200 rpm for 10 min at 4°C. Supernatant (protein extract) was collected into a new 1.5mL Eppendorf tube and spun in a centrifuge at 13,200 rpm for 10 min at 4°C. Supernatant (soluble protein extracts) were collected into a new 1.5 mL Eppendorf tube. Protein concentration of supernatants was determined using the Pierce™ BCA protein assay kit (ThermoFisher, #23227) following the manufacturer's protocol. Proteins extracts were aliquoted and stored at -80°C until use.

SDS-PAGE: Dentate gyri protein extracts (4 knockout, 3 control) stored at -80°C were thawed quickly at room temperature and place on ice. Loading buffer (4x Laemmli buffer with β -mercaptoethanol) was added to protein extracts. Protein extracts were boiled at 95°C for 10 min. For each sample, 30 μ g of protein extract was loaded onto BioRad 4-20% precast gels (one gel for control samples, one gel for knockout samples, leaving one empty well between each sample) and ran at 120 V for 25 min (to about half of the total gel length).

Western Blotting: Proteins ran on 4-20% BioRad precast TGX gels were transferred onto a nitrocellulose membrane at 300 mA for 2 hours in a BioRad Criterion™ Blotter (560BR) in an ice-water bath. The transferred membrane was blocked with TBST (1X Tris-buffered saline, 0.1% tween) with 2% bovine serum albumin for 1 hour at room temperature with agitation. Primary antibody incubation was conducted at 4°C overnight. The following day, the membrane was washed with TBST (0.1% Tween) at room temperature three times, 10 min each. Secondary antibody incubation was conducted at room temperature with agitation in the dark for 1 hour. Blot was washed three times, 10 min each with 0.1% tween TBST. Primary antibodies used were: Rabbit anti-CRMP4 (Sigma/Millipore; AB5454; 1:1000), rabbit anti-CRMP4 (Alyson Fournier in-house; 1:1000), rabbit anti-phospho-Ser9 GSK3B (Cell signaling; D85E12; 1:1000), and mouse anti-GAPDH (Advanced immunochemical Inc; 2-RGM2; 1:10000). Secondary antibodies used were: Goat anti-rabbit 680 (Invitrogen; A32734; 1:10,000) and goat anti-mouse 800 (Licor ID dye; 925-32210; 1:10000). Blot were imaged using a Li-Cor Odyssey CLx Imager.

Statistical analyses: Three-way comparisons of control (*Cic^{lox/lox}*), heterozygous (*Emx1-Cre; Cic^{lox/+}*) and knockout (*Emx1-Cre; Cic^{lox/lox}*) were conducted using one-way ANOVA with Tukey's *post hoc* test. * $P < 0.05$; ** $P < 0.01$; **** $P < 0.0001$. Two-way control versus knockout comparisons were conducted with t-test assuming non-equal variance.

CHAPTER 3: CAPICUA IS IMPORTANT FOR ADULT HIPPOCAMPAL NEUROGENESIS

CIC shows a dynamic expression pattern during granule neuron generation in the adult

brain: While the expression pattern for CIC has been determined for embryonic and early postnatal neurogenesis, CIC expression had never been previously examined in the adult brain. Through immunostaining, it was observed that CIC was widely expressed in the adult mouse brain, with the highest expression observed in the DG of the hippocampus (**Fig. 6**), where adult neurogenesis takes place. There are several cell types contained in the DG (**Fig. 7A**). Quiescent RGL cells reside in the SGZ; upon activation, RGL cells differentiate into rapidly amplifying type 2a/b IPCs [152]. IPCs give rise to neuroblasts that eventually exit the cell cycle to become immature and then mature granule neurons that localize to the granule layer [124]. To assess CIC expression within adult DG neuronal cells, I immunostained for SOX2⁺ RGLs and IPCs, DCX^{hi} neuroblasts, and DCX^{lo} immature neurons. Moderate CIC expression was observed in SOX2⁺ RGLs and IPCs [**Fig. 7D** (white dash line), **7G-I**] that decreases upon differentiation into DCX^{hi} neuroblasts [**Fig. 7D-G** (white asterisks)]. Nonetheless, CIC expression in DCX⁺ cells was detectable (**Fig. 8**), which was followed by an increase in expression during maturation (**Fig. 7G-I**). These results show that CIC exhibits a dynamic expression pattern throughout the cellular stages of AHN, peaking during the proliferation and maturation stages. This expression pattern of CIC suggests that CIC may contribute to these stages of AHN. Furthermore, CIC was expressed at comparable levels in SOX2⁺ NES⁺ RGL cells and SOX2⁺ GFAP⁻ IPCs (**Fig. 7H, I**).

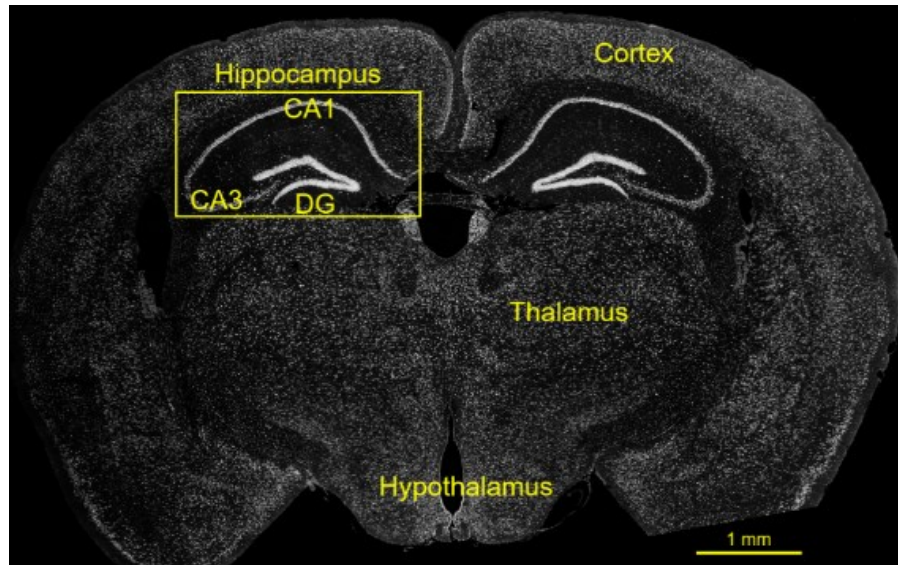


Figure 6: CIC expression in the adult mouse brain. Wildtype mouse brains were immunostained for CIC (grey). CIC is expressed most strongly in the DG of the hippocampus. Scale bar = 1 mm.

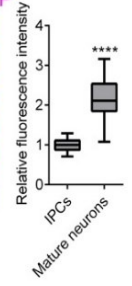
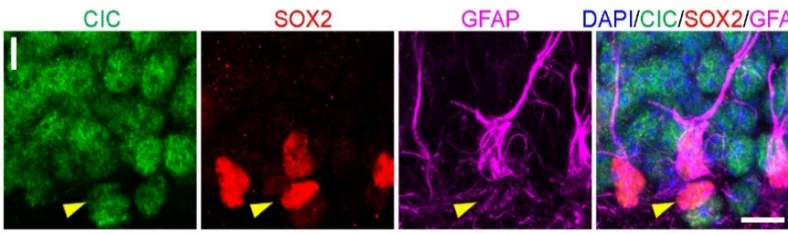
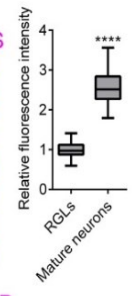
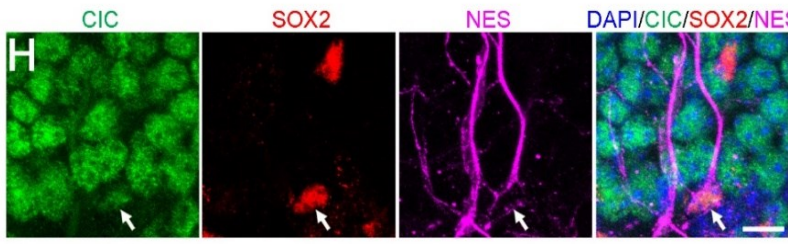
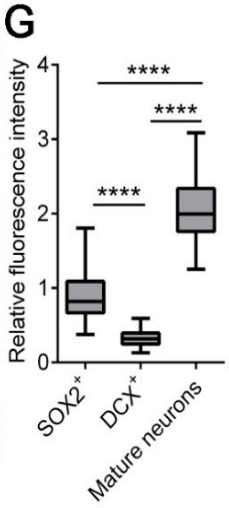
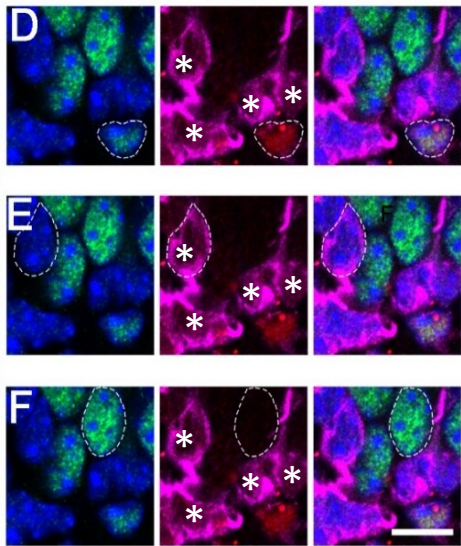
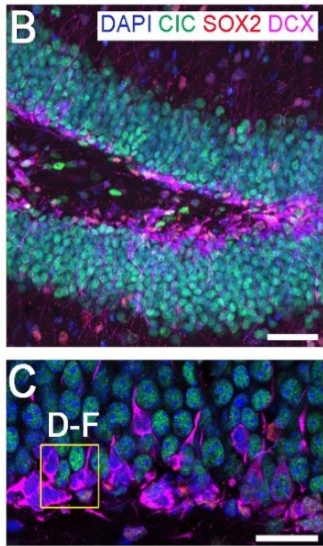
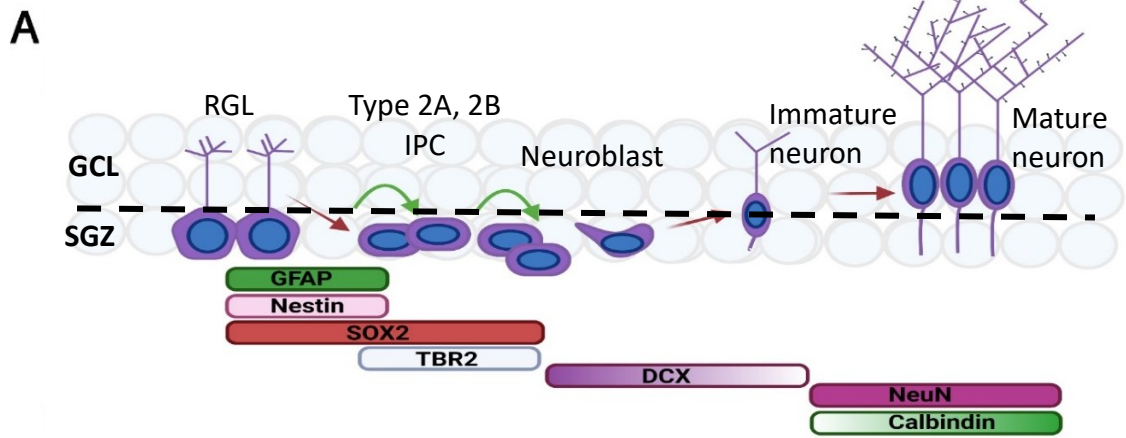
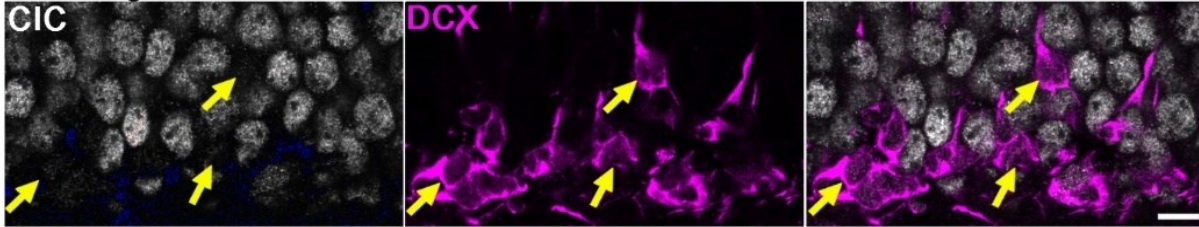


Figure 7: CIC expression along the neurogenic lineage in the adult dentate gyrus (page 28).

(A) Schematic of AHN. AHN encompasses three phases with six developmental milestones classifiable through cell morphology and expression of specific protein markers. RGL cells are mostly quiescent stem cells that reside in the SGZ. Upon activation, RGLs give rise to rapidly amplifying type 2a and subsequently, type 2b IPCs. IPCs differentiate to neuroblasts which eventually exit the cell cycle to become immature and then mature granule neurons. SOX2 and GFAP are expressed by RGL and type 2a cells. DCX starts to be expressed by type 2b cells but is turned off when neurons become mature. (B) A representative image showing CIC, SOX2 and DCX expression in the dentate gyrus of 8-week-old wildtype mice. Scale bar = 50 μm . (C) CIC, SOX2 and DCX expression in the DG SGZ. Scale bar = 25 μm . (D) During AHN, SOX2⁺ neural progenitor cells express moderate levels of CIC. (E) Minimal CIC expression is observed in DCX⁺ cells. (F) Mature neurons have the highest levels of CIC. Scale bar = 10 μm . (G) Quantification of relative fluorescence intensity of CIC immunostaining in different cell stages. N = 60 cells from a total of three 8-week-old wildtype mice. (H) CIC is expressed in SOX2⁺ Nes⁺ RGL cells. Arrow points to a RGL cell. Scale bar = 10 μm . Quantification is shown to the right. N = 59 RGL cells and 80 mature neurons from a total of four 12-week-old control mice. (I) CIC is expressed in SOX2⁺ GFAP⁻ IPCs. Arrowhead points to an IPC. Scale bar = 10 μm . Quantification is shown to the right. N = 15 IPCs and 51 mature neurons from a total of three 12-week-old control mice. Data are presented in box-and-whisker plots, where centre lines represent medians, box limits represent interquartile ranges, and whiskers represent minimum to maximum data ranges. Statistical analyses were performed with one-way ANOVA with Tukey's *post hoc* test (in G) or two-tailed Student's *t*-test (H and I). **** $P < 0.0001$.

Below signal saturation



Above signal saturation

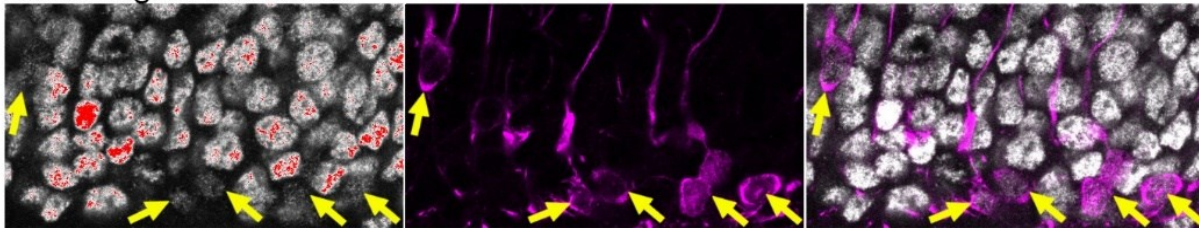


Figure 8: CIC is expressed at a low but detectable level in DCX⁺ cells. Upper panel, same images as in **Fig. 7C**. To quantify the expression levels of CIC in multiple cell stages and to keep the fluorescence signals within the dynamic range, these images were taken below signal saturation in mature neurons using relatively low laser power and detector gain (**upper panel**; saturated pixels in red; few pixels in the image are saturated). As a result, CIC appears to be not expressed in DCX⁺ cells (yellow arrows). The **lower panel**, however, represents images taken above signal saturation using high laser power and detector gain (saturated pixels in red), and CIC is clearly visible in DCX⁺ cells (yellow arrows). Scale bar = 10 μ m.

Reduced progenitor pool in the *Emx1-Cre; Cic^{flx/flx}* knockout mice is not due to reduced

proliferation capacity of neural progenitor cells:

I next assessed the role of CIC during the progenitor proliferation phase of AHN. To do so, a *Cic* knockout mouse strain was generated using the Cre-lox system to genetically remove *Cic*. *Emx1-Cre; Cic^{flx/+}* conditional heterozygous mice were bred with *Cic^{flx/flx}* mice to generate *Emx1-Cre; Cic^{flx/flx}* (herein referred to as the *Emx1-Cre; Cic* knockout mice). These mice express a Cre recombinase in forebrain neural progenitor cells starting at embryonic day 9.5 [153]. Cre mediates the recombination of the two *loxP* sites flanking exons 9-11 of the *Cic* gene. The floxed exons are excised, leading to a premature stop codon which results in nonsense-mediated decay of *Cic* mRNAs. First, I assessed whether Cre-mediated recombination in the adult DG was complete in the *Emx1-Cre; Cic* knockout mice. Immunostaining for CIC in the control and knockout mice showed that CIC was not expressed in *Emx1*-lineage, adult neurogenic cell stages, including SOX2⁺ neural progenitor cells, DCX⁺ cells and mature granule neurons (**Fig. 9**). CIC⁺ cells were occasionally found in the DG of the knockout mice in what were likely non-*Emx1*-lineage cells. As the *Emx1-Cre* driver is turned on during early embryonic development, it was determined whether *Cic* deletion in these mice affected the formation of the adult SGZ. The SGZ cell layer was defined as “a layer of cells expanding 5µm into the hilus and 15µm into the granular cell layer” as previously described [30]. The analysis of 11-week-old control and *Emx1-Cre; Cic* knockout mice showed that the size of the SGZ was not significantly altered in the knockout mice (**Fig. 10**). For this analysis and all subsequent analysis, these µm measurements were used to define the SGZ. While these stereological measurements were done with consistent brain tissue µm size (40µm), the same mice strain and age, as well as consistent sampling of a specific region of the DG (in the middle of the DG), there are caveats. Of note, adult neurogenesis is dependent on factors such as species, age, and which DG section is being analyzed (dorsal versus ventral DG) [154-156]. Therefore, the values we obtained are consistent with independent literature (as described below, where applicable for each result), but would vary if the variables mentioned above (age, species, selection of DG section to analyze) changed. Technical methods such as tissue fixing and staining protocols can also affect quantifications of adult neurogenesis [154]. For example, fixation by formalin can affect protein tertiary structure and thus affect antibody recognition [157, 158]. While tissue shrinkage through formalin is reduced in relevance to other fixatives such as ethanol, shrinkage can occur [159]. Next, the proliferation of SOX2⁺ neural precursors

was examined by utilizing EdU labeling in combination with immunofluorescence staining of Ki67, a proliferation marker. EdU labels cells that had entered the S phase of the cell cycle during a 4-hour labelling period. The length of S phase for SGZ neural progenitor cells is 2-2.5 hours and the total cell cycle length is about 22-24 hours [35]. Therefore, this experimental paradigm labelled only those cells that had recently entered, and remained in, the cell cycle. *Emx1-Cre; Cic* knockout mice showed reduced total EdU and Ki67 co-expressing cells in comparison to the control and heterozygous mice (**Fig. 11A-I**), indicating a reduction in neural progenitor proliferation within these mice. This could be due to a decrease in the overall neural progenitor cell pool, a decline of the proliferation capacity of neural progenitor cells, or both. To tease apart these possibilities, I compared the number of SGZ SOX2⁺ progenitor cells between the control and the *Emx1-Cre; Cic* knockout mice. Cell counts indicate that the total number of SOX2⁺ neural precursors is reduced in the *Emx1-Cre; Cic* knockout mice relative to the control and heterozygous mice (**Fig. 11H, I**). Analyses further showed that both NES⁺ GFAP⁺ RGL cells and TBR2⁺ IPCs were significantly reduced in the knockout DG (**Fig. 12**). I also observed a decrease in the total number of SOX2⁺ Ki67⁺ cells in the *Emx1-Cre; Cic* knockout mice in comparison to control and heterozygous mice (**Fig. 11I**). To determine the proliferation capacity of neural progenitor cells, I calculated the proportion of SOX2⁺ cells that were also co-labelled with Ki67. In the SGZ of control adult mice, about 20% of SOX2⁺ cells were actively dividing (**Fig. 11J**), which is comparable to findings from other studies [160-162]. The percentage of proliferating SOX2⁺ cells in the *Emx1-Cre; Cic* knockout mice was similar to that of the control mice, thus the proliferation capacity of neural progenitor cells did not appear to be altered in the knockout mice. This suggests that the reduction in the proliferating SOX2⁺ population is not due to reduced proliferation potential of the amplifying population within the *Emx1-Cre; Cic* knockout mice.

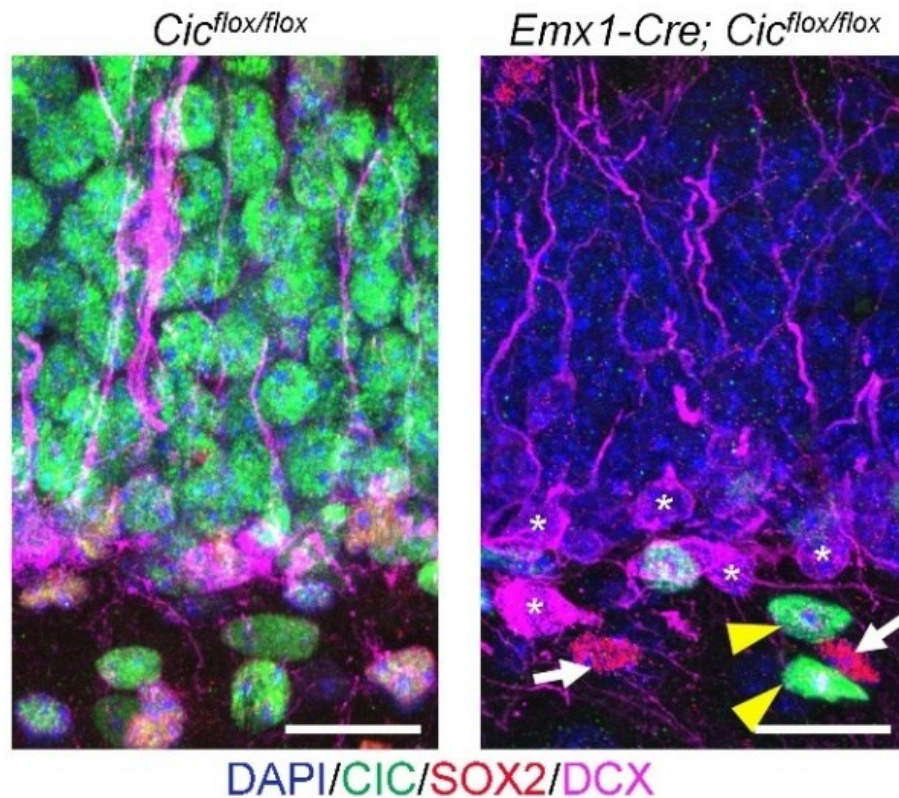


Figure 9: Knockout efficiency of *Emx1-Cre; Cic* knockout mice. Control (*Cic^{flox/flox}*) and *Emx1-Cre; Cic* knockout mice dentate gyri were assessed for CIC levels using immunofluorescence staining with the cell stage-specific markers SOX2 (red) and DCX (magenta) alongside CIC (green). White arrows indicate SOX2⁺ neuronal lineage cells; white asterisks indicate DCX⁺ neuronal cells and yellow wedges correspond to non-*Emx1*-lineage cell.

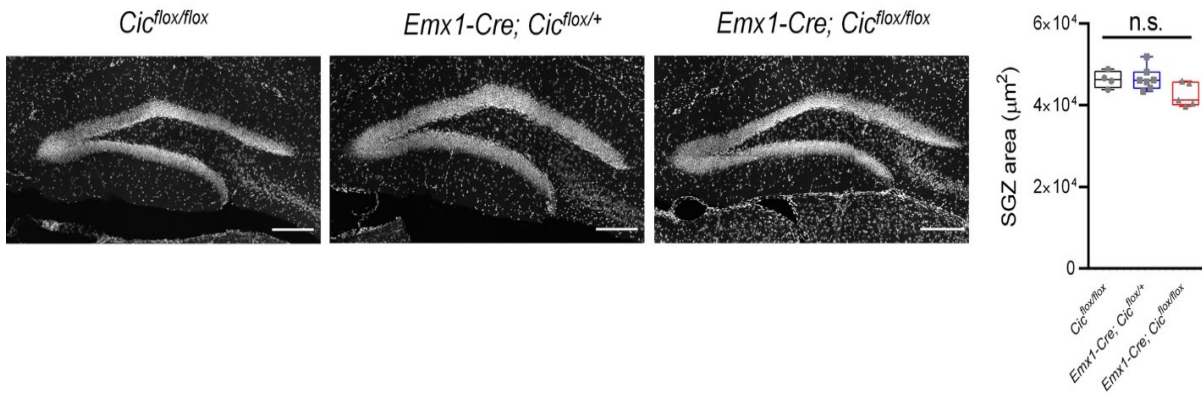


Figure 10: The size of the adult subgranular zone is not significantly altered in the *Emx1-Cre; Cic* knockout mice. Representative confocal images of 11-week-old mice stained for DAPI (gray) to show the overall morphology of the adult DG. Quantification of the areas of the SGZ is shown to the right. SGZ is defined as “a layer of cells expanding 5 μm into the hilus and 15 μm into the granular cell layer” as previously described. $N = 4-7$ animals. Data are presented in box-and-whisker plots showing all data points, where centre lines represent medians, box limits represent interquartile ranges, and whiskers represent minimum to maximum data ranges. Statistical analysis was performed with one-way ANOVA with Tukey’s *post hoc* test. n.s., not significant.

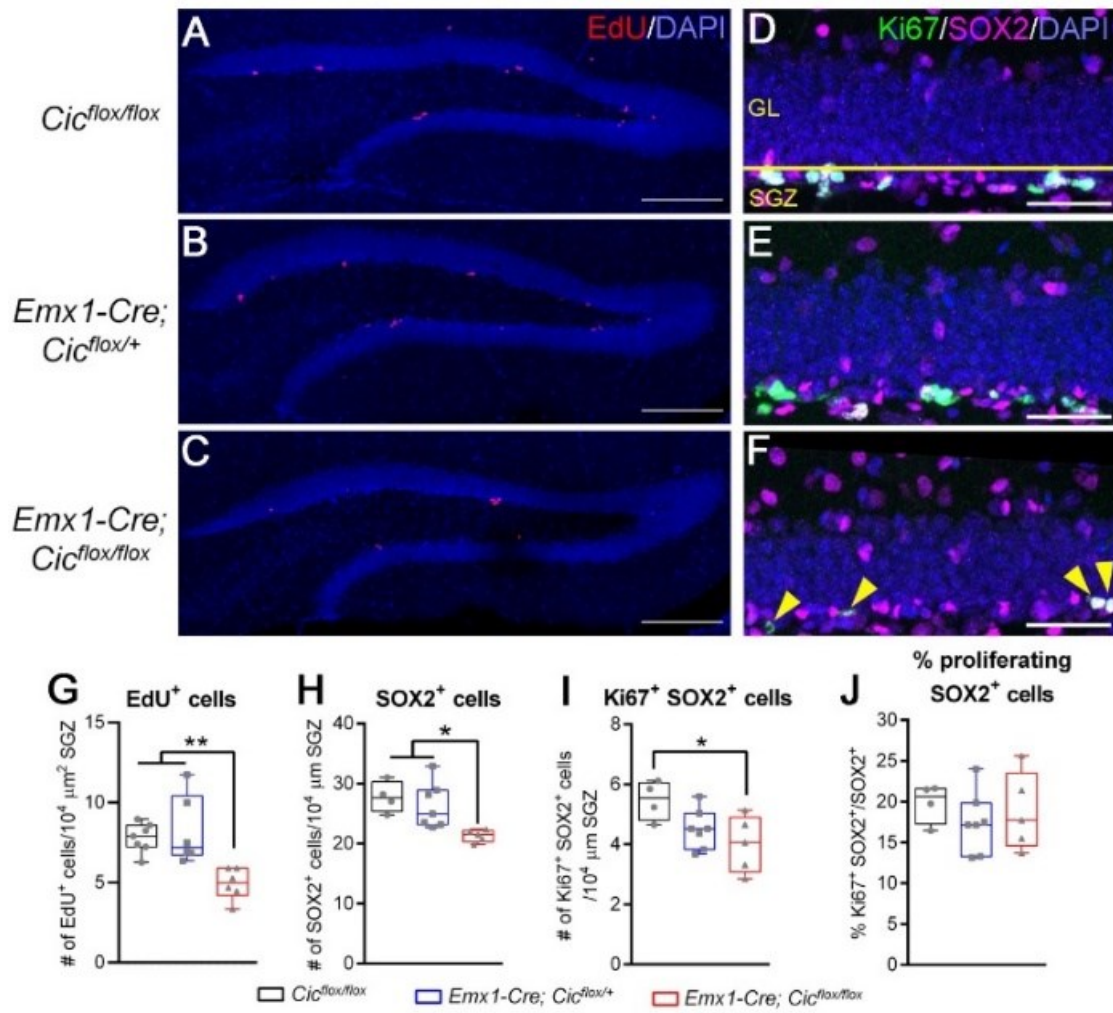


Figure 11: *Emx1-Cre; Cic* knockout mice have a diminished pool of adult hippocampal neural progenitor cells (page 35). (A-C) Representative images of the DG four hours post EdU injection showing staining for EdU (red) and DAPI (blue). EdU staining is mainly found in the neurogenic SGZ. Scale bars = 200 μm . (D-F) Representative images of the SGZ showing staining for Ki67 (green), SOX2 (magenta), and DAPI (blue). Yellow line in (D) indicates the boundary between the SGZ and the granule layer. Yellow arrowheads in (F) point to cells double positive for SOX2 and Ki67. Scale bars = 50 μm . Quantifications of EdU⁺ cells (G), SOX2⁺ cells (H), Ki67⁺ SOX2⁺ cells (I), and the percentage of proliferating SOX2⁺ neural progenitor cells (J) are shown at the bottom. N = 4–7 animals per group. Box-and-whisker plots show all data points; centre lines represent medians, box limits represent interquartile ranges, and whiskers represent minimum to maximum data ranges. Statistical analyses were performed with one-way ANOVA with Tukey's *post hoc* test. * $P < 0.05$.

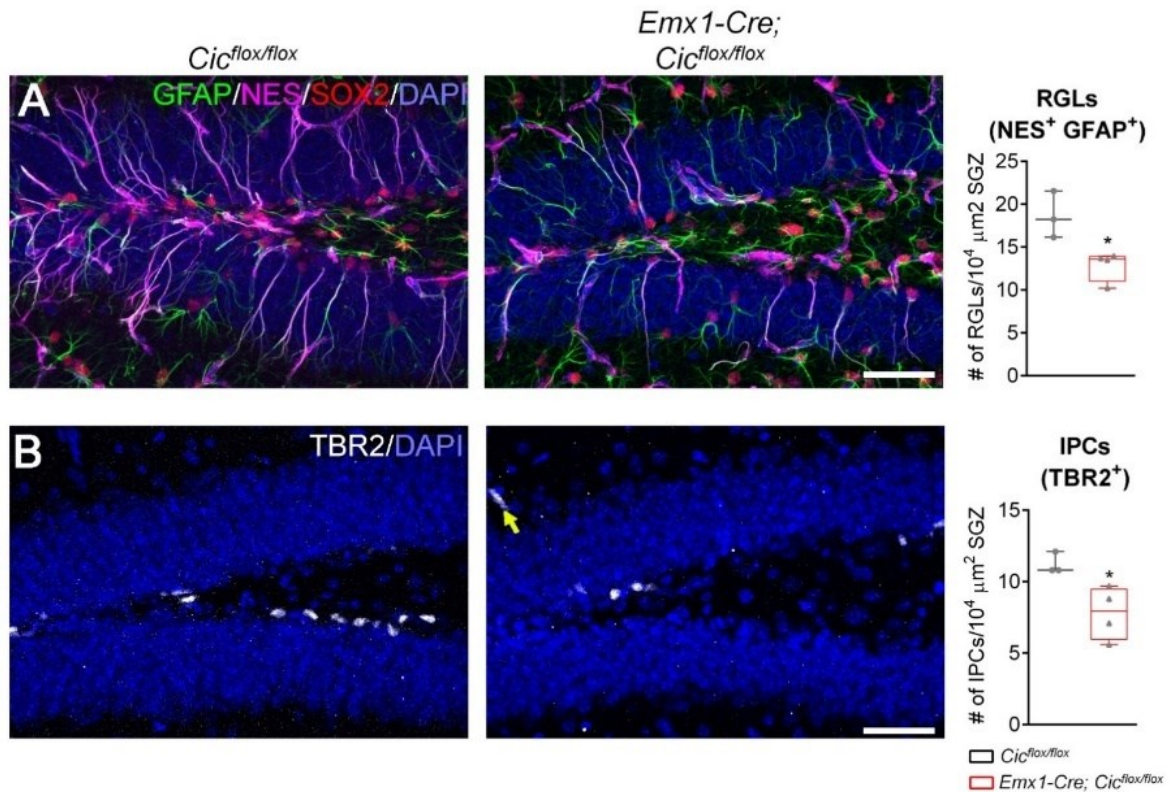


Figure 12. Adult neural progenitor cells are reduced in the dentate gyrus of the *Emx1-Cre; Cic* knockout mice. (A) The *Emx1-Cre; Cic* knockout mice have fewer GFAP⁺ Nes⁺ RGL cells. Note that GFAP also marks astrocytes, and NES also marks pericytes of the vasculature, but only RGL cells are double positive for GFAP and NES. Quantification is shown to the right. (B) The *Emx1-Cre; Cic* knockout mice have fewer TBR2⁺ IPCs. An abnormally located TBR2⁺ IPC in the molecular layer is indicated by an arrow. Scale bars = 50 μm. N = 3–4 animals per group. Data are presented in box-and-whisker plots showing all data points, where centre lines represent medians, box limits represent interquartile ranges, and whiskers represent minimum to maximum data ranges. Statistical analysis was performed with one-way ANOVA with Tukey's *post hoc* test. *, *P* < 0.05.

CIC deletion does not affect the total number of DCX⁺ cells but impairs their development into mature neurons: Next, the role of CIC outside of the precursor cell phase was investigated since dynamic regulation of CIC as neuronal differentiation progresses was observed (**Fig. 7B-I**). In the adult DG, all newly generated neurons express DCX during the survival and maturation phases [58, 163, 164]. DCX⁺ cells thus encompass cells before selective cell death and those that have survived and will persist for a long time. When I examined the DCX⁺ cell population in the control and *Emx1-Cre; Cic* knockout mice, I did not find a difference in the total number of these cells among the three genotypes (**Fig. 13B**). In this context, an unchanged DCX⁺ cell population could be due to reduced cell death or altered differentiation progression. To examine whether there was reduced cell death, the total number of DCX⁺ cells that expressed the apoptosis marker cleaved caspase 3 (cCASP3) were counted. There was no detectable differences in cCASP3⁺ cells among the three genotypes (**Fig. 14**). However, it needs to be recognized that CASP3 activation is transient and that CASP3-independent programmed cell death pathways have been shown to regulate adult neurogenesis [165]. Next EdU was injected into mice (two injections that were two hours apart) and were analysed three weeks after injections (**Fig. 13C**). The three-week time point was chosen because this is when the EdU-labelled cells start to become mature neurons that express CALB1 [166-168]. Reasonably, this experimental paradigm would allow the assessment of the effects of *Cic* deletion on the development of the DCX⁺ cells and their transition into CALB1⁺ mature neurons. I calculated the proportion of EdU-labelled DCX⁺ cells and found that the *Emx1-Cre; Cic* knockout mice had a significantly higher percentage of these cells compared to the controls, indicative of increased cell survival and/or increased neuronal differentiation from progenitor cells (**Fig. 13D, E**). Within the EdU-labelled DCX⁺ cell population, CALB1 expression was observed in ~25% of the cells in the control and heterozygous mice (**Fig. 13D, F**). Interestingly, no DCX and CALB1 co-expressing cells in the EdU-labelled population were detected in the *Emx1-Cre; Cic* knockout mice, suggesting impaired development of DCX⁺ immature neurons into mature neurons. Overall, this strongly suggest that, in the *Emx1-Cre; Cic* knockout mice, despite the reduction in the progenitor cell pool (**Fig. 11, 12**), the population of DCX⁺ cells remain similar in size with no obvious effect on cell death. Thus, the reduced NPC pool is likely due to increased progenitor differentiation into DCX⁺ cells.

Loss of CIC leads to reduced dendritic arborization of DCX⁺ cells: The period of DCX expression is associated with neuronal migration and neurite outgrowth: immature cells start expressing DCX when they begin to migrate and grow their dendrites, then they turn off DCX expression when they become fully mature [58, 163, 164]. As DCX expression spans the entire process of dendritic development, DCX⁺ cells exhibit varying degree of dendrite maturation. The least mature DCX⁺ cells have no or very short, plump processes. Then they develop an intermediate-length primary process perpendicular to the granular layer, followed by the establishment of a strong apical primary dendrite with elaborate dendritic branching in the molecular layer [58]. As such, the length of the primary dendrite and complexity of the dendritic architecture correlates with the maturity of DCX⁺ cells. The initial dendrite analysis showed that DCX⁺ cells in the knockout mice had shorter primary dendrites when compared to the control mice, an indication of reduced maturity (**Fig. 15A, B**). When I focused on DCX⁺ cells with a primary dendrite, about 85% of these cells in the control and conditional heterozygous mice formed higher-order branching in the molecular layer. Only 15% of DCX⁺ cells in these mice had one single primary process lacking any secondary branches (**Fig. 15C, 15**). In the knockout mice, however, only 50% of DCX⁺ cells had higher-order dendrites, and the rest of the 50% showed an immature morphology with a single intermediate-length primary dendrite that lacked any branches (**Fig. 15C, 16**). This data demonstrates impaired dendrite development in the knockout mice. To further analyze dendritogenesis in the *Emx1-Cre; Cic* knockout mice, I categorized DCX⁺ cells into three different developmental stages using a previously described morphology-based criteria: the most immature subgroup with no or short processes, the intermediate subgroup with a medium-length process, and the most mature subgroup with a strong primary process and elaborate branching [58]. While I found no difference in the number of DCX⁺ cells of the most immature subgroup (**Fig. 15D**), there was a significant increase in the intermediate subgroup (**Fig. 15E**) and a concomitant decrease in the most mature subgroup of DCX⁺ cells in the knockout mice (**Fig. 15F**). Altogether, the data demonstrates dendritic branching defects of DCX⁺ cells in the knockout mice and pinpoints the dendrite development stage at which CIC plays a critical role.

Loss of CIC leads to aberrant migration of DCX⁺ cells: Next, it was asked whether loss of CIC had any effect on cell migration. During AHN, tangential and radial migration occurs in DCX-expressing cell stages [31]. Radial migration of DCX⁺ cells is typically confined to the

inner two thirds of the granule layer [31, 68]. In agreement with this, I observed characteristic radial migration of DCX⁺ cells in the control and conditional heterozygous mice: most cells remained within the inner half of the granule cell layer and they seldomly migrate past the granule cell layer. In the knockout mice, while majority of DCX⁺ cells were seen in granule cell layer, I frequently and consistently found DCX⁺ cells in the molecular layer of the DG (**Fig. 15G, H, and 16**). These abnormally located DCX⁺ cells lacked primary processes and extended their dendrites in a random fashion, features of a relatively immature phenotype. To further refine the molecular identity of these abnormally migrated DCX⁺ cells, I co-labelled DCX with other neural cell type-specific markers. The cells were negative for the neural progenitor cell marker SOX2, the mature neuron marker NeuN, the astrocyte marker GFAP, and the oligodendroglial marker OLIG2, indicating that these were bona fide DG immature cells (**Fig. 17**). Indeed, I also observed some TBR2⁺ IPCs abnormally located to the molecular layer of the *Emx1-Cre; Cic* knockout mice (**Fig. 12**), further demonstrating aberrant localization of immature neuronal lineage cells. In brief, CIC regulates dendritic development of immature neurons in the adult dentate gyrus. Loss of CIC impairs dendritic arborization of DCX⁺ cells, concomitant with uncontrolled radial migration of some of these cells.

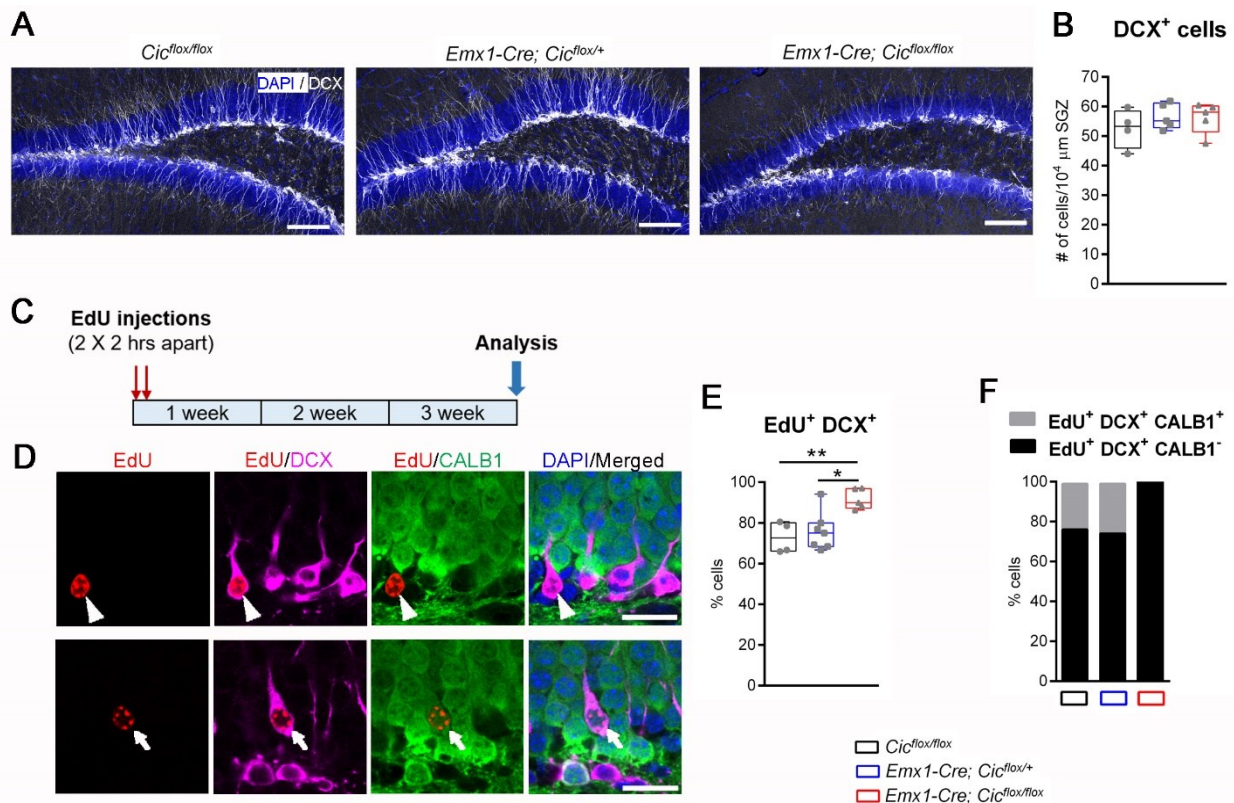


Figure 13. Impaired development of DCX⁺ cells in the *Emx1-Cre; Cic* knockout mice.

(A) Representative images of the dentate gyrus in the three mouse lines show severe dendritic morphology defects in DCX⁺ cells of the knockout mice. DAPI (blue) and DCX (grey). Scale bars = 100 μm. (B) Quantification of the total number of DCX⁺ cells in the three genotypes. No statistically significant difference was found. (C) A schematic of the EdU-labelling study. Mice were injected with two doses of EdU that were separated by two hours and were analysed three weeks post injections. (D) Representative images of the subgranular zone three weeks post EdU injection showing staining for EdU (red), DCX (magenta), CALB1 (green), and DAPI (blue). The arrowhead points to an EdU-labelled cell that is positive for DCX but negative for CALB1. The arrow points to an EdU-labelled cell that is double positive for DCX and CALB1. Scale bars = 20 μm. (E) Quantification of the percentage of EdU-labelled cells that were DCX⁺ in mice of the three genotypes. (F) Quantification of the relative proportion of EdU⁺ DCX⁺ cells that were CALB1⁻ or CALB1⁺ in mice of the three genotypes. $P < 0.0001$ using Chi-square test. $N = 4-7$ animals per group. In (B) and (E), data are presented in box-and-whisker plots showing all data points, where centre lines represent medians, box limits represent interquartile ranges, and whiskers represent minimum to maximum data ranges. Statistical analyses were performed with one-way ANOVA with Tukey's *post hoc* test. * $P < 0.05$; ** $P < 0.01$.

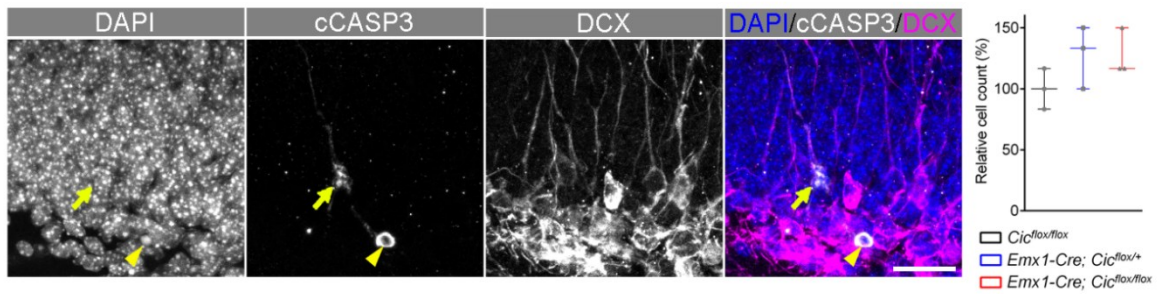


Figure 14. Apoptotic cell death of DCX⁺ cells is unaltered in the *Emx1-Cre; Cic* knockout mice. Immunostaining for the apoptosis marker cleaved-caspase 3 (cCASP3). Quantification is shown to the right. Scale bars = 25 μ m. N = 3 animals per group. Data are presented in box-and-whisker plots showing all data points, where centre lines represent medians, box limits represent interquartile ranges, and whiskers represent minimum to maximum data ranges. Statistical analysis was performed with one-way ANOVA with Tukey's *post hoc* test.

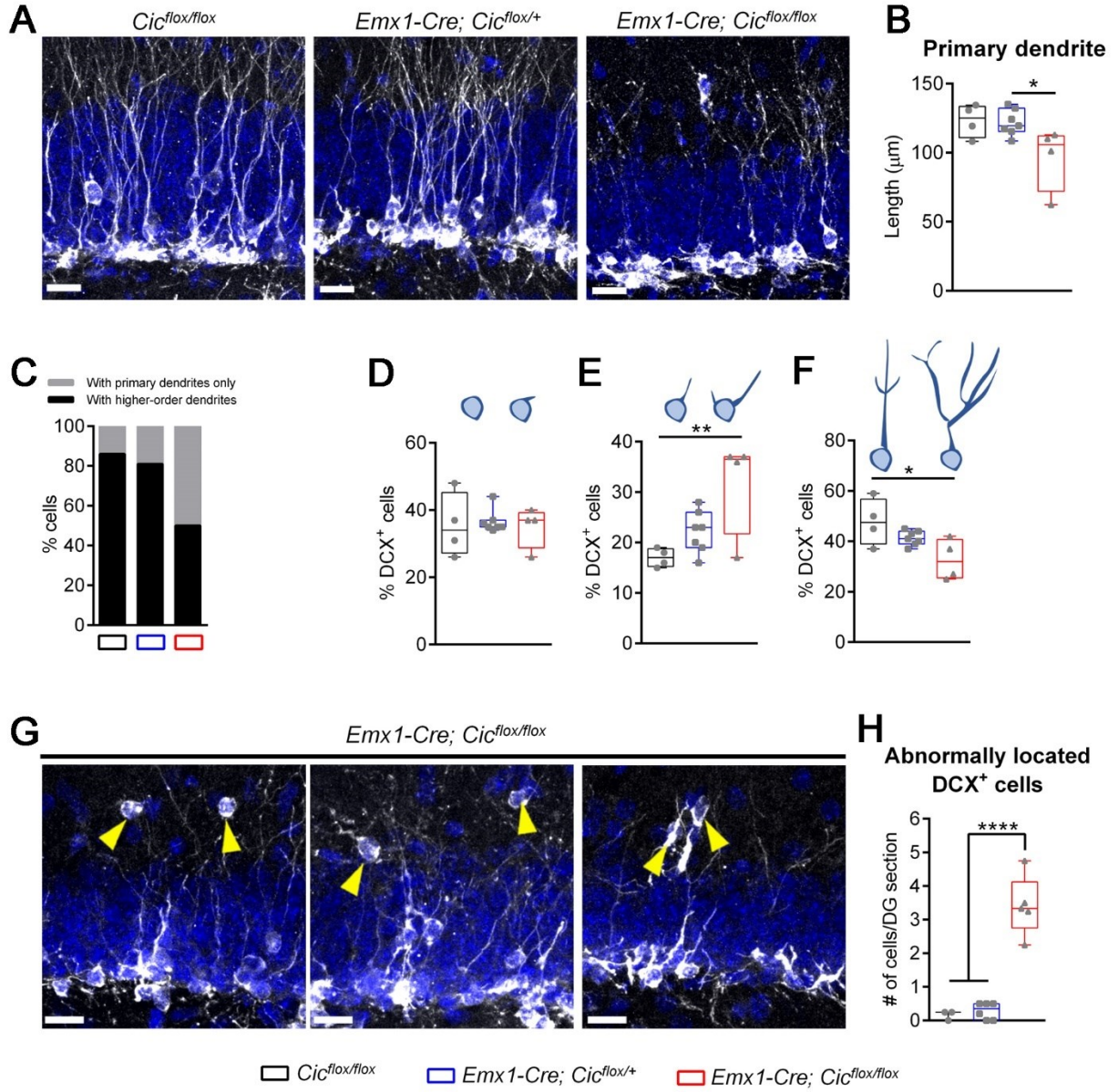


Figure 15. Reduced dendritic branching and abnormal migration of DCX⁺ cells in the *Emx1-Cre; Cic* knockout mice (page 43). (A) Representative images of the dentate gyrus show abnormal dendritic morphology in knockout DCX⁺ cells. DAPI (blue) and DCX (grey). (B) Quantification of primary dendrite length. (C) Dendrite analysis shows reduced dendritic complexity in the knockout mice. $P < 0.0001$ using Chi-square test. (D-F) DCX⁺ cells are categorized into distinct subgroups based on their dendrite morphology. The *Emx1-Cre; Cic* knockout mice show no difference in the number of the most immature subgroup with no or short processes (D), an increase in the intermediate subgroup with a medium-length process (E), and a decrease in the most mature subgroup with a thick long apical dendrite or an elaborate dendritic tree (F). (G) Representative images of the dentate gyrus show ectopically located DCX⁺ cells in the *Emx1-Cre; Cic* knockout mice. Each image is from a different animal. DAPI (blue) and DCX (grey). (H) Quantification of abnormally located DCX⁺ cells. N = 3–6 animals per group. Scale bars = 20 μ m. Three dentate gyri sections per animal was used. Data are presented in box-and-whisker plots showing all data points, where centre lines represent medians, box limits represent interquartile ranges, and whiskers represent minimum to maximum data ranges. Statistical analyses were performed with one-way ANOVA with Tukey's *post hoc* test. * $P < 0.05$; ** $P < 0.01$; **** $P < 0.0001$.

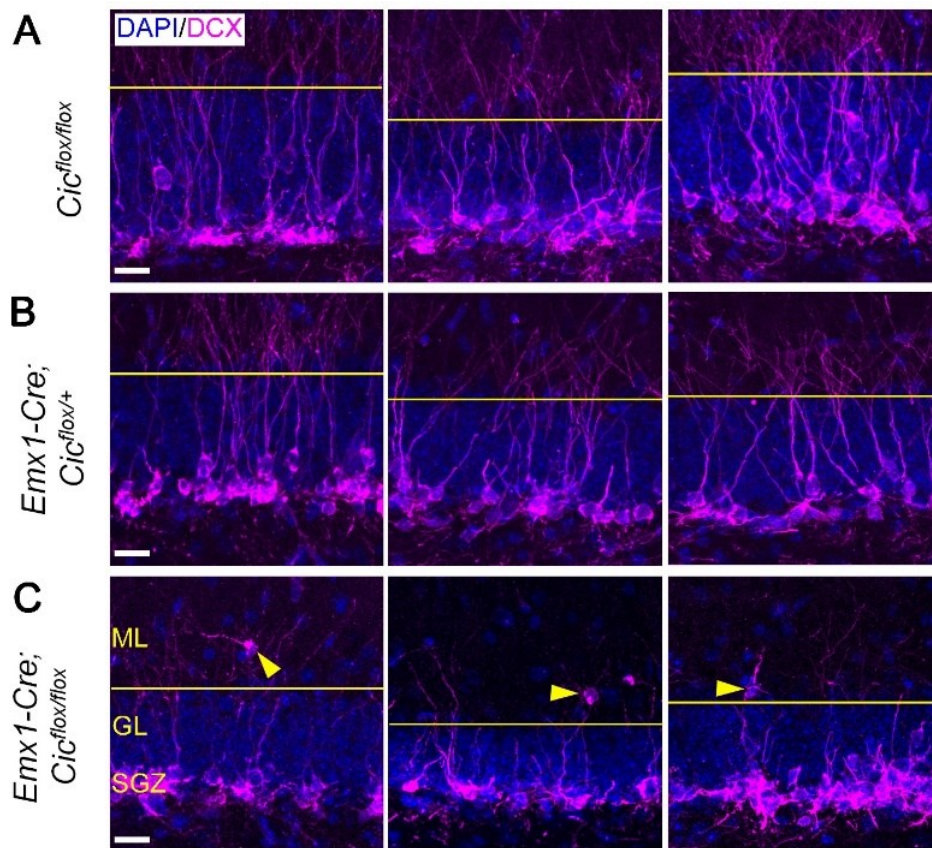


Figure 16. DCX⁺ cells in *Emx1-Cre; Cic* knockout mice show morphological and migration defects. Representative images of the dentate gyrus in (A) control, (B) heterozygous, and (C) knockout mice, with DAPI staining (blue) and DCX (magenta). The yellow lines mark the boundary of granule cell layer (GL) and molecular layer (ML). Majority of DCX⁺ cells in the control (A) and conditional heterozygous (B) mice have similar morphology: they project a single apical dendritic process radially through the granule cell layer; these processes then branch to form dendritic arbours in the molecular layer. In contrast, most DCX⁺ cells in the knockout mice (C) fail to extend an apical dendritic process and instead produced random, non-radial outgrowths. DCX⁺ cells normally do not migrate into the molecular layer. However, DCX⁺ cells are frequently found in the molecular layer of the knockout mice (yellow arrowheads). These abnormalities were found in all knockout animals examined (N = 6). Representative images from three different animals from each genotype are shown. SGZ, subgranular zone. Scale bars = 20 μ m.

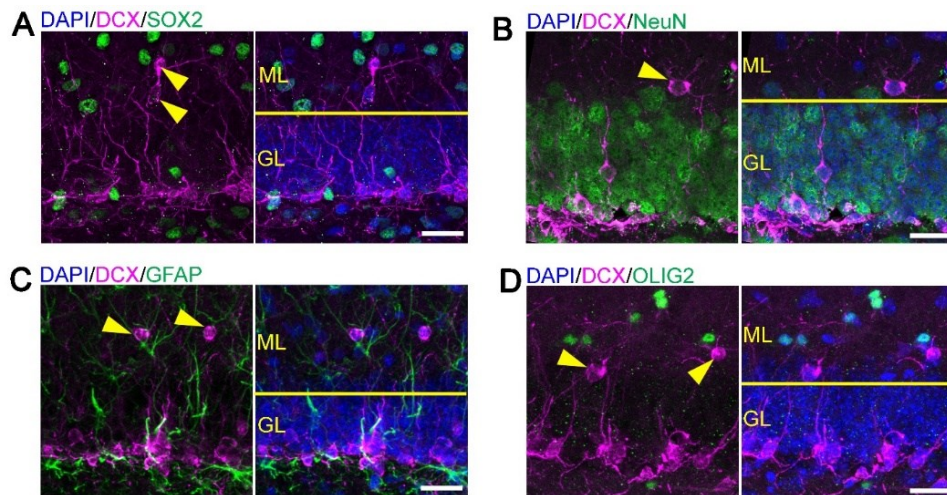


Figure 17. Molecular characteristics of abnormally migrated DCX⁺ cells in the *Emx1-Cre; Cic* knockout mice. Representative images of the dentate gyrus in the *Emx1-Cre; Cic* knockout mice show that DCX-expressing cells that have abnormally migrated into the molecular layer (yellow arrowheads) are negative for the neural progenitor cell marker SOX2 (A), the mature neuron marker NeuN (B), the astrocyte marker GFAP (C) and the oligodendroglial marker OLIG2 (D). Yellow lines mark the boundary between the granule cell layer (GL) and the molecular layer (ML). Scale bars = 25 μ m.

Increased NFIB expression is associated with abnormal development and migration of DCX⁺ cells in *Emx1-Cre; Cic* knockout mice: AHN is driven by a coordinated network of transcription factors that orchestrate the developmental sequence of proliferation, differentiation and maturation [169]. As CIC regulates the expression of other transcription factors involved in cell growth and differentiation [170, 171], I hypothesized that deletion of CIC from the adult DG disrupted downstream transcription factor networks. The reason being that a transcription factor repressed by CIC would have an expression pattern inversely correlated with the expression of CIC along the neurogenic lineage. To identify such factors, a chromatin immunoprecipitation-sequencing (ChIP-Seq) list from literature data was taken containing CIC-bound transcription factor genes in neural stem cells and looked for genes with low expression in neural progenitor cells and mature neurons but high expression in neuroblasts/immature neurons using a single-cell RNA sequencing dataset of the adult DG [149, 172]. This analysis revealed only two candidates, *Nfia* and *Nfib*, which are both members of the nuclear factor I (NFI) family (**Fig. 18A, 19A**). By co-labelling NFIA and NFIB with cell-stage specific markers, NFIA and NFIB expression was observed, and were most highly expressed in DCX⁺ cells, with NFIB experiencing a greater increase in expression from the transition of SOX2⁺ neural progenitor cells to DCX⁺ cells (**Fig. 18B, C, 19B-F**). Moreover, within the DCX⁺ population, strong NFIB expression was seen in majority of the cells except those possessing the most mature morphology, namely, an elaborate dendritic tree, an enlarged cell body and low DCX expression [58, 173, 174]. As DCX⁺ cells developed into mature neurons, NFIA and NFIB levels dropped. Thus, expression of NFIA and NFIB along the granule cell lineage development inversely correlates with the expression of CIC. Following this, NFIA or NFIB expression was assessed to indicate whether it altered in the DG of the *Emx1-Cre; Cic* knockout mice. While deletion of CIC did not lead to ectopic NFIA or NFIB expression in neural progenitor cells or mature neurons, NFIB (but not NFIA) levels were significantly upregulated in DCX⁺ cells of the *Emx1-Cre; Cic* knockout mice compared with the control mice [**Figs. 20A-H** (NFIB), **21** (NFIA)], supporting the idea that CIC regulates NFIB expression in DCX⁺ cells. Next, whether increased levels of NFIB in the *Emx1-Cre; Cic* knockout mice would alter the development of DCX⁺ cells was assessed as downregulation of NFIB is associated with neuronal maturation (**Fig. 19**). In the control mice, about 50% of DCX⁺ cells expressed NFIB at levels higher than those in SOX2⁺ progenitor cells; these NFIB^{hi} DCX⁺ cells exhibited a relatively immature morphology compared to DCX⁺ cells with low NFIB

expression. In the knockout mice, however, roughly 75% of DCX⁺ cells co-expressed high levels of NFIB (**Fig. 20C, F, H**). With high NFIB expression in DCX⁺ cells molecularly defining a less mature phenotype (**Fig. 19**), this result indicates an expansion of the less mature DCX⁺ subgroups in the knockout mice. Since the total number of DCX⁺ cells did not differ between the different lines of mice (**Fig. 13B**), this result further points to a reduction in the most mature DCX⁺ subgroup in the knockout mice. Interestingly, all *Cic*-knockout DCX⁺ cells that had abnormally migrated into the molecular layer had strong NFIB expression (**Fig. 20I-K**), raising the possibility that aberrant NFIB levels might contribute to abnormal neuronal migration. Altogether, these data suggest that deletion of CIC from the adult hippocampus leads to upregulation of NFIB in DCX⁺ cells, concomitant with an expansion of the less mature subgroups of these cells and occasional abnormal migration.

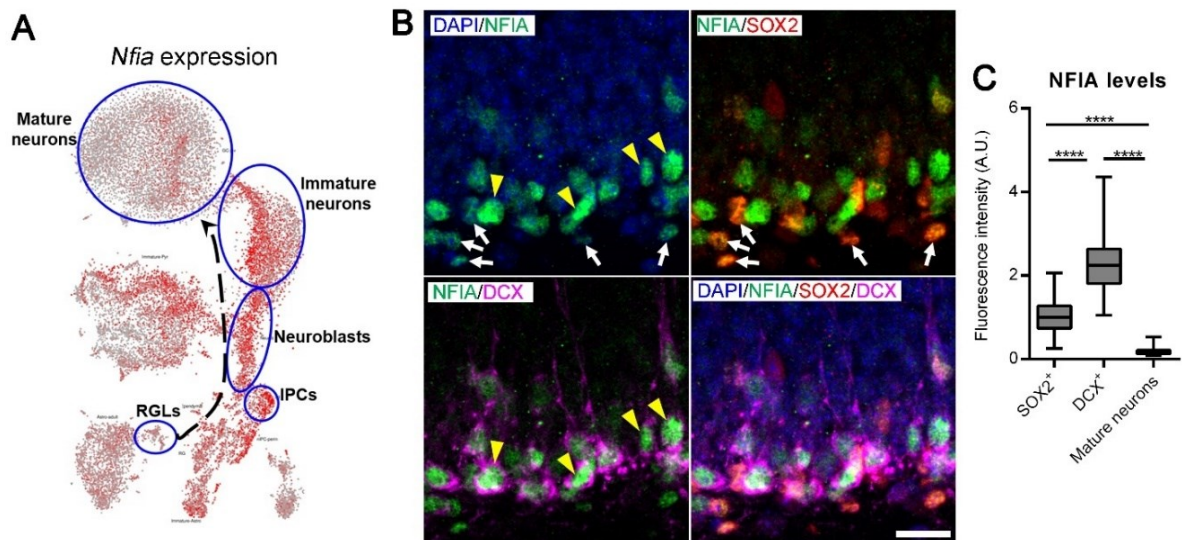
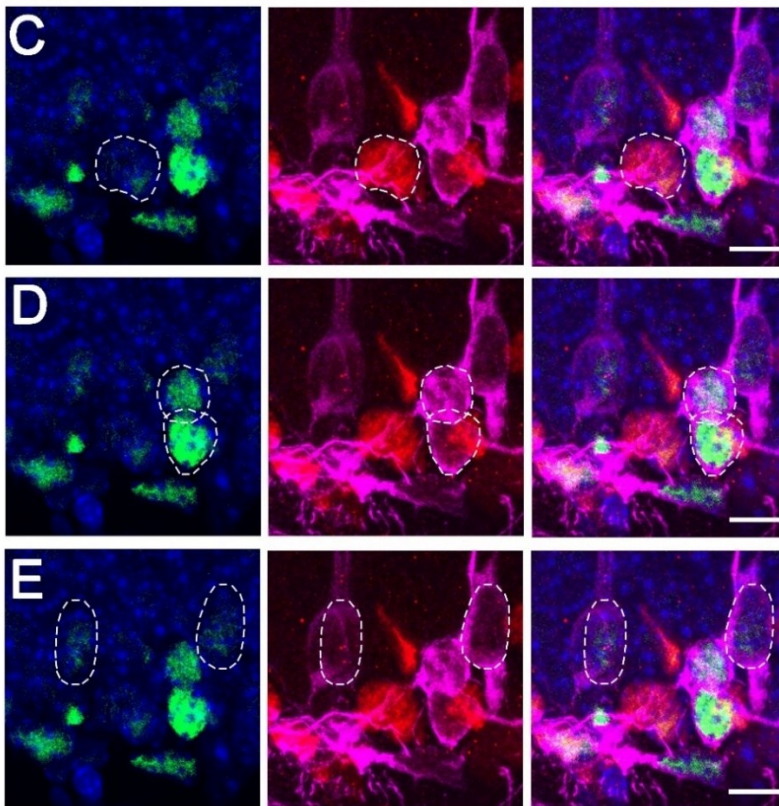
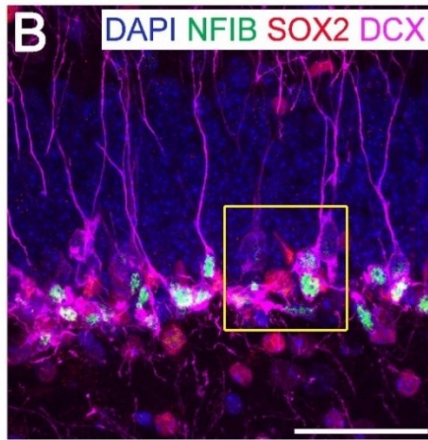
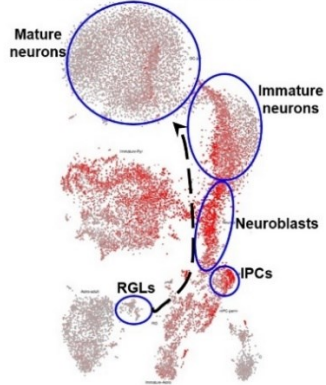


Figure 18. Expression pattern of NFIA during adult hippocampal neurogenesis. (A) tSNE plot of adult dentate gyrus single-cell RNA sequencing data showing *Nfia* gene expression along the developmental trajectory. Highest mRNA levels of *Nfia* are found in intermediate progenitor cells (IPCs), neuroblasts, and immature neurons. RGLs, radial glial like cells. *Nfia* levels drop when neurons become mature. The data is generated using an online browser from the Linnarsson lab (<http://linnarssonlab.org/dentate/>). (B) Representative images of NFIA and cell stage-specific marker expression in the dentate gyrus of adult control mice, showing DAPI (blue), NFIA (green), SOX2 (red) and DCX (magenta) staining. During adult hippocampal neurogenesis, peak NFIA levels are found in DCX⁺ cells (yellow arrowheads). NFIA is not detectable in mature granule neurons. White arrows point to SOX2⁺ neural progenitor cells, in which NFIA shows moderate expression. The expression pattern of NFIA protein is similar to its mRNA expression shown in (A). Scale bar = 20 μ m. (C) Quantification of relative fluorescence intensity of NFIA immunostaining in different cell stages. N = 99 SOX2⁺ cells, 109 DCX⁺ cells, and 41 mature neurons from three 11-week-old control mice. Data are presented in box-and-whisker plots, where centre lines represent medians, box limits represent interquartile ranges, and whiskers represent minimum to maximum data ranges. Statistical analysis was performed with one-way ANOVA with Tukey's *post hoc* test. **** $P < 0.0001$.

A *Nfib* gene expression



F NFIB levels

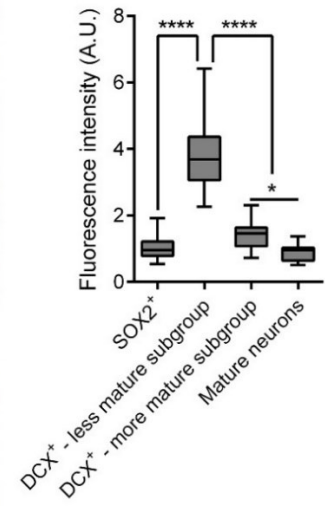


Figure 19. Expression pattern of NFIB during adult hippocampal neurogenesis (page 50). (A) tSNE plot of adult dentate gyrus single-cell RNA sequencing data showing *Nfib* gene expression along the neurogenic lineage. Highest mRNA levels of *Nfib* are found in neuroblasts. *Nfib* levels drop during neuronal maturation. The data is generated using an online browser from the Linnarsson lab (<http://linnarssonlab.org/dentate/>). (B) NFIB and cell stage-specific marker expression in the dentate gyrus of adult control mice, showing DAPI (blue), NFIB (green), SOX2 (red) and DCX (magenta) staining. Scale bar = 50 μm . (C) NFIB shows low expression in a SOX2⁺ neural progenitor cell. (D) Within the DCX⁺ cell population, strongest NFIB expression is found in the less mature subgroups, which are the ones without a radial process or with strong DCX expression and a small cell body. (E) NFIB level drops in the most mature subgroup of DCX⁺ cells, which have low DCX expression and a large cell body with elaborate dendrites. Scale bars in C-E = 10 μm . (F) Quantification of relative fluorescence intensity of NFIB immunostaining in different cell stages. N = 44 SOX2⁺ cells, 74 DCX⁺ cells from the less mature subgroups, 15 DCX⁺ cell from the most mature subgroup, and 30 mature neurons from three 11-week-old control mice. Data are presented in box-and-whisker plots, where centre lines represent medians, box limits represent interquartile ranges, and whiskers represent minimum to maximum data ranges. Statistical analysis was performed with one-way ANOVA with Tukey's *post hoc* test. * $P < 0.05$; **** $P < 0.0001$.

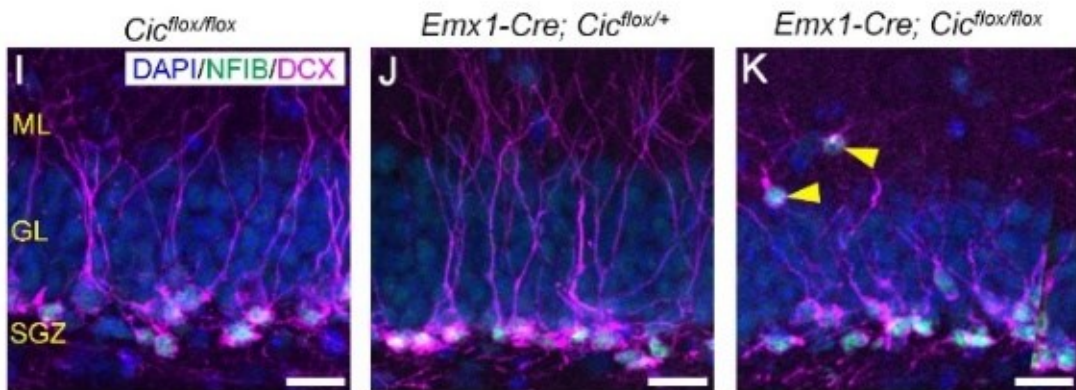
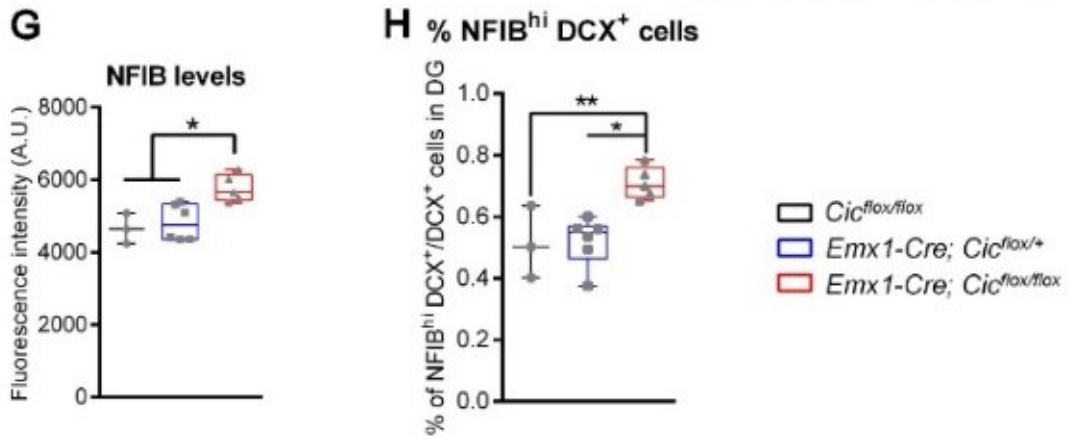
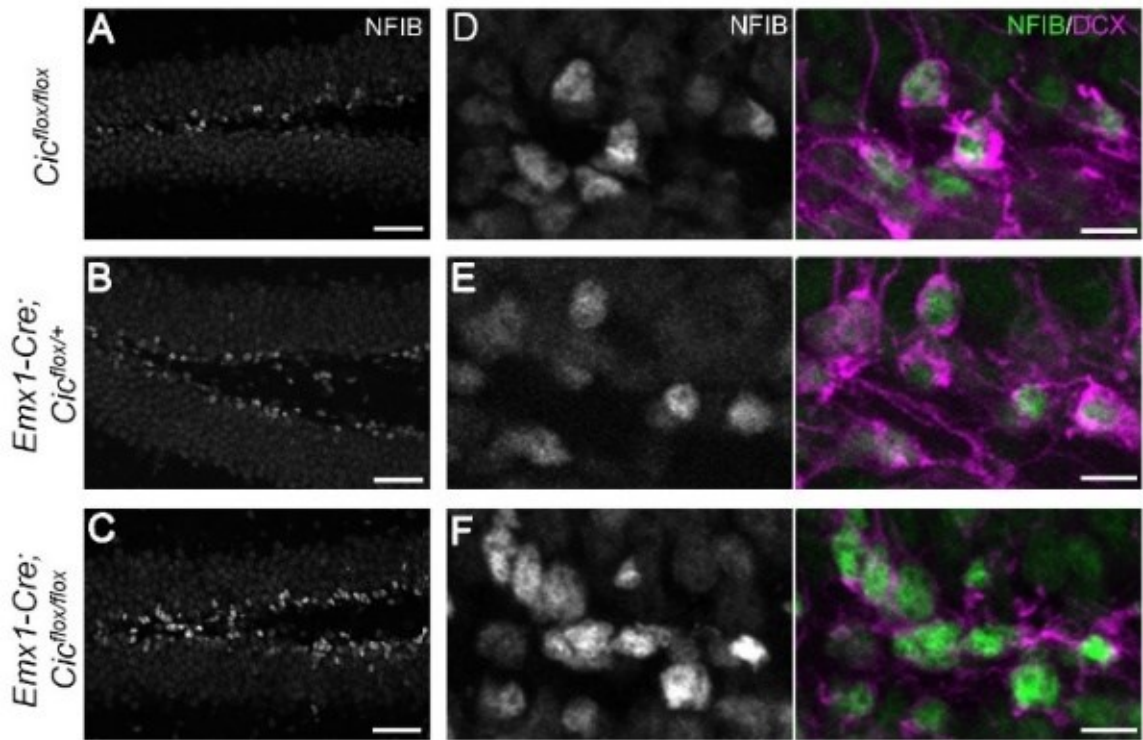


Figure 20. Upregulation of NFIB in neuroblasts of the *Emx1-Cre; Cic* knockout mice (page 52). (A-C) Representative images of NFIB immunostaining (grey) in the dentate gyrus. Cells with the highest NFIB expression are found in the neurogenic subgranular zone. Scale bars = 50 μm . (D-F) Representative images of NFIB staining at higher magnification showing increased NFIB immunoreactivity and more NFIB^{hi} cells in the knockout mice. Scale bars = 10 μm . (G) Quantification of fluorescent staining intensity of NFIB in DCX⁺ cells. More than 150 cells per animal were analysed. Each data point represents the average value from multiple cells per animal. (H) Quantification of the percentage of DCX⁺ neuroblasts co-express high levels of NFIB. N = 3–6 animals per group. (I-K) In the knockout mice, DCX⁺ cells abnormally located to the molecular layer express high levels of NFIB (yellow arrowheads). Scale bars = 20 μm . Data are presented in box-and-whisker plots showing all data points, where centre lines represent medians, box limits represent interquartile ranges, and whiskers represent minimum to maximum data ranges. Statistical analyses were performed with one-way ANOVA with Tukey's *post hoc* test. * $P < 0.05$; ** P

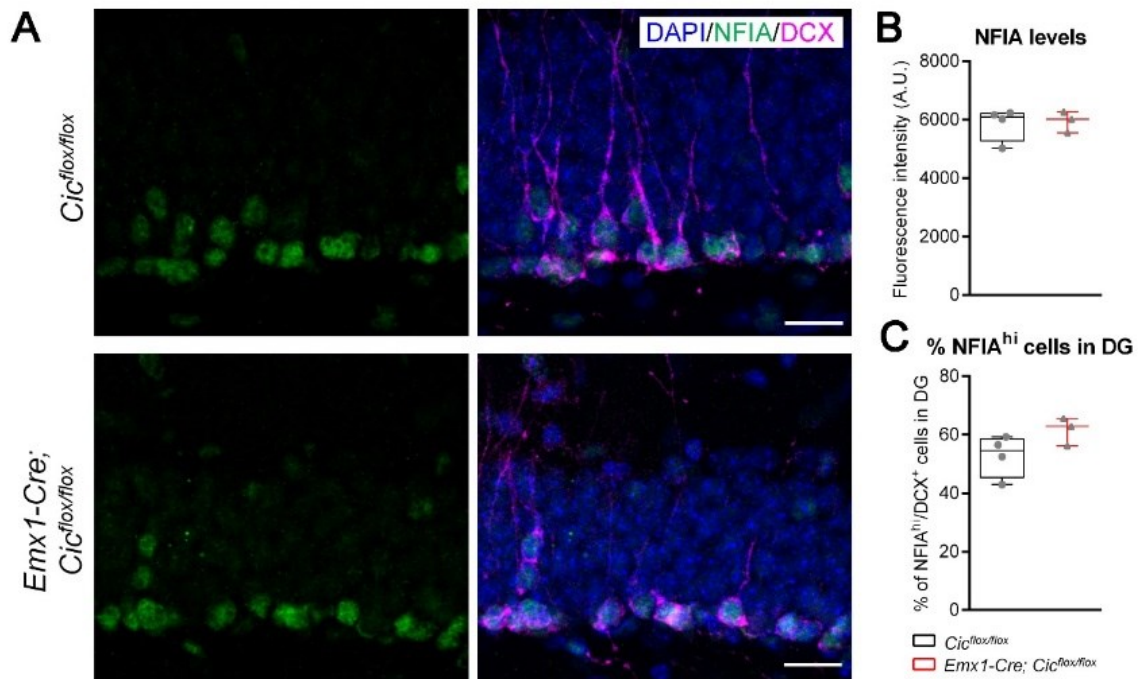


Figure 21. NFIA levels in DCX⁺ cells are not altered in the *Emx1-Cre; Cic* knockout mice. (A) Representative images of DAPI (blue), NFIA (green) and DCX (magenta) staining in the dentate gyrus. The highest NFIA expression is found in DCX⁺ cells. Scale bars = 20 μ m. (B) Quantification of fluorescent staining intensity of NFIA in neuroblasts. More than 50 cells per animal were analysed. Each data point represents the average value from multiple cells per animal. There is no difference between control and knockout mice. (C) Quantification of the percentage of DCX⁺ neuroblasts co-expressing NFIA. No significant difference is reported. N = 3-4 animals per group. Data are presented in box-and-whisker plots showing all data points, where centre lines represent medians, box limits represent interquartile ranges, and whiskers represent minimum to maximum data ranges. Statistical analysis was performed with one-way ANOVA with Tukey's *post hoc* test.

Discussion:

Summary and Significance: I demonstrated that CIC is dynamically regulated during neuronal lineage progression in the adult DG. Using the *Emx1-Cre; Cic* knockout mice, I have made three key observations: (1) Deletion of CIC from the hippocampus reduces the adult DG neuronal progenitor cell pool without affecting the proliferation potential of progenitors. (2) Despite the reduction in the progenitor cell pool, *Cic* deletion does not alter the number of DCX⁺ cells. This is likely due to increased neural progenitor differentiation into neurons, as I did not find an apparent effect on cell death of the DCX⁺ population. (3) Loss of CIC impedes dendritic development and migration of maturing neurons. These findings provide evidence for an important role of CIC in AHN.

CIC is critical for timely differentiation, survival and maturation of adult hippocampal neuronal lineage cells: CIC is a transcriptional repressor that recruits other co-repressor proteins, such as the mSWI/SNF and SIN3-HDAC complexes, to repress target gene expression [147]. It is widely expressed in the embryonic and adult brains [145]. Within neurogenic regions, CIC expression is low in neural stem and progenitor cells but high in fully differentiated neurons [147]. However, whether CIC upregulation during neurogenesis is strictly linear or has additional dynamics is unknown. Here, by comparing CIC expression in different cell stages, I made the discovery that CIC is first downregulated in DCX⁺ cells and then upregulated as new neurons exit the DCX-expressing stage. The reduction in CIC levels in DCX⁺ cells may allow for the onset of a unique transcriptional program required for differentiation and/or survival. This notion is supported by the results of our EdU-labelling study showing increased percentage of EdU⁺ DCX⁺ cells in the knockout mice, which suggests increased DCX⁺ cell survival and/or increased progenitor cell differentiation into DCX⁺ cells. New neurons begin to express DCX when they start to migrate and grow their dendrites [58, 163]. CIC may regulate specific genes necessary for cell motility and proper neurite outgrowth as we observed impaired dendritic development and migration of DCX⁺ cells when we deleted CIC from the DG. What mediates the dynamic expression of CIC during neurogenesis remains to be investigated, but CIC is known to be negatively regulated by the growth factor Ras/MAPK signalling pathway [170, 171]. Therefore, CIC downregulation in DCX⁺ cells may serve to integrate external cues, such as growth factor signalling, to neuronal lineage development by enabling appropriate regulation of genes involved in survival and/or neuronal differentiation, cell motility and dendritic outgrowth.

The role of CIC in progenitor proliferation and differentiation: As a gatekeeper of the Ras/MAPK pathway, CIC restricts cell proliferation in the contexts of development and cancer [175]. Surprisingly, I did not find a change in the proliferation potential of SOX2⁺ progenitor cells when CIC was deleted from the DG. This observation is consistent with a previous study demonstrating with *Emx1-Cre; Cic* knockout mice that loss of CIC does not alter the proliferation rate of embryonic ventricular zone neural progenitor cells [145]. On the other hand, deletion of CIC increases proliferation of cultured neural progenitor cells isolated from the embryonic ventricular zone and perinatal subventricular zone. Such discrepancy may arise from the use of *in vivo* versus *in vitro* systems. It is possible that when taken out of the neurogenic microenvironment and cultured *in vitro*, *Cic*-null neural stem cells sustain cell proliferation *via* a cell-autonomous mechanism. *In vivo*, however, proliferation of progenitor cells is regulated by a plethora of extracellular signals in the neurogenic niche [152]. Diverse regulatory feedback signals might keep the proliferation capacity of *Cic* knockout progenitor cells in check to prevent precocious stem cell pool exhaustion. Although the proliferation potential of neural progenitor cells is not changed, the progenitor cell pool is reduced in the *Emx1-Cre; Cic* knockout mice. This could be due to increased progenitor cell differentiation into DCX⁺ cells as our data suggest. Alternatively, there might be a defect during the postnatal period where the initial establishment of adult neural progenitors in the knockout DG occurs. Future studies are needed to determine whether CIC plays a role in the early DG development to establish adult neural progenitors.

The role of CIC in dendrite development: A striking phenotype uncovered in the absence of CIC is the disruption of DCX⁺ cell development. This is supported by 1) EdU-labelling study showing impaired progression of knockout DCX⁺ cells into CALB1⁺ mature neurons, 2) morphological analysis revealing reduced dendritic complexity in knockout DCX⁺ cells, and 3) molecular analysis demonstrating an expansion of DCX⁺ cells co-expressing high levels of NFIB, which marks the less mature subgroups. Previous studies have demonstrated a role for CIC in dendrite development and neuronal maturation during early brain development. Deletion of CIC reduces dendritic arborization of layers 2-4 neurons in the cerebral cortex during early postnatal development [145]. Therefore, CIC may regulate dendritic development across different neuronal subtypes. Moreover, deletion of CIC using the pan-neural *Nestin-Cre* driver expands the pool of neuroblasts with a less mature phenotype in the early postnatal (2-week-old) DG. CIC thus seems to play a consistent role in DG neurogenesis whether in early postnatal or

adult periods. In addition to highlighting the requirement of CIC for dendritic development of DCX⁺ cells, this data suggest that CIC also plays a role in the regulation of migration of these cells. DCX⁺ cells normally do not migrate pass the granule cell layer [31, 68]. However, I consistently observed DCX⁺ cells abnormally located in the molecular layer of the *Emx1-Cre; Cic* knockout mice. Notably, only a small fraction of DCX⁺ cells in the *Cic* knockout mice exhibit abnormal migration. This might be due to other redundant/compensatory pathways that ensure proper neuronal migration in the absence of CIC. As little is known about the molecular mechanisms underlying neuronal migration in the adult DG, future studies that aim to capture these abnormally migrated DCX⁺ cells and interrogate their molecular signatures using single-cell approaches may yield new insight into the regulation of migration of adult-born neurons.

The role of NFI factors during adult hippocampal neurogenesis: The NFI family of transcription factors are important players in brain development. These results demonstrate that within the AHN lineage, NFIA and NFIB both have peak expression at the DCX⁺ cell stage, a pattern similar to that of NFIX [124]. While NFIX has been shown to be required for neuroblast maturation and dendritic development, the role of NFIA and NFIB in the adult DG has not been investigated. Much of our knowledge of the NFI factors in normal brain development comes from loss-of-function studies [176]. The consequences of ectopic or overexpression of these factors remain largely unexplored. Nonetheless, evidence suggests that the brain is highly sensitive to the dosage of NFI factors. Astrocyte differentiation is reduced and delayed due to NFIB loss, while precocious astrogliosis is observed upon ectopic expression of NFIB [177-179]. AHN is biased toward an oligodendrocyte cell fate by NFIX deletion or NFIB overexpression in neural stem cells [124, 180]. Importantly, inhibition of NFI factors in developing cerebellar granule neurons impedes neuronal process formation and migration by downregulating cell adhesion molecules [181]. Our finding that upregulation of NFIB in *CIC* knockout DCX⁺ cells is associated with abnormal dendritic development and migration further attests to the importance of NFI factors in neuronal maturation and raises the possibility that proper neuronal migration and maturation requires an optimal dosage of NFI factors. Overexpression of NFI factors might lead to increased expression of cell adhesion molecules, disrupting the normal migratory behaviour of DCX⁺ cells. Interestingly, I observe upregulation only of NFIB and not NFIA in the *Emx1-Cre; Cic* knockout mice, suggesting differential regulation of the two factors by CIC or compensatory mechanisms that maintain the steady-state levels of NFIA in the absence of CIC.

The NFI factors have very similar expression patterns during brain development and overlapping transcriptional targets [182, 183], but how they might be regulated differently in diverse cellular contexts is not well understood. Our results open the door for future investigative studies to dissect the mechanisms by which NFI factors are differentially modulated in the adult neurogenic lineage. Moreover, it is intriguing that loss of CIC only increased NFIB levels in DCX⁺ cells, where CIC is normally kept at a very low level. Future studies are required to test if CIC directly regulates *Nfib* and whether upregulation of NFIB is a cause or consequence of altered development of DCX⁺ cells.

CHAPTER 4: DYSREGULATION OF GENES IMPORTANT FOR AXON GROWTH AND GUIDANCE IN THE *Emx1-Cre; Cic* KNOCKOUT MICE

Preliminary data: Axon growth and guidance genes are upregulated in the *Emx1-Cre; Cic* knockout mice dentate gyri. The finding that deletion of *Cic* affects neuronal maturation during AHN (chapter 3) directed the study to focus on the neuroblasts and immature neuron populations that undergo maturation. Since *Cic* is a transcriptional repressor, I wondered whether genes important for neuronal maturation (i.e., migration, dendrite and axon development, synaptic integration) were altered in the *Emx1-Cre; Cic* knockout mice. To answer this question, bulk RNA sequencing and data analysis of dentate gyri from adult (11-week-old) *Cic^{flox/flox}* control and *Emx1-Cre; Cic* knockout mice was conducted by the Tan lab and revealed the top 30 differentially expressed genes (DEGs) (**Fig. 22**). Gene set enrichment analysis (GSEA) of the data showed that genes associated with negative regulation of axon guidance were upregulated in the knockout mice (**Fig. 23**). Interestingly, one gene on the top 30 DEG list, dihydropyrimidinase-like 3 (*Dpysl3*, encodes the protein CRMP4), has been shown to play a role in neuronal maturation. The focus then became whether CRMP4 plays a role in the neuronal maturation defects in the *Emx1-Cre; Cic* knockout mice.

***Dpysl3* encodes collapsin response mediator protein 4 (CRMP4):** Dihydropyrimidinase-like 3 (*dpysl3*) encodes a member of the collapsin response mediator protein (CRMP) family, collapsin response mediator protein 4 [CRMP4, also known as turned on division-64 (TOAD-64), unc-33 like phosphoprotein (ULIP), and TUC-4 (toad/ulip/crmp-4)] [184]. Initially identified through 2D-gel electrophoresis as a gene that changes expression during early cerebral cortex and spinal cord development [185, 186], CRMP4 was shown to be an early post-mitotic neuron-specific protein and was used as a marker for immature neurons [187]. Studies show that CRMP4 expression peaks during embryonic days 14-21 (E14-E21) and is downregulated in adulthood [188, 189]. Subcellularly, CRMP4 expression has been observed in the actin and tubulin-associated areas of growth cones in axons and lipid rafts [187-190]. There are two protein variants of CRMP4 produced by *Dpysl3*, through the alternative usage of a different first exon, resulting in one variant (CRMP4b) with an extended N-terminal region, which is not present in the other isoform (CRMP4a) [191, 192]. CRMP4 forms tetramers with other CRMP family members and is regulated post-translationally by phosphorylation on the residues serine (Ser)522, Ser518, threonine (Thr)514 and Thr509 by different kinases [193-195]. It is thought

that either cyclin dependent kinase 5 (CDK5) or dual specificity tyrosine phosphorylation regulated kinase 2 (DYRK2) prime CRMP4 for phosphorylation of other residues by phosphorylating Ser522. After Ser522 is phosphorylated, glycogen synthase kinase (GSK3B) phosphorylates Ser518, Thr509 and Thr514 [196-199]. One report has also suggested phosphorylation of CRMP4 by Ca²⁺/calmodulin-dependent protein kinase 2 (CAMKII) in the postsynaptic density at three residues [197]. However, the biological significance of CAMKII-mediated phosphorylation on CRMP4 remains to be explored. Post-translational regulation of CRMP4 has also been reported through calpain protease cleavage. When calpain is upregulated in response to n-methyl-d-aspartate (NMDA) and H₂O₂-mediated neuron toxicity, a part of the C-terminus of CRMP4 is cleaved off [200, 201]. While the full sequence of CRMP4 resides in the cytoplasm, calpain-truncated CRMP4 can be localized to the nucleus and bind to E2 promoter binding factor 1 (E2F1) and activating its transcription. This leads to an increase in DNA methylase 1 (DNMT1) and subsequent feedback negative regulation of *Dpysl3* by methylation of CpG islands through recruitment of DNMT1 by p65/NF-κB, and rRELA [202].

Roles of collapsin response mediator protein 4 in axon outgrowth, guidance, pruning:

While CRMP4 has been implicated in axon generation/inhibition through functional studies of other CRMP family members, the specific role of CRMP4 is less well understood. CRMP4 has been shown to interact with F-actin to regulate actin bundling in the actin filopodial skeleton of the growth cone [203]. It is thought that the F-actin bundling regulation is necessary for proper fine tuning of filopodial vs lamellipodial actin structures in the growth cone. CRMP4 has also been implicated in tubulin assembly, which is thought to directly affect the rate and process of microtubule spraying, a component of the microtubule growth phase and resultingly, the size of the growth cone [192, 204]. These actin and microtubule interactions maybe a result of CRMP4 and CRMP2 cooperation in the growth cone [204, 205]. In terms of isoform-specific functions, CRMP4b has been shown to interact with RhoA upon Nogo-66 stimulation to mediate neurite outgrowth by dephosphorylation through the inhibition of GSK3B [206, 207]. CRMP4 is required for early commissure fissure and fornix development through semaphorin 3A (Sema3A)/neuropilin 1 (NRP1) and semaphorin 3E/plexin D1/neuropilin 1 (Sema3E/PLXND1/NRP1) signaling respectfully [208, 209]. In the DG of adult CRMP2/CRMP4 double knockout mice, abnormal mossy fiber termination, pruning, and innervation of synaptic terminals into CA3 region of the hippocampus have been observed. While this was partially explained by

the actions of CRMP2/NRP2/Sema3F signaling, CRMP4 appears to contribute to DG mossy fiber pathfinding in a NRP2/Sema3F-independent pathway [208]. CRMP4 is also involved in fast endophilin-mediate endocytosis (FEME), which influences axon growth and growth cone regulation by binding to endophilin and dynamin-1 [210]. CRMP4 interacts with the C terminus of the gluk5 KAR (kainate-type glutamate receptor 5) which is thought to be important for neurite outgrowth [211]. CRMP4 also affects dendrite bifurcation and orientation of basal dendrites of neurons in cortical layer 5 [212, 213]. In the DG, CRMP4^{-/-} mice have ectopic DCX cell localization and impaired neuron maturation [214].

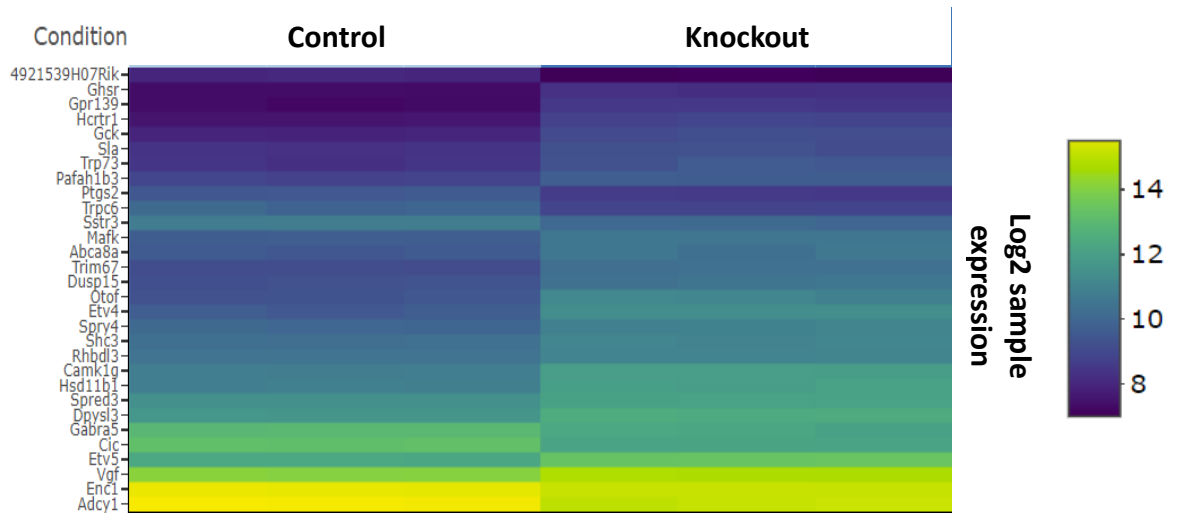


Figure 22: Biclustering heatmap of top 30 differentially expressed genes in adult *Cic^{flox/flox}* and *Emx1-Cre; Cic* knockout mice. The top 30 DEGs were plotted by their condition (control versus knockout) and by their sample log₂ expression values. Higher values and lighter shades correspond to increased expression. Genes with an adjusted *p*-value < 0.05 and absolute log₂ fold change > 1 were called as differentially expressed genes for each comparison.

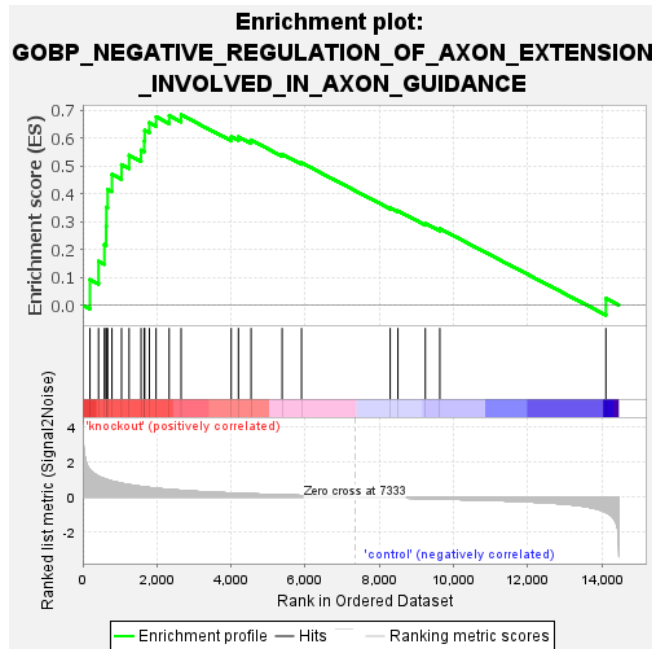


Figure 23: Gene set enrichment analysis (GSEA) of bulk RNA sequencing data. GSEA is a computational method that determines whether a gene set (bulk RNA sequencing data) is randomly distributed throughout a defined set of GO lists or if the set of genes are predominately present at the top or bottom of a GO term list. A positive enrichment store (ES) indicates gene set enrichment at the top of the GO term, while a negative score indicate enrichment at the bottom. **Top portion of chart:** The running ES for the gene set as the analysis moves down the gene list; the plot’s peak value is the ES. **Middle portion of chart:** Members of the gene set (black lines) appear in the ranked list of genes. The leading-edge subset of the gene set is the subset of members that contribute most to the ES. A positive ES has its gene members appear in the ranked list prior to the peak value. **Bottom portion of chart:** The value of the ranking metric moving down the list of ranked genes. The ranking metric measures a gene’s correlation with a phenotype. The value goes from positive to negative as one moves down the list. A positive value indicates correlation with the first phenotype and a negative value indicates correlation with the second phenotype (control and knockout). GSEA analysis of the bulk RNA sequencing data revealed a normalized enrichment score (ES) OF 1.8044127 and Nominal p-value 0.0029239766, indicating enrichment or genes involved with the GOBP term “negative regulation of axon extension involved in axon guidance”.

Results

Collapsin response mediator protein 4 protein levels are upregulated in the *Emx1-Cre; Cic* dentate gyri: Since the Tan lab RNAseq data indicated a transcriptional upregulation of *Dpysl3*, I assessed protein levels of CRMP4 utilizing mass spectrometry and immunoblot analysis of control and knockout dentate gyri protein extracts. Protein visualization of dentate gyri control and *Emx1-Cre; Cic* knockout mice was also conducted with immunofluorescence staining.

Mass spectrometry: A whole-proteome analysis to quantify proteome changes in 11-week-old control *Emx1-Cre; Cic* knockout mice (N = 3 for each genotype) dentate gyri was conducted. Over 4000 proteins were quantified, using proteome discoverer (v 2.4.1.15) in control and knockout protein lysates. A high reproducibility between replicates (>93%) was achieved. Protein abundance changes between knockout and control brains with a significant *p*-value below 0.01 and a fold change (FC) greater than 1.5 or smaller than 0.5 was used to define significant changes. Using these parameters, 102 downregulated and 85 up-regulated proteins were identified in the *Emx1-cre; Cic* knockout mice. CRMP4 was identified as a significantly upregulated protein with a fold-change of 1.6 and adjusted *p*-value of 0.004.

Immunoblot analysis of CRMP4: Eight-week-old control and *Emx1-cre; Cic* dentate gyri were dissected, and protein was extracted. With these DG protein extracts and two different CRMP4 antibodies [Sigma Cat# AB5454 and an antibody made in-house by the Alyson Fournier lab (herein referred to as the AF in-house CRMP4 antibody)], I probed for CRMP4. I first validated the reduction of CIC protein in the *Emx1-Cre; Cic* knockout mice DG extracts in comparison to controls (**Fig. 24**). Using either the Sigma or the AF in-house CRMP4 antibody, I found a ~2-fold increase in CRMP4 levels in the knockout mice compared to the controls (**Figs. 24-25**). This is in line with the RNA-seq data showing a 2.3-fold increase, suggesting that the upregulation of CRMP4 protein is likely due to transcriptional upregulation of *Dpysl3*.

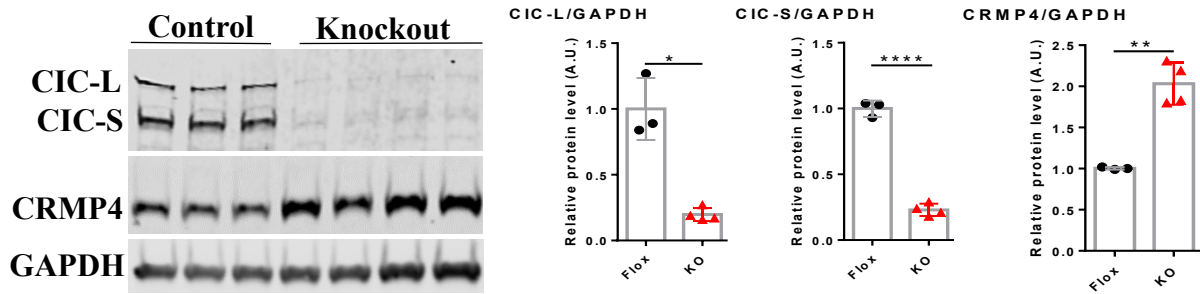


Figure 24: Immunoblot of CIC -L and CIC-S and CRMP4 (Sigma). Left panel: Representative immunoblot of CIC-L, CIC-S, CRMP4 and GAPDH. Right panel: Relative protein levels of CIC-L, CIC-S and CRMP4, normalized to GAPDH. Three control (*Cic^{lox/lox}*) and four knockout (*Emx1-Cre; Cic^{lox/lox}*) mice were used. * $P > 0.05$, ** $P > 0.01$, **** $P > 0.0001$.

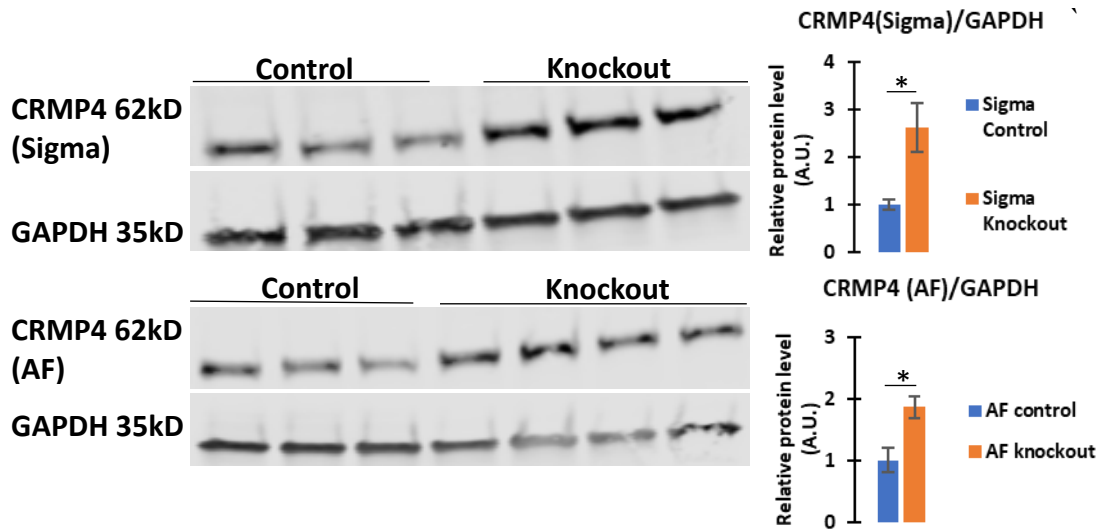


Figure 25: Immunoblot analysis of Alyson Fournier (AF)-in house versus Sigma CRMP4 antibodies. Left Panel: Immunoblots of CRMP4 (Sigma)(top) and CRMP4 (AF-inhouse)(bottom). **Right Panel:** Quantification of CRMP4 (Sigma) and (AF-inhouse) normalized to GAPDH.

Immunofluorescence studies of CRMP4 in dendrites and axons of dentate gyri neuronal

populations: I next immunostained for CRMP4 in the adult control and *Emx1-Cre; Cic* knockout mice using the AF in-house CRMP4 antibody as it was found to yield a more reproducible staining pattern and higher signal-to-noise ratio compared to the Sigma antibody. I first examined CRMP4 expression patterns in the DCX⁺ neuroblast and immature neuron populations of the control and *Emx1-cre; Cic* knockout mice (**Fig. 26**). CRMP4 is specifically expressed in the DCX⁺ populations of both genotypes, consistent with a previous report [215]. Of note, there was no obvious increase in CRMP4 immunoreactivity in cell bodies and dendrites of DCX⁺ populations in the knockout mice. To determine whether CRMP4 was expressed in other parts of the DG, I examined CRMP4 expression in the DG hilus and CA3 region of the hippocampus, which consists of the mossy fibers of immature and mature granule neurons. CRMP4 expression was evident in both control and knockout mice in the mossy fibers projecting from DG granule neurons to the CA3 (**Fig. 27**). Interestingly, I observed more intense CRMP4 immunofluorescence signals in the knockout mice, suggesting that the granule neuron axon fiber tract may be impacted in the knockout mice. To assess this possibility, I used CALB1, an established marker of the mossy fiber tract to visualize the axon pathway [216] (**Fig. 28**). While the mossy fiber tracts were comparable in control and knockout mice up to the CA3 stratum lucidum region, I observed innervation of the mossy fibers into the CA3 pyramidal cellular layer (**Fig. 28**), indicating abnormal synaptic termination of the mossy fibers.

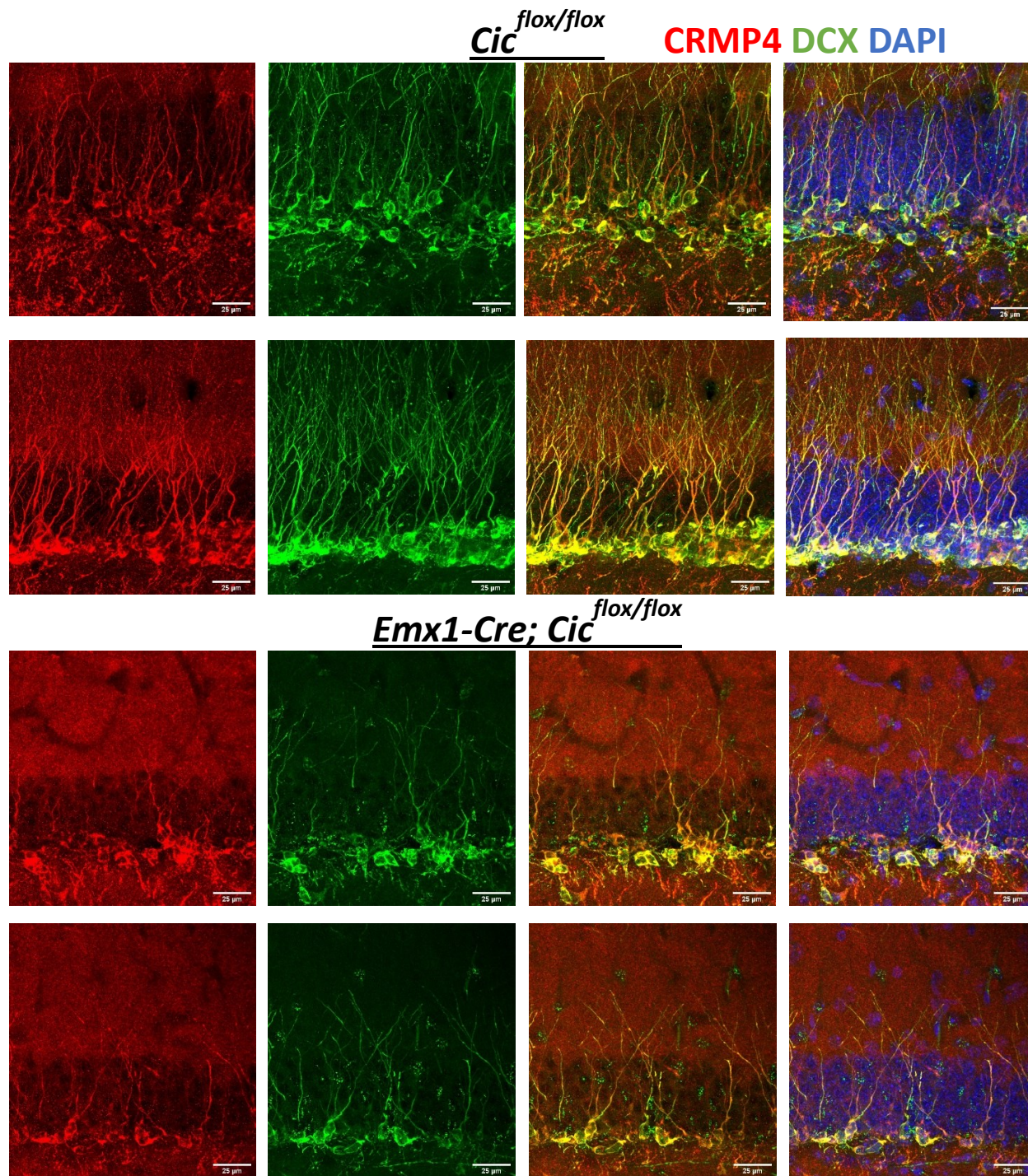


Figure 26: Immunofluorescence staining of CRMP4 in dentate gyrus of control and the *Emx1-Cre; Cic* knockout mice. Representative images from two mice are shown. Scale bars = 25µm, Red = CRMP4, Green = DCX, Blue = DAPI, Yellow = Green/Red merge.

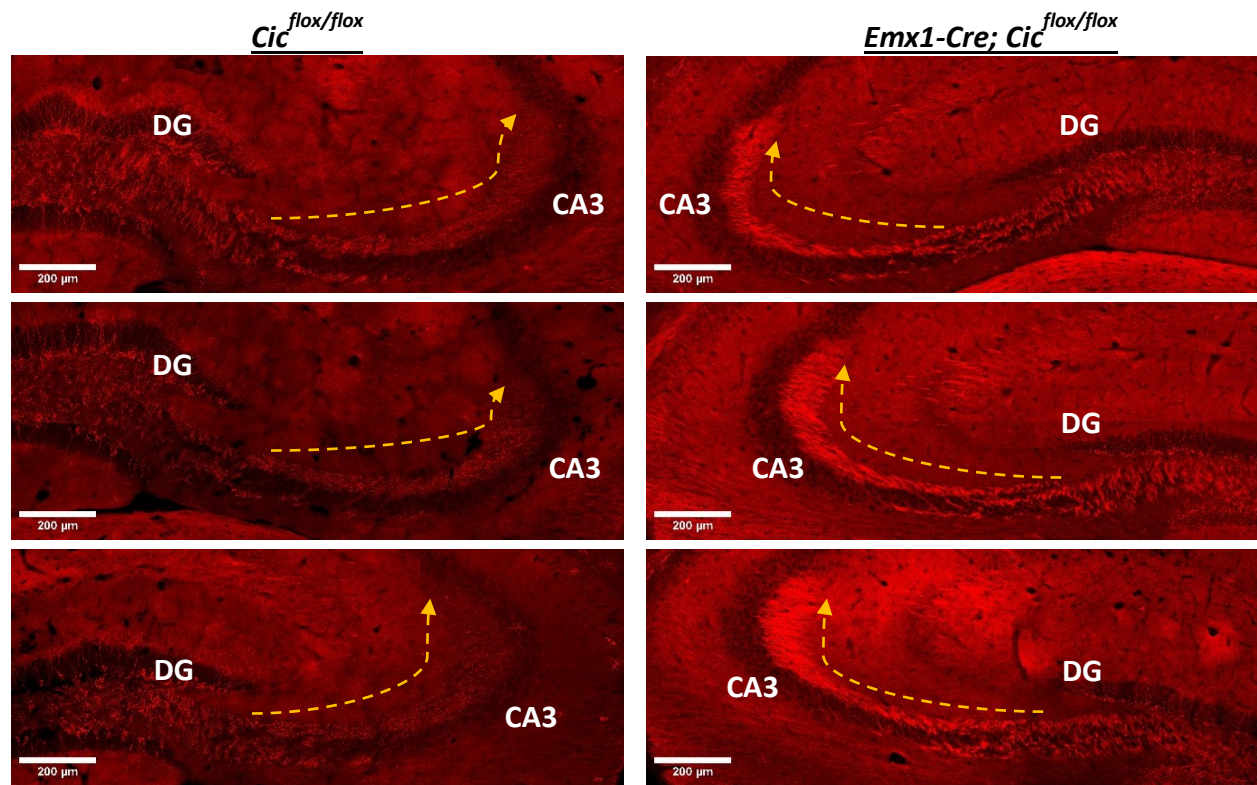


Figure 27: CRMP4 expression in mossy fibers of control and *Emx1-Cre; Cic* knockout mice. Control (left panels) show weak CRMP4 expression in the suprapyramidal mossy fibers (tracked with yellow arrow from DG to CA3). Knockout mice (right panels) show increased expression in the suprapyramidal mossy fibers. Scale bars = 200 μm . DG = dentate gyrus, CA3 = cornu ammonis 3.

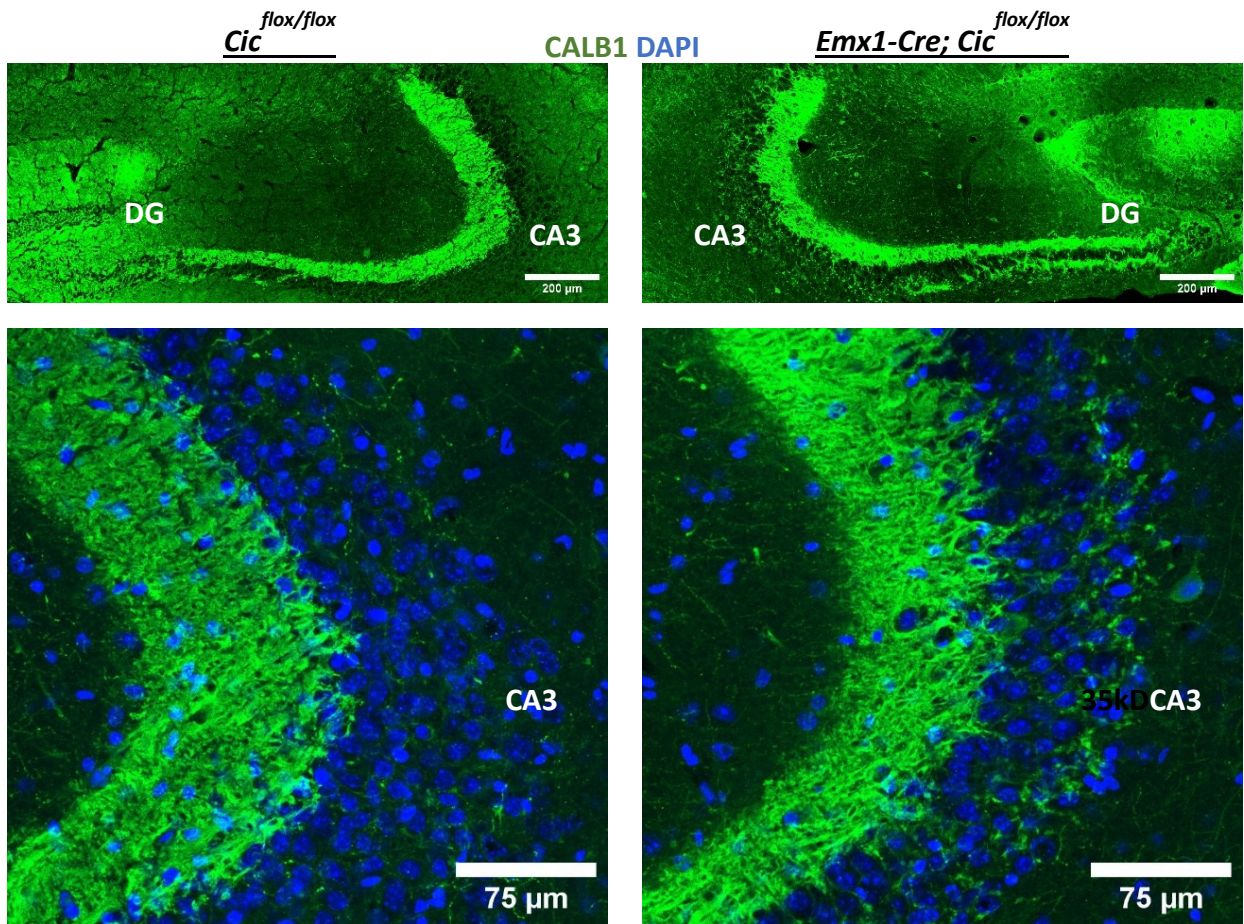


Figure 28: Abnormal synaptic termination in CA3 hippocampal region. Top panels: Representative images show CALB1 immunoreactivity in mossy fibers. Scale bars = 200 μm . **Bottom panels:** Representative images of higher magnification of the CA3 region. SP-MF = suprapyramidal mossy fibers, CA3 = cornu ammonis 3. Scale bars = 75 μm .

Phospho-Ser9 GSK3B levels are not changed in the *Emx1-Cre; Cic* knockout mice: GSK3B is a kinase that phosphorylates key residues on CRMP4 to regulate CRMP4 function [206]. It has been shown that inhibition of GSK3B affects the phosphorylation of CRMP4 and therefore activity of CRMP4 [206]. The main cellular method of inhibiting GSK3B is through phosphorylation of Ser9 on GSK3B [217]. Thus, I assessed whether GSK3B was in an active or inhibited state in the knockout mice to influence CRMP4 signaling by immunoblotting with a phospho-Ser9 GSK3B antibody. Our results revealed that, while there was a trend towards an increase of phospho-Ser9 GSK3B in the knockout mice, this was not statistically significant (**Fig. 29**).

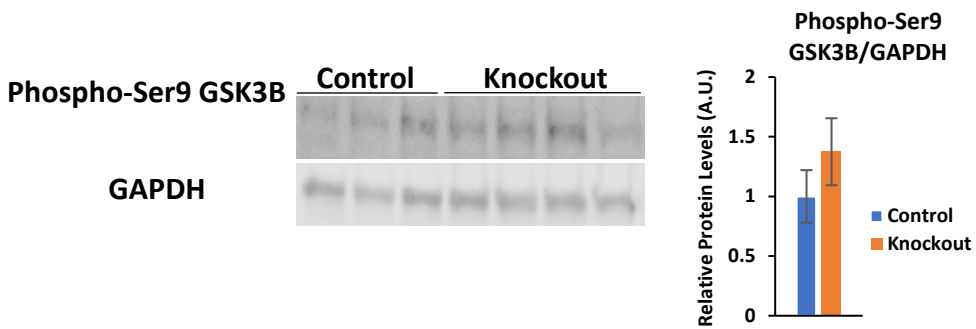


Figure 29: Immunoblot analysis of phospho-Ser9 GSK3B. Left panel: Immunoblot of phospho-Ser9 GSK3B. Three control (*Cic^{fllox/fllox}*) and four knockout (*Emx1-Cre; Cic^{fllox/fllox}*) mice were used for the analysis. Right panel: Quantification of phospho-Ser9 GSK3B after normalization to GAPDH.

Discussion and future directions: All together, I show that CRMP4 is upregulated in the *Emx1-Cre; Cic* knockout mice, specifically in the mossy fibers of the DG. I also report abnormal innervation of mossy fibers in the CA3 pyramidal cell layer of the hippocampus in the knockout mice. The proteomics and RNA sequencing data revealed a concordant two-fold upregulation of CRMP4. This, together with the finding that GSK3B phosphorylation was not affected suggests that CRMP4 upregulation in the knockout mice is largely due to transcriptional regulation. Since *Cic* is a transcriptional repressor, whether *Dpysl3* is a direct or indirect gene target of *Cic* needs to be tested. We found that CRMP4 expression in the *Emx1-Cre; Cic* knockout mice was altered in comparison to the control. The upregulation of CRMP4 expression in mossy fibers of the knockout mice could suggest the presence of CRMP4 in knockout mature neurons. However, CRMP4 is not normally expressed in mature granule neurons, thus this would suggest potential axon dysfunction in mature neurons of the knockout mice. To examine the mature neuron population in the DG, the ideal method would be to generate a mature neuron-specific knockout of *Cic* and assess whether the axon-dysregulation is still present. In addition to CRMP4 expression, we also observed abnormal mossy fiber innervation in the CA3 region, indicating abnormal synaptic integration of the mossy fibers. If this phenotype is verified using synaptic terminal markers, one approach to study this further would be to examine other signaling factors that exhibit similar synaptic termination defect. Of note, *Crmp2^{-/-}/Crmp4^{-/-}* double knockout mice and *Nrp2^{-/-}* mice also exhibit abnormal mossy fiber terminal pruning [208, 218]. NRP1 and CRMP4 have both been associated with Sema3E and Sema3F signaling, as well as NRP2 and Sema3D signaling [209, 219]. Since we observed dysregulation of semaphorin genes, it may be important to examine the Sema/NRP/Plxn signaling components as potential effectors that could lead to abnormal synaptic termination. Alternatively, CRMP4 is also involved in Ephrin/EphB2 signaling that can also affect axon guidance and pruning [220, 221]. Our data revealed many genes upregulated in the *Cic* knockout mice. Of note, a set of these genes are involved in negative regulation of axon extension. Further examination of these genes shows that a number of these genes are semaphorin-encoding genes. Semaphorin signaling make up major pathways implicated in axon guidance and thus provides a source of effector molecules to further probe for [222]. One major limitation with the bulk RNA sequencing data was that it was not population selective. Therefore, this data did not indicate in which cell populations those genes were dysregulated. Further information can be pried apart by assessing gene expression changes,

specifically in the immature neuron populations, either by isolating the DCX⁺ DG population or single-cell RNA sequencing.

CHAPTER 5: DISCUSSION AND FUTURE DIRECTIONS

Summary of thesis and main findings: Adult hippocampal neurogenesis is the process of generating new neurons in the adult hippocampus. Studies on the early progenitor cell phase have revealed that it is controlled by myriads of extrinsic and intrinsic signals that lead to an orchestrated transcriptional regulatory network. Whether such coordination and elaborated regulatory network occurs during later phases of AHN, namely neuronal differentiation, survival, and maturation is less known because these later stages have been understudied. Since many transcriptional regulators have conserved roles in the developing and adult brain, the goal of this thesis was to ask whether transcriptional regulators of neuronal migration and maturation in the developing brain may be required for similar processes in the adult brain [149]. CIC was chosen because it is important for neuronal maturation and dendrite development during early postnatal brain development, but whether CIC is similarly required for neurons to mature during adult neurogenesis remained unknown [145, 147]. I also began to examine the putative molecular mechanisms of how CIC may be a key factor in neuron maturation. I explored that the overexpression of CRMP4, (an actin and microtubule-binding protein expressed in immature neurons) may be a direct effector of the dendrite deficit that we observed in the *Emx1-Cre; Cic* knockout mice. Altogether, the experiments suggest that CIC is involved in the proper regulation of neuron maturation in AHN, as I found aberrant differentiation, localization, and dendrite formation of immature neurons in the adult DG, in conjunction with dysregulation of axon growth and guidance genes, including CRMP4, when CIC is deleted from the DG.

The role of capicua in neuronal maturation in the adult brain: This data implicates that CIC plays a conserved role in neuron maturation in the adult and early postnatal brain. CIC is a transcriptional repressor widely expressed in the embryonic and adult brains [145]. This data supporting a role for CIC in neuron maturation comes from (1) EdU-labelling study showing impaired progression of knockout DCX⁺ cells into CALB1⁺ mature neurons, (2) morphological analysis revealing reduced dendritic complexity in knockout DCX⁺ cells, and (3) molecular analysis demonstrating an expansion of DCX⁺ cells co-expressing high levels of NFIB, which marks the less mature subgroups. Previous studies have demonstrated a role for CIC in dendrite development and neuronal maturation during early brain development. Deletion of CIC reduces dendritic arborization of layers 2-4 neurons in the cerebral cortex during early postnatal

development [145]. Therefore, CIC may regulate dendritic development across different neuronal subtypes. Moreover, deletion of CIC using the pan-neural *Nestin-Cre* driver expands the pool of neuroblasts with a less mature phenotype in the early postnatal (2-week-old) DG [147]. CIC thus seems to play a consistent role in DG neurogenesis whether in early postnatal or adult periods. In addition to highlighting the requirement of CIC for dendritic development of DCX⁺ cells, our data suggest that CIC also plays a role in the regulation of migration of these cells. DCX⁺ cells normally do not migrate past the granule cell layer [31, 68]. However, we consistently observed DCX⁺ cells abnormally located in the molecular layer of the *Emx1-Cre; Cic* knockout mice. Notably, only a small fraction of DCX⁺ cells in the *Cic* knockout mice exhibit abnormal migration. This might be due to other redundant/compensatory pathways that ensure proper neuronal migration in the absence of CIC. While we observed such defects in the DCX⁺ immature neurons, our examination of CIC during AHN revealed that these immature neurons express relatively, the lowest amount of CIC during AHN. What mediates the dynamic expression of CIC during neurogenesis remains to be investigated, but CIC is known to be negatively regulated by the growth factor Ras/MAPK signalling pathway [170, 171]. Therefore, CIC downregulation in DCX⁺ cells may serve to integrate external cues, such as growth factor signalling to neuronal lineage development by enabling appropriate regulation of genes involved in survival and/or neuronal differentiation, cell motility and dendritic outgrowth. This idea that CIC regulates a network of genes involved in neurite development is further supported by our RNA sequencing and gene set enrichment analysis, which reveal an upregulation of negative regulation of axon guidance and growth genes. The regulation of axon guidance and growth requires the emergence of external and internal cues onto gene regulatory networks. How these signals converge and integrate to regulate the tempo of specific maturation events (axon and dendrite growth, proper migration) is not well understood. How CIC situates in these external and/or internal signals of immature neurons to regulate axon guidance and growth needs to be further explored. While insight was provided by studying CRMP4, more *Cic* targets need to be examined. Although it is possible that *Dpysl3* (encodes CRMP4) is a direct target of CIC-mediated gene repression, the promoter region of *Dpysl3* does not harbor consensus CIC binding sequences (unpublished observations). Thus, upregulation of *Dpysl3* and CRMP4 might be an indirect effect of *Cic* deletion.

CRMP4 upregulation in mossy fibers: I found that CRMP4 was upregulated in the dentate gyrus of *Emx1-Cre; Cic* knockout mice, particularly in the mossy fibers of granule neurons. I also observed aberrant axon termination in the CA3 region. CRMP4 expression is normally restricted to immature neurons and is an immature neuron marker [215]. Studies have revealed overexpression of CRMP4 in three pathological conditions: cancer, the mutant superoxide dismutase 1 (mSOD1) amyotrophic lateral sclerosis (ALS) mouse model, and sciatic nerve injury. CRMP4 overexpression has been observed in prostate cancer and suppresses the ability of tumor cells to metastasize [223]. However, CRMP4 mRNA and protein expression was significantly increased in colon cancer and siRNA knockdown of CRMP4 reduced invasion [224]. The possible reason for opposing effects may be due to cancer type and/or different CRMP4 isoforms studied, as one study showed CRMP4a overexpression and CRMP4b silencing suppressed gastric cancer cell proliferation [225]. At the molecular level, CRMP4 is downstream by the semaphorin 3A/neuropilin-1 (Sema3A-NRP1) signaling, which is implicated in tumor metastasis [226]. Furthermore, CRMP4 overexpression reduced NRP1 expression in prostate cancer, suggesting a potential role of CRMP4 in tumor metastasis involving NRP1 [223]. In a mSOD1 mouse model of ALS, overexpression of CRMP4a *in vivo* triggers both motor neuron death and muscle denervation [227]. Inhibiting CRMP4a expression in mSOD1 motor neurons *in vivo* prevented nitric oxide-induced death, while hippocampal neurons were not affected by CRMP4a overexpression [227]. A later study revealed a potential mechanism when they observed in ALS neurons that CRMP4 protein in distal axons was mislocalized to the proximal axons and cell bodies [228]. This local elevation in CRMP4 is mediated by dynein and Sema3A, likely by CRMP4 binding and retrograde transport to the cell body [228]. In sciatic nerve injury, increased phosphorylated and total CRMP4 was observed and *Crmp4*^{-/-} knockout mice exhibit neuroprotective effects against sciatic nerve injury [229, 230]. Further work has suggested that full length CRMP4 supports sensory axon regrowth, while its calpain-mediated cleavage form in the distal degenerating fibers facilitates Wallerian degeneration [231]. In the *Emx1-Cre; Cic* knockout mice, does overexpression of CRMP4 in the mossy fibers have any effect on the mature granule neurons? This is a question that will need to be further investigated. Although several signaling mechanisms have been shown to increase CRMP4 levels in other cell types, CRMP4 overexpression in hippocampal neurons *in vivo* has never been explored and thus warrants further investigation to assess the significance of CRMP4 (over)expression.

Future directions

Are the defects in AHN in the *Emx1-Cre; Cic* knockout mice cell or non-cell autonomous?

Although this data reveal several abnormalities of AHN in the *Emx1-Cre; Cic* knockout mice, these observed defects may arise from *Cic* deletion in the developing brain, as the Cre recombinase is turned on in forebrain progenitors from embryonic day 9.5 [153]. Furthermore, loss of *Cic* in mature granule neurons in the *Emx1-Cre; Cic* knockout mice may change the local environment of adult neurogenesis, contributing to the observed defects in a non-cell autonomous manner. Therefore, I cannot ascertain whether the defects are adult or development related nor whether it is due to cell or non-cell autonomous effects [153]. Establishing a mechanistic or a causative link will require further studies using knockout mice with conditional *Cic* inactivation in adult neural stem cells. I have attempted to remove *Cic* from adult neural stem cells using the *Nestin-Cre/ERT2* and *Hopx-Cre/ERT2* mice, but the *Nestin-Cre/ERT2* line was non-specific, expressing Cre in multiple hippocampal lineage cells (unpublished observations) [232]. *Hopx-Cre/ERT2* was more specific, but knockout efficiency was extremely low [233] (unpublished observations). I therefore was not able to delete *Cic* in adult neural stem cells by genetic crosses to inducible Cre-drive mouse lines. Future studies could explore the use of retrovirus-Cre, which will only infect dividing cells, and stereotaxic injection into the subtriangular zone of the *Cic^{flx/flx}* mice to specifically delete *Cic* from adult neural stem and progenitor cells [80, 85].

Study the role of CIC in axon guidance and growth: The whole-DG transcriptomic data identify *Cic* as a regulator of axon guidance genes. However, I do not know which cell population within the DG exhibit these gene alterations. Studies that aim to capture DCX⁺ cells and interrogate their molecular signatures such as single-cell RNA sequencing can be conducted if a single population from the DG can be isolated in adequate cell numbers. Alternatively, *Cic* may be deleted from different cell populations, for example, DCX⁺ immature neurons or mature granule neurons, to dissect the consequences of *Cic* deletion in different cell populations.

Final comments and conclusion: In this thesis, I show that *Cic* is important for proper lineage progression during AHN by facilitating neuron maturation. This work reveals that CIC regulates neuron maturation through proper dendrite development of DCX⁺ cells. The branched dendrites of DCX⁺ immature neurons provide the anatomical basis for receiving information from the entorhinal cortex, enabling ongoing learning in the adult brain [85, 234]. Therefore, dendritic

arborization defects in these cells could contribute to the previously observed learning and memory deficits in the *Emx1-Cre; Cic* knockout mice [145]. Moreover, heterozygous loss-of-function mutations in *CIC* cause a rare neurodevelopmental syndrome characterized by prominent intellectual disability/learning difficulties in affected individuals [145, 235]. Given that these pathologies persist into adulthood, the finding that CIC is required for AHN sets the stage for future investigative studies to understand whether the loss of CIC triggers ongoing learning difficulties in adult patients by impairing adult neurogenesis. Beyond the CIC haploinsufficiency syndrome, CIC may also play a broader role in age-related cognitive decline, as impaired AHN is believed to contribute to age-associated cognitive deficits [236-238]. Aging leads to a reduction in neural progenitor cells [14, 239, 240] and a delay in morphological maturation of adult-born granule neurons [241]. Both defects were observed in the *Emx1-Cre; Cic* knockout mice. In future studies, it will be interesting to determine whether CIC expression along the adult neurogenic lineage is altered by aging, and whether aging exacerbates the neurogenesis defects of the *Emx1-Cre; Cic* knockout mice

Bibliography

1. Jones, E.G., *The Neuron Doctrine 1891*. J Hist Neurosci, 1994. **3**(1): p. 3-20.
2. Ramón y Cajal, S., J. DeFelipe, and E.G. Jones, *Cajal's degeneration and regeneration of the nervous system*. History of neuroscience. 1991, New York: Oxford University Press. xvi, 769 p.
3. Allen, E., *The cessation of mitosis in the central nervous system of the albino rat*. 1912, Baltimore, cover-title, p. 547-568 illus., diags.
4. Taylor, J.H., P.S. Woods, and W.L. Hughes, *The Organization and Duplication of Chromosomes as Revealed by Autoradiographic Studies Using Tritium-Labeled Thymidine*. Proc Natl Acad Sci U S A, 1957. **43**(1): p. 122-8.
5. Altman, J. and G.D. Das, *Autoradiographic and histological evidence of postnatal hippocampal neurogenesis in rats*. J Comp Neurol, 1965. **124**(3): p. 319-35.
6. Altman, J., *Are new neurons formed in the brains of adult mammals?* Science, 1962. **135**(3509): p. 1127-8.
7. Altman, J., *Autoradiographic study of degenerative and regenerative proliferation of neuroglia cells with tritiated thymidine*. Exp Neurol, 1962. **5**: p. 302-18.
8. Kaplan, M.S. and J.W. Hinds, *Neurogenesis in the adult rat: electron microscopic analysis of light radioautographs*. Science, 1977. **197**(4308): p. 1092-4.
9. Kaplan, M.S. and D.H. Bell, *Mitotic neuroblasts in the 9-day-old and 11-month-old rodent hippocampus*. J Neurosci, 1984. **4**(6): p. 1429-41.
10. Rakic, P. and R.S. Nowakowski, *The time of origin of neurons in the hippocampal region of the rhesus monkey*. J Comp Neurol, 1981. **196**(1): p. 99-128.
11. Bayer, S.A., *Development of the hippocampal region in the rat. I. Neurogenesis examined with 3H-thymidine autoradiography*. J Comp Neurol, 1980. **190**(1): p. 87-114.
12. Starr, T.J., *Fluorescence Microscopy and Autoradiography of Colchicine-Induced Micronucleated Cells*. Nature, 1963. **200**: p. 608-9.
13. del Rio, J.A. and E. Soriano, *Immunocytochemical detection of 5'-bromodeoxyuridine incorporation in the central nervous system of the mouse*. Brain Res Dev Brain Res, 1989. **49**(2): p. 311-7.
14. Kuhn, H.G., H. Dickinson-Anson, and F.H. Gage, *Neurogenesis in the dentate gyrus of the adult rat: age-related decrease of neuronal progenitor proliferation*. J Neurosci, 1996. **16**(6): p. 2027-33.
15. Eriksson, P.S., et al., *Neurogenesis in the adult human hippocampus*. Nat Med, 1998. **4**(11): p. 1313-7.
16. Yamaguchi, M., et al., *Visualization of neurogenesis in the central nervous system using nestin promoter-GFP transgenic mice*. Neuroreport, 2000. **11**(9): p. 1991-6.
17. Filippov, V., et al., *Subpopulation of nestin-expressing progenitor cells in the adult murine hippocampus shows electrophysiological and morphological characteristics of astrocytes*. Mol Cell Neurosci, 2003. **23**(3): p. 373-82.
18. Kronenberg, G., et al., *Subpopulations of proliferating cells of the adult hippocampus respond differently to physiologic neurogenic stimuli*. J Comp Neurol, 2003. **467**(4): p. 455-63.
19. Feng, R., et al., *Deficient neurogenesis in forebrain-specific presenilin-1 knockout mice is associated with reduced clearance of hippocampal memory traces*. Neuron, 2001. **32**(5): p. 911-26.

20. Tsien, J.Z., et al., *Subregion- and cell type-restricted gene knockout in mouse brain*. Cell, 1996. **87**(7): p. 1317-26.
21. Naldini, L., et al., *Efficient transfer, integration, and sustained long-term expression of the transgene in adult rat brains injected with a lentiviral vector*. Proc Natl Acad Sci U S A, 1996. **93**(21): p. 11382-8.
22. van Praag, H., et al., *Exercise enhances learning and hippocampal neurogenesis in aged mice*. J Neurosci, 2005. **25**(38): p. 8680-5.
23. Yoshimura, S., et al., *FGF-2 regulation of neurogenesis in adult hippocampus after brain injury*. Proc Natl Acad Sci U S A, 2001. **98**(10): p. 5874-9.
24. Duan, X., et al., *Disrupted-In-Schizophrenia 1 regulates integration of newly generated neurons in the adult brain*. Cell, 2007. **130**(6): p. 1146-58.
25. Boyden, E.S., et al., *Millisecond-timescale, genetically targeted optical control of neural activity*. Nat Neurosci, 2005. **8**(9): p. 1263-8.
26. Gu, Y., et al., *Optical controlling reveals time-dependent roles for adult-born dentate granule cells*. Nat Neurosci, 2012. **15**(12): p. 1700-6.
27. Ash, A.M., et al., *Adult-born neurons inhibit developmentally-born neurons during spatial learning*. Neurobiol Learn Mem, 2023. **198**: p. 107710.
28. Encinas, J.M., A. Vaahtokari, and G. Enikolopov, *Fluoxetine targets early progenitor cells in the adult brain*. Proc Natl Acad Sci U S A, 2006. **103**(21): p. 8233-8.
29. Fukuda, S., et al., *Two distinct subpopulations of nestin-positive cells in adult mouse dentate gyrus*. J Neurosci, 2003. **23**(28): p. 9357-66.
30. Sierra, A., et al., *Microglia shape adult hippocampal neurogenesis through apoptosis-coupled phagocytosis*. Cell Stem Cell, 2010. **7**(4): p. 483-95.
31. Sun, G.J., et al., *Tangential migration of neuronal precursors of glutamatergic neurons in the adult mammalian brain*. Proc Natl Acad Sci U S A, 2015. **112**(30): p. 9484-9.
32. Brandt, M.D., et al., *Transient calretinin expression defines early postmitotic step of neuronal differentiation in adult hippocampal neurogenesis of mice*. Mol Cell Neurosci, 2003. **24**(3): p. 603-13.
33. Sloviter, R.S., *Calcium-binding protein (calbindin-D28k) and parvalbumin immunocytochemistry: localization in the rat hippocampus with specific reference to the selective vulnerability of hippocampal neurons to seizure activity*. J Comp Neurol, 1989. **280**(2): p. 183-96.
34. Bonaguidi, M.A., et al., *In vivo clonal analysis reveals self-renewing and multipotent adult neural stem cell characteristics*. Cell, 2011. **145**(7): p. 1142-55.
35. Encinas, J.M., et al., *Division-coupled astrocytic differentiation and age-related depletion of neural stem cells in the adult hippocampus*. Cell Stem Cell, 2011. **8**(5): p. 566-79.
36. Mineyeva, O.A., G. Enikolopov, and A.A. Koulakov, *Spatial geometry of stem cell proliferation in the adult hippocampus*. Sci Rep, 2018. **8**(1): p. 3444.
37. Martin-Suarez, S., et al., *Phenotypical and functional heterogeneity of neural stem cells in the aged hippocampus*. Aging Cell, 2019. **18**(4): p. e12958.
38. Lugert, S., et al., *Quiescent and active hippocampal neural stem cells with distinct morphologies respond selectively to physiological and pathological stimuli and aging*. Cell Stem Cell, 2010. **6**(5): p. 445-56.
39. Gebara, E., et al., *Heterogeneity of Radial Glia-Like Cells in the Adult Hippocampus*. Stem Cells, 2016. **34**(4): p. 997-1010.

40. Dong, J., et al., *A neuronal molecular switch through cell-cell contact that regulates quiescent neural stem cells*. Sci Adv, 2019. **5**(2): p. eaav4416.
41. Ashton, R.S., et al., *Astrocytes regulate adult hippocampal neurogenesis through ephrin-B signaling*. Nat Neurosci, 2012. **15**(10): p. 1399-406.
42. Semerci, F., et al., *Lunatic fringe-mediated Notch signaling regulates adult hippocampal neural stem cell maintenance*. Elife, 2017. **6**.
43. Ables, J.L., et al., *Notch1 is required for maintenance of the reservoir of adult hippocampal stem cells*. J Neurosci, 2010. **30**(31): p. 10484-92.
44. Ehm, O., et al., *RBPJkappa-dependent signaling is essential for long-term maintenance of neural stem cells in the adult hippocampus*. J Neurosci, 2010. **30**(41): p. 13794-807.
45. Imayoshi, I., et al., *Essential roles of Notch signaling in maintenance of neural stem cells in developing and adult brains*. J Neurosci, 2010. **30**(9): p. 3489-98.
46. Favaro, R., et al., *Hippocampal development and neural stem cell maintenance require Sox2-dependent regulation of Shh*. Nat Neurosci, 2009. **12**(10): p. 1248-56.
47. Ellis, P., et al., *SOX2, a persistent marker for multipotential neural stem cells derived from embryonic stem cells, the embryo or the adult*. Dev Neurosci, 2004. **26**(2-4): p. 148-65.
48. Graham, V., et al., *SOX2 functions to maintain neural progenitor identity*. Neuron, 2003. **39**(5): p. 749-65.
49. Hodge, R.D., et al., *Tbr2 is essential for hippocampal lineage progression from neural stem cells to intermediate progenitors and neurons*. J Neurosci, 2012. **32**(18): p. 6275-87.
50. Hodge, R.D., et al., *Intermediate progenitors in adult hippocampal neurogenesis: Tbr2 expression and coordinate regulation of neuronal output*. J Neurosci, 2008. **28**(14): p. 3707-17.
51. Lie, D.C., et al., *Wnt signalling regulates adult hippocampal neurogenesis*. Nature, 2005. **437**(7063): p. 1370-5.
52. Okamoto, M., et al., *Reduction in paracrine Wnt3 factors during aging causes impaired adult neurogenesis*. FASEB J, 2011. **25**(10): p. 3570-82.
53. Bilic, J., et al., *Wnt induces LRP6 signalosomes and promotes dishevelled-dependent LRP6 phosphorylation*. Science, 2007. **316**(5831): p. 1619-22.
54. Aberle, H., et al., *beta-catenin is a target for the ubiquitin-proteasome pathway*. EMBO J, 1997. **16**(13): p. 3797-804.
55. Daniels, D.L. and W.I. Weis, *Beta-catenin directly displaces Groucho/TLE repressors from Tcf/Lef in Wnt-mediated transcription activation*. Nat Struct Mol Biol, 2005. **12**(4): p. 364-71.
56. Qu, Q., et al., *Wnt7a regulates multiple steps of neurogenesis*. Mol Cell Biol, 2013. **33**(13): p. 2551-9.
57. Kuwabara, T., et al., *Wnt-mediated activation of NeuroD1 and retro-elements during adult neurogenesis*. Nat Neurosci, 2009. **12**(9): p. 1097-105.
58. Plumpe, T., et al., *Variability of doublecortin-associated dendrite maturation in adult hippocampal neurogenesis is independent of the regulation of precursor cell proliferation*. BMC Neurosci, 2006. **7**: p. 77.
59. Zhao, C., Teng, M., Summers, R.G., Ming, G., and Gage, F.H., *Distinct morphological stages of dentate gyrus granule neuron maturation in the adult mouse hippocampus*. Journal of Neuroscience, 2006. **26**(1): p. 3-11.

60. Piatti, V.C., et al., *The timing for neuronal maturation in the adult hippocampus is modulated by local network activity*. J Neurosci, 2011. **31**(21): p. 7715-28.
61. Kim, J.Y., et al., *Interplay between DISC1 and GABA signaling regulates neurogenesis in mice and risk for schizophrenia*. Cell, 2012. **148**(5): p. 1051-64.
62. Namba, T., et al., *NMDA receptor regulates migration of newly generated neurons in the adult hippocampus via Disrupted-In-Schizophrenia 1 (DISC1)*. J Neurochem, 2011. **118**(1): p. 34-44.
63. Flavell, S.W., et al., *Activity-dependent regulation of MEF2 transcription factors suppresses excitatory synapse number*. Science, 2006. **311**(5763): p. 1008-12.
64. Flavell, S.W., et al., *Genome-wide analysis of MEF2 transcriptional program reveals synaptic target genes and neuronal activity-dependent polyadenylation site selection*. Neuron, 2008. **60**(6): p. 1022-38.
65. Fiore, R., et al., *Mef2-mediated transcription of the miR379-410 cluster regulates activity-dependent dendritogenesis by fine-tuning Pumilio2 protein levels*. EMBO J, 2009. **28**(6): p. 697-710.
66. Latchney, S.E., et al., *Inducible knockout of Mef2a, -c, and -d from nestin-expressing stem/progenitor cells and their progeny unexpectedly uncouples neurogenesis and dendritogenesis in vivo*. FASEB J, 2015. **29**(12): p. 5059-71.
67. Vazquez, L.E., et al., *SynGAP regulates spine formation*. J Neurosci, 2004. **24**(40): p. 8862-72.
68. Kempermann, G., et al., *Early determination and long-term persistence of adult-generated new neurons in the hippocampus of mice*. Development, 2003. **130**(2): p. 391-9.
69. Esposito, M.S., et al., *Neuronal differentiation in the adult hippocampus recapitulates embryonic development*. J Neurosci, 2005. **25**(44): p. 10074-86.
70. Acsady, L., et al., *GABAergic cells are the major postsynaptic targets of mossy fibers in the rat hippocampus*. J Neurosci, 1998. **18**(9): p. 3386-403.
71. Lim, C., et al., *Connections of the hippocampal formation in humans: I. The mossy fiber pathway*. J Comp Neurol, 1997. **385**(3): p. 325-51.
72. Sun, G.J., et al., *Seamless reconstruction of intact adult-born neurons by serial end-block imaging reveals complex axonal guidance and development in the adult hippocampus*. J Neurosci, 2013. **33**(28): p. 11400-11.
73. Laplagne, D.A., et al., *Functional convergence of neurons generated in the developing and adult hippocampus*. PLoS Biol, 2006. **4**(12): p. e409.
74. Mongiat, L.A., et al., *Reliable activation of immature neurons in the adult hippocampus*. PLoS One, 2009. **4**(4): p. e5320.
75. Markwardt, S.J., J.I. Wadiche, and L.S. Overstreet-Wadiche, *Input-specific GABAergic signaling to newborn neurons in adult dentate gyrus*. J Neurosci, 2009. **29**(48): p. 15063-72.
76. Overstreet Wadiche, L., et al., *GABAergic signaling to newborn neurons in dentate gyrus*. J Neurophysiol, 2005. **94**(6): p. 4528-32.
77. Toni, N., et al., *Synapse formation on neurons born in the adult hippocampus*. Nat Neurosci, 2007. **10**(6): p. 727-34.
78. Mu, Y., C. Zhao, and F.H. Gage, *Dopaminergic modulation of cortical inputs during maturation of adult-born dentate granule cells*. J Neurosci, 2011. **31**(11): p. 4113-23.

79. Tozuka, Y., et al., *GABAergic excitation promotes neuronal differentiation in adult hippocampal progenitor cells*. *Neuron*, 2005. **47**(6): p. 803-15.
80. Ge, S., et al., *GABA regulates synaptic integration of newly generated neurons in the adult brain*. *Nature*, 2006. **439**(7076): p. 589-93.
81. Markwardt, S.J., et al., *Ivy/neurogliaform interneurons coordinate activity in the neurogenic niche*. *Nat Neurosci*, 2011. **14**(11): p. 1407-9.
82. Schmidt-Hieber, C., P. Jonas, and J. Bischofberger, *Enhanced synaptic plasticity in newly generated granule cells of the adult hippocampus*. *Nature*, 2004. **429**(6988): p. 184-7.
83. Wang, S., B.W. Scott, and J.M. Wojtowicz, *Heterogenous properties of dentate granule neurons in the adult rat*. *J Neurobiol*, 2000. **42**(2): p. 248-57.
84. Snyder, J.S., N. Kee, and J.M. Wojtowicz, *Effects of adult neurogenesis on synaptic plasticity in the rat dentate gyrus*. *J Neurophysiol*, 2001. **85**(6): p. 2423-31.
85. Ge, S., et al., *A critical period for enhanced synaptic plasticity in newly generated neurons of the adult brain*. *Neuron*, 2007. **54**(4): p. 559-66.
86. Massa, F., et al., *Conditional reduction of adult neurogenesis impairs bidirectional hippocampal synaptic plasticity*. *Proc Natl Acad Sci U S A*, 2011. **108**(16): p. 6644-9.
87. Li, Y., et al., *Development of GABAergic inputs controls the contribution of maturing neurons to the adult hippocampal network*. *Proc Natl Acad Sci U S A*, 2012. **109**(11): p. 4290-5.
88. Marin-Burgin, A., et al., *Unique processing during a period of high excitation/inhibition balance in adult-born neurons*. *Science*, 2012. **335**(6073): p. 1238-42.
89. Claiborne, B.J., D.G. Amaral, and W.M. Cowan, *Quantitative, three-dimensional analysis of granule cell dendrites in the rat dentate gyrus*. *J Comp Neurol*, 1990. **302**(2): p. 206-19.
90. Hama, K., T. Arai, and T. Kosaka, *Three-dimensional morphometrical study of dendritic spines of the granule cell in the rat dentate gyrus with HVEM stereo images*. *J Electron Microscop Tech*, 1989. **12**(2): p. 80-7.
91. Krueppel, R., S. Remy, and H. Beck, *Dendritic integration in hippocampal dentate granule cells*. *Neuron*, 2011. **71**(3): p. 512-28.
92. Frotscher, M., et al., *The mossy cells of the fascia dentata: a comparative study of their fine structure and synaptic connections in rodents and primates*. *J Comp Neurol*, 1991. **312**(1): p. 145-63.
93. Buckmaster, P.S., et al., *Mossy cell axonal projections to the dentate gyrus molecular layer in the rat hippocampal slice*. *Hippocampus*, 1992. **2**(4): p. 349-62.
94. Amaral, D.G., *A Golgi study of cell types in the hilar region of the hippocampus in the rat*. *J Comp Neurol*, 1978. **182**(4 Pt 2): p. 851-914.
95. Han, Z.S., et al., *A high degree of spatial selectivity in the axonal and dendritic domains of physiologically identified local-circuit neurons in the dentate gyrus of the rat hippocampus*. *Eur J Neurosci*, 1993. **5**(5): p. 395-410.
96. Henze, D.A., L. Wittner, and G. Buzsaki, *Single granule cells reliably discharge targets in the hippocampal CA3 network in vivo*. *Nat Neurosci*, 2002. **5**(8): p. 790-5.
97. Torborg, C.L., et al., *Control of CA3 output by feedforward inhibition despite developmental changes in the excitation-inhibition balance*. *J Neurosci*, 2010. **30**(46): p. 15628-37.
98. Marr, D., *Simple memory: a theory for archicortex*. *Philos Trans R Soc Lond B Biol Sci*, 1971. **262**(841): p. 23-81.

99. Lee, I. and R.P. Kesner, *Encoding versus retrieval of spatial memory: double dissociation between the dentate gyrus and the perforant path inputs into CA3 in the dorsal hippocampus*. *Hippocampus*, 2004. **14**(1): p. 66-76.
100. Nanry, K.P., W.R. Mundy, and H.A. Tilson, *Colchicine-induced alterations of reference memory in rats: role of spatial versus non-spatial task components*. *Behav Brain Res*, 1989. **35**(1): p. 45-53.
101. Ramirez, S., et al., *Creating a false memory in the hippocampus*. *Science*, 2013. **341**(6144): p. 387-91.
102. Liu, X., et al., *Optogenetic stimulation of a hippocampal engram activates fear memory recall*. *Nature*, 2012. **484**(7394): p. 381-5.
103. Fortin, N.J., S.P. Wright, and H. Eichenbaum, *Recollection-like memory retrieval in rats is dependent on the hippocampus*. *Nature*, 2004. **431**(7005): p. 188-91.
104. Gilbert, P.E. and R.P. Kesner, *The role of the dorsal CA3 hippocampal subregion in spatial working memory and pattern separation*. *Behav Brain Res*, 2006. **169**(1): p. 142-9.
105. Sutherland, R.J., I.Q. Wishaw, and B. Kolb, *A behavioural analysis of spatial localization following electrolytic, kainate- or colchicine-induced damage to the hippocampal formation in the rat*. *Behav Brain Res*, 1983. **7**(2): p. 133-53.
106. Jung, M.W. and B.L. McNaughton, *Spatial selectivity of unit activity in the hippocampal granular layer*. *Hippocampus*, 1993. **3**(2): p. 165-82.
107. Pernia-Andrade, A.J. and P. Jonas, *Theta-gamma-modulated synaptic currents in hippocampal granule cells in vivo define a mechanism for network oscillations*. *Neuron*, 2014. **81**(1): p. 140-52.
108. Campbell, S., et al., *Lower hippocampal volume in patients suffering from depression: a meta-analysis*. *Am J Psychiatry*, 2004. **161**(4): p. 598-607.
109. Frodl, T., et al., *Reduced hippocampal volume correlates with executive dysfunctioning in major depression*. *J Psychiatry Neurosci*, 2006. **31**(5): p. 316-23.
110. Videbech, P. and B. Ravnkilde, *Hippocampal volume and depression: a meta-analysis of MRI studies*. *Am J Psychiatry*, 2004. **161**(11): p. 1957-66.
111. Bannerman, D.M., et al., *Ventral hippocampal lesions affect anxiety but not spatial learning*. *Behav Brain Res*, 2003. **139**(1-2): p. 197-213.
112. Pothuizen, H.H., et al., *Dissociation of function between the dorsal and the ventral hippocampus in spatial learning abilities of the rat: a within-subject, within-task comparison of reference and working spatial memory*. *Eur J Neurosci*, 2004. **19**(3): p. 705-12.
113. Wu, M.V. and R. Hen, *Functional dissociation of adult-born neurons along the dorsoventral axis of the dentate gyrus*. *Hippocampus*, 2014. **24**(7): p. 751-61.
114. Banasr, M., et al., *Serotonin-induced increases in adult cell proliferation and neurogenesis are mediated through different and common 5-HT receptor subtypes in the dentate gyrus and the subventricular zone*. *Neuropsychopharmacology*, 2004. **29**(3): p. 450-60.
115. Malberg, J.E., et al., *Chronic antidepressant treatment increases neurogenesis in adult rat hippocampus*. *J Neurosci*, 2000. **20**(24): p. 9104-10.
116. Santarelli, L., et al., *Requirement of hippocampal neurogenesis for the behavioral effects of antidepressants*. *Science*, 2003. **301**(5634): p. 805-9.

117. David, D.J., et al., *Neurogenesis-dependent and -independent effects of fluoxetine in an animal model of anxiety/depression*. *Neuron*, 2009. **62**(4): p. 479-93.
118. Surget, A., et al., *Drug-dependent requirement of hippocampal neurogenesis in a model of depression and of antidepressant reversal*. *Biol Psychiatry*, 2008. **64**(4): p. 293-301.
119. Amador-Arjona, A., et al., *SOX2 primes the epigenetic landscape in neural precursors enabling proper gene activation during hippocampal neurogenesis*. *Proc Natl Acad Sci U S A*, 2015. **112**(15): p. E1936-45.
120. Gao, Z., et al., *The master negative regulator REST/NRSF controls adult neurogenesis by restraining the neurogenic program in quiescent stem cells*. *J Neurosci*, 2011. **31**(26): p. 9772-86.
121. Abrajano, J.J., et al., *REST and CoREST modulate neuronal subtype specification, maturation and maintenance*. *PLoS One*, 2009. **4**(12): p. e7936.
122. Nishihara, S., L. Tsuda, and T. Ogura, *The canonical Wnt pathway directly regulates NRSF/REST expression in chick spinal cord*. *Biochem Biophys Res Commun*, 2003. **311**(1): p. 55-63.
123. Mukherjee, S., et al., *REST regulation of gene networks in adult neural stem cells*. *Nat Commun*, 2016. **7**: p. 13360.
124. Harris, L., et al., *Neurogenic differentiation by hippocampal neural stem and progenitor cells is biased by NFIX expression*. *Development*, 2018. **145**(3).
125. Jagasia, R., et al., *GABA-cAMP response element-binding protein signaling regulates maturation and survival of newly generated neurons in the adult hippocampus*. *J Neurosci*, 2009. **29**(25): p. 7966-77.
126. Magill, S.T., et al., *microRNA-132 regulates dendritic growth and arborization of newborn neurons in the adult hippocampus*. *Proc Natl Acad Sci U S A*, 2010. **107**(47): p. 20382-7.
127. Jimenez, G., et al., *Relief of gene repression by torso RTK signaling: role of capicua in Drosophila terminal and dorsoventral patterning*. *Genes Dev*, 2000. **14**(2): p. 224-31.
128. Lee, C.J., W.I. Chan, and P.J. Scotting, *CIC, a gene involved in cerebellar development and ErbB signaling, is significantly expressed in medulloblastomas*. *J Neurooncol*, 2005. **73**(2): p. 101-8.
129. Lee, C.J., et al., *CIC, a member of a novel subfamily of the HMG-box superfamily, is transiently expressed in developing granule neurons*. *Brain Res Mol Brain Res*, 2002. **106**(1-2): p. 151-6.
130. Roch, F., G. Jimenez, and J. Casanova, *EGFR signalling inhibits Capicua-dependent repression during specification of Drosophila wing veins*. *Development*, 2002. **129**(4): p. 993-1002.
131. Lam, Y.C., et al., *ATAXIN-1 interacts with the repressor Capicua in its native complex to cause SCA1 neuropathology*. *Cell*, 2006. **127**(7): p. 1335-47.
132. Astigarraga, S., et al., *A MAPK docking site is critical for downregulation of Capicua by Torso and EGFR RTK signaling*. *EMBO J*, 2007. **26**(3): p. 668-77.
133. Bunda, S., et al., *CIC protein instability contributes to tumorigenesis in glioblastoma*. *Nat Commun*, 2019. **10**(1): p. 661.
134. Ni, C., et al., *LncRNA-AC006129.1 reactivates a SOCS3-mediated anti-inflammatory response through DNA methylation-mediated CIC downregulation in schizophrenia*. *Mol Psychiatry*, 2021. **26**(8): p. 4511-4528.

135. Kawamura-Saito, M., et al., *Fusion between CIC and DUX4 up-regulates PEA3 family genes in Ewing-like sarcomas with t(4;19)(q35;q13) translocation*. Hum Mol Genet, 2006. **15**(13): p. 2125-37.
136. Bettgowda, C., et al., *Mutations in CIC and FUBP1 contribute to human oligodendroglioma*. Science, 2011. **333**(6048): p. 1453-5.
137. Tan, Q., et al., *Loss of Capicua alters early T cell development and predisposes mice to T cell lymphoblastic leukemia/lymphoma*. Proc Natl Acad Sci U S A, 2018. **115**(7): p. E1511-E1519.
138. Rousseaux, M.W.C., et al., *ATXN1-CIC Complex Is the Primary Driver of Cerebellar Pathology in Spinocerebellar Ataxia Type 1 through a Gain-of-Function Mechanism*. Neuron, 2018. **97**(6): p. 1235-1243 e5.
139. Wong, D., et al., *Transcriptomic analysis of CIC and ATXN1L reveal a functional relationship exploited by cancer*. Oncogene, 2019. **38**(2): p. 273-290.
140. Lee, Y., et al., *ATXN1 protein family and CIC regulate extracellular matrix remodeling and lung alveolarization*. Dev Cell, 2011. **21**(4): p. 746-57.
141. Kim, E., et al., *Deficiency of Capicua disrupts bile acid homeostasis*. Sci Rep, 2015. **5**: p. 8272.
142. Park, S., et al., *The Capicua/ETS Translocation Variant 5 Axis Regulates Liver-Resident Memory CD8(+) T-Cell Development and the Pathogenesis of Liver Injury*. Hepatology, 2019. **70**(1): p. 358-371.
143. Kim, S., et al., *Regulation of positive and negative selection and TCR signaling during thymic T cell development by capicua*. Elife, 2021. **10**.
144. Park, S., et al., *Capicua deficiency induces autoimmunity and promotes follicular helper T cell differentiation via derepression of ETV5*. Nat Commun, 2017. **8**: p. 16037.
145. Lu, H.C., et al., *Disruption of the ATXN1-CIC complex causes a spectrum of neurobehavioral phenotypes in mice and humans*. Nat Genet, 2017. **49**(4): p. 527-536.
146. Rocha, M., et al., *Deficits in hippocampal-dependent memory across different rodent models of early life stress: systematic review and meta-analysis*. Transl Psychiatry, 2021. **11**(1): p. 231.
147. Hwang, I., et al., *CIC is a critical regulator of neuronal differentiation*. JCI Insight, 2020. **5**(9).
148. Ahmad, S.T., et al., *Capicua regulates neural stem cell proliferation and lineage specification through control of Ets factors*. Nat Commun, 2019. **10**(1): p. 2000.
149. Hochgerner, H., et al., *Conserved properties of dentate gyrus neurogenesis across postnatal development revealed by single-cell RNA sequencing*. Nat Neurosci, 2018. **21**(2): p. 290-299.
150. Bond, A., et al., *A Common Embryonic Origin of Stem Cells Drives Developmental and Adult Neurogenesis*. Cell, 2019. **177**.
151. Hagihara, H., et al., *Dissection of hippocampal dentate gyrus from adult mouse*. J Vis Exp, 2009(33).
152. Kempermann, G., H. Song, and F.H. Gage, *Neurogenesis in the Adult Hippocampus*. Cold Spring Harb Perspect Biol, 2015. **7**(9): p. a018812.
153. Gorski, J.A., et al., *Cortical excitatory neurons and glia, but not GABAergic neurons, are produced in the Emx1-expressing lineage*. J Neurosci, 2002. **22**(15): p. 6309-14.
154. Zhao, X. and H. van Praag, *Steps towards standardized quantification of adult neurogenesis*. Nat Commun, 2020. **11**(1): p. 4275.

155. Paredes, M.F., et al., *Brain size and limits to adult neurogenesis*. J Comp Neurol, 2016. **524**(3): p. 646-64.
156. Noori, H.R. and C.A. Fornal, *The appropriateness of unbiased optical fractionators to assess cell proliferation in the adult hippocampus*. Front Neurosci, 2011. **5**: p. 140.
157. Ramos-Vara, J.A. and M.E. Beissenherz, *Optimization of immunohistochemical methods using two different antigen retrieval methods on formalin-fixed paraffin-embedded tissues: experience with 63 markers*. J Vet Diagn Invest, 2000. **12**(4): p. 307-11.
158. Sompuram, S.R., K. Vani, and S.A. Bogen, *A molecular model of antigen retrieval using a peptide array*. Am J Clin Pathol, 2006. **125**(1): p. 91-8.
159. Rodgers, G., et al., *Virtual histology of an entire mouse brain from formalin fixation to paraffin embedding. Part 1: Data acquisition, anatomical feature segmentation, tracking global volume and density changes*. J Neurosci Methods, 2021. **364**: p. 109354.
160. Micheli, L., et al., *Fluoxetine or Sox2 reactivate proliferation-defective stem and progenitor cells of the adult and aged dentate gyrus*. Neuropharmacology, 2018. **141**: p. 316-330.
161. Farioli-Vecchioli, S., et al., *Running rescues defective adult neurogenesis by shortening the length of the cell cycle of neural stem and progenitor cells*. Stem Cells, 2014. **32**(7): p. 1968-82.
162. Suh, H., et al., *In vivo fate analysis reveals the multipotent and self-renewal capacities of Sox2+ neural stem cells in the adult hippocampus*. Cell Stem Cell, 2007. **1**(5): p. 515-28.
163. Spampanato, J., et al., *Properties of doublecortin expressing neurons in the adult mouse dentate gyrus*. PLoS One, 2012. **7**(9): p. e41029.
164. Gao, Y., et al., *Integrative Single-Cell Transcriptomics Reveals Molecular Networks Defining Neuronal Maturation During Postnatal Neurogenesis*. Cereb Cortex, 2017. **27**(3): p. 2064-2077.
165. Ryu, J.R., et al., *Control of adult neurogenesis by programmed cell death in the mammalian brain*. Mol Brain, 2016. **9**: p. 43.
166. Gage, F.H., *Adult neurogenesis in mammals*. Science, 2019. **364**(6443): p. 827-828.
167. Knoth, R., et al., *Murine features of neurogenesis in the human hippocampus across the lifespan from 0 to 100 years*. PLoS One, 2010. **5**(1): p. e8809.
168. Kempermann, G., et al., *Milestones of neuronal development in the adult hippocampus*. Trends Neurosci, 2004. **27**(8): p. 447-52.
169. Beckervordersandforth, R., C.L. Zhang, and D.C. Lie, *Transcription-Factor-Dependent Control of Adult Hippocampal Neurogenesis*. Cold Spring Harb Perspect Biol, 2015. **7**(10): p. a018879.
170. Lee, Y., *Regulation and function of capicua in mammals*. Experimental & Molecular Medicine, 2020.
171. Wong, D. and S. Yip, *Making heads or tails - the emergence of capicua (CIC) as an important multifunctional tumour suppressor*. J Pathol, 2020.
172. Weissmann, S., et al., *The Tumor Suppressor CIC Directly Regulates MAPK Pathway Genes via Histone Deacetylation*. Cancer Res, 2018. **78**(15): p. 4114-4125.
173. Rodriguez-Iglesias, N., A. Sierra, and J. Valero, *Rewiring of Memory Circuits: Connecting Adult Newborn Neurons With the Help of Microglia*. Front Cell Dev Biol, 2019. **7**: p. 24.

174. Encinas, J.M. and A. Sierra, *Neural stem cell deforestation as the main force driving the age-related decline in adult hippocampal neurogenesis*. Behavioural Brain Research, 2012. **227**(2): p. 433-439.
175. Simon-Carrasco, L., et al., *The Capicua tumor suppressor: a gatekeeper of Ras signaling in development and cancer*. Cell Cycle, 2018: p. 1-33.
176. Harris, L., et al., *Nuclear factor one transcription factors: Divergent functions in developmental versus adult stem cell populations*. Dev Dyn, 2015. **244**(3): p. 227-38.
177. Deneen, B., et al., *The transcription factor NFIA controls the onset of gliogenesis in the developing spinal cord*. Neuron, 2006. **52**(6): p. 953-68.
178. Piper, M., et al., *Multiple non-cell-autonomous defects underlie neocortical callosal dysgenesis in Nfib-deficient mice*. Neural Dev, 2009. **4**: p. 43.
179. Barry, G., et al., *Specific glial populations regulate hippocampal morphogenesis*. J Neurosci, 2008. **28**(47): p. 12328-40.
180. Rolando, C., et al., *Multipotency of Adult Hippocampal NSCs In Vivo Is Restricted by Droscha/NFIB*. Cell Stem Cell, 2016. **19**(5): p. 653-662.
181. Wang, W., et al., *Nuclear factor I coordinates multiple phases of cerebellar granule cell development via regulation of cell adhesion molecules*. J Neurosci, 2007. **27**(23): p. 6115-27.
182. Fraser, J., et al., *Common Regulatory Targets of NFIA, NFIX and NFIB during Postnatal Cerebellar Development*. Cerebellum, 2020. **19**(1): p. 89-101.
183. Bunt, J., et al., *Combined allelic dosage of Nfia and Nfib regulates cortical development*. Brain and Neuroscience Advances, 2017. **1**: p. 2398212817739433.
184. Matsuo, T., et al., *Structure and promoter analysis of the human unc-33-like phosphoprotein gene. E-box required for maximal expression in neuroblastoma and myoblasts*. J Biol Chem, 2000. **275**(22): p. 16560-8.
185. Geschwind, D.H. and S. Hockfield, *Identification of proteins that are developmentally regulated during early cerebral corticogenesis in the rat*. J Neurosci, 1989. **9**(12): p. 4303-17.
186. Geschwind, D.H., F.R. Thormodsson, and S. Hockfield, *Changes in protein expression during neural development analyzed by two-dimensional gel electrophoresis*. Electrophoresis, 1996. **17**(11): p. 1677-82.
187. Minturn, J.E., et al., *Early postmitotic neurons transiently express TOAD-64, a neural specific protein*. J Comp Neurol, 1995. **355**(3): p. 369-79.
188. Minturn, J.E., et al., *TOAD-64, a gene expressed early in neuronal differentiation in the rat, is related to unc-33, a C. elegans gene involved in axon outgrowth*. J Neurosci, 1995. **15**(10): p. 6757-66.
189. Wang, L.H. and S.M. Strittmatter, *A family of rat CRMP genes is differentially expressed in the nervous system*. J Neurosci, 1996. **16**(19): p. 6197-207.
190. Rosslenbroich, V., et al., *Subcellular localization of collapsin response mediator proteins to lipid rafts*. Biochem Biophys Res Commun, 2003. **305**(2): p. 392-9.
191. Quinn, C.C., et al., *TUC-4b, a novel TUC family variant, regulates neurite outgrowth and associates with vesicles in the growth cone*. J Neurosci, 2003. **23**(7): p. 2815-23.
192. Yuasa-Kawada, J., et al., *Axonal morphogenesis controlled by antagonistic roles of two CRMP subtypes in microtubule organization*. Eur J Neurosci, 2003. **17**(11): p. 2329-43.
193. Wang, L.H. and S.M. Strittmatter, *Brain CRMP forms heterotetramers similar to liver dihydropyrimidinase*. J Neurochem, 1997. **69**(6): p. 2261-9.

194. Ponnusamy, R., et al., *Crystal structure of human CRMP-4: correction of intensities for lattice-translocation disorder*. Acta Crystallogr D Biol Crystallogr, 2014. **70**(Pt 6): p. 1680-94.
195. Fukada, M., et al., *Molecular characterization of CRMP5, a novel member of the collapsin response mediator protein family*. J Biol Chem, 2000. **275**(48): p. 37957-65.
196. Gaetano, C., T. Matsuo, and C.J. Thiele, *Identification and characterization of a retinoic acid-regulated human homologue of the unc-33-like phosphoprotein gene (hUlip) from neuroblastoma cells*. J Biol Chem, 1997. **272**(18): p. 12195-201.
197. Yoshimura, Y., et al., *Identification of protein substrates of Ca(2+)/calmodulin-dependent protein kinase II in the postsynaptic density by protein sequencing and mass spectrometry*. Biochem Biophys Res Commun, 2002. **290**(3): p. 948-54.
198. Cole, A.R., et al., *Distinct priming kinases contribute to differential regulation of collapsin response mediator proteins by glycogen synthase kinase-3 in vivo*. J Biol Chem, 2006. **281**(24): p. 16591-8.
199. Cole, A.R., et al., *GSK-3 phosphorylation of the Alzheimer epitope within collapsin response mediator proteins regulates axon elongation in primary neurons*. J Biol Chem, 2004. **279**(48): p. 50176-80.
200. Kowara, R., et al., *Calpain-mediated truncation of dihydropyrimidinase-like 3 protein (DPYSL3) in response to NMDA and H2O2 toxicity*. J Neurochem, 2005. **95**(2): p. 466-74.
201. Kowara, R., K.L. Moraleja, and B. Chakravarthy, *Involvement of nitric oxide synthase and ROS-mediated activation of L-type voltage-gated Ca²⁺ channels in NMDA-induced DPYSL3 degradation*. Brain Res, 2006. **1119**(1): p. 40-9.
202. Gao, X., et al., *Calpain-2 triggers prostate cancer metastasis via enhancing CRMP4 promoter methylation through NF-kappaB/DNMT1 signaling pathway*. Prostate, 2018. **78**(9): p. 682-690.
203. Rosslenbroich, V., et al., *Collapsin response mediator protein-4 regulates F-actin bundling*. Exp Cell Res, 2005. **310**(2): p. 434-44.
204. Khazaei, M.R., et al., *Collapsin response mediator protein 4 regulates growth cone dynamics through the actin and microtubule cytoskeleton*. J Biol Chem, 2014. **289**(43): p. 30133-43.
205. al, T.e., *CRMP4 and CRMP2 interact to coordinate cytoskeleton dynamics, regulating growth cone development and axon elongation*. Neural Plasticity, 2015. **2015**: p. 1-13.
206. Alabed, Y.Z., et al., *GSK3 beta regulates myelin-dependent axon outgrowth inhibition through CRMP4*. J Neurosci, 2010. **30**(16): p. 5635-43.
207. Alabed, Y.Z., et al., *Identification of CRMP4 as a convergent regulator of axon outgrowth inhibition*. J Neurosci, 2007. **27**(7): p. 1702-11.
208. Nakanishi, Y., et al., *Regulation of axon pruning of mossy fiber projection in hippocampus by CRMP2 and CRMP4*. Dev Neurobiol, 2022. **82**(1): p. 138-146.
209. Guo, Y., C.F. Oliveros, and T. Ohshima, *CRMP2 and CRMP4 are required for the formation of commissural tracts in the developing zebrafish forebrain*. Dev Neurobiol, 2022. **82**(6): p. 533-544.
210. Ferreira, A.P.A., et al., *Cdk5 and GSK3beta inhibit fast endophilin-mediated endocytosis*. Nat Commun, 2021. **12**(1): p. 2424.
211. Marques, J.M., et al., *CRMP2 tethers kainate receptor activity to cytoskeleton dynamics during neuronal maturation*. J Neurosci, 2013. **33**(46): p. 18298-310.

212. Niisato, E., et al., *CRMP4 suppresses apical dendrite bifurcation of CA1 pyramidal neurons in the mouse hippocampus*. Dev Neurobiol, 2012. **72**(11): p. 1447-57.
213. Takaya, R., et al., *CRMP1 and CRMP4 are required for proper orientation of dendrites of cerebral pyramidal neurons in the developing mouse brain*. Brain Res, 2017. **1655**: p. 161-167.
214. Osawa, K., et al., *CRMP4 is required for the positioning and maturation of newly generated neurons in adult mouse hippocampus*. Neurosci Lett, 2022. **773**: p. 136503.
215. Seki, T., *Expression patterns of immature neuronal markers PSA-NCAM, CRMP-4 and NeuroD in the hippocampus of young adult and aged rodents*. J Neurosci Res, 2002. **70**(3): p. 327-34.
216. Kohara, K., et al., *Cell type-specific genetic and optogenetic tools reveal hippocampal CA2 circuits*. Nat Neurosci, 2014. **17**(2): p. 269-79.
217. Frame, S., P. Cohen, and R.M. Biondi, *A common phosphate binding site explains the unique substrate specificity of GSK3 and its inactivation by phosphorylation*. Mol Cell, 2001. **7**(6): p. 1321-7.
218. Chen, H., et al., *Neuropilin-2 regulates the development of selective cranial and sensory nerves and hippocampal mossy fiber projections*. Neuron, 2000. **25**(1): p. 43-56.
219. Boulan, B., et al., *CRMP4-mediated fornix development involves Semaphorin-3E signaling pathway*. Elife, 2021. **10**.
220. Xu, N.J. and M. Henkemeyer, *Ephrin-B3 reverse signaling through Grb4 and cytoskeletal regulators mediates axon pruning*. Nat Neurosci, 2009. **12**(3): p. 268-76.
221. Liu, X.D., et al., *Retrograde regulation of mossy fiber axon targeting and terminal maturation via postsynaptic Lnx1*. J Cell Biol, 2018. **217**(11): p. 4007-4024.
222. Bagri, A., et al., *Stereotyped pruning of long hippocampal axon branches triggered by retraction inducers of the semaphorin family*. Cell, 2003. **113**(3): p. 285-99.
223. Zhou, W., et al., *Upregulation of CRMP4, a new prostate cancer metastasis suppressor gene, inhibits tumor growth in a nude mouse intratibial injection model*. Int J Oncol, 2015. **46**(1): p. 290-8.
224. Chen, S.L., et al., *Targeting CRMP-4 by lentivirus-mediated RNA interference inhibits SW480 cell proliferation and colorectal cancer growth*. Exp Ther Med, 2016. **12**(4): p. 2003-2008.
225. Guo, H. and B. Xia, *Collapsin response mediator protein 4 isoforms (CRMP4a and CRMP4b) have opposite effects on cell proliferation, migration, and invasion in gastric cancer*. BMC Cancer, 2016. **16**: p. 565.
226. Chakraborty, G., et al., *Semaphorin 3A suppresses tumor growth and metastasis in mice melanoma model*. PLoS One, 2012. **7**(3): p. e33633.
227. Duplan, L., et al., *Collapsin response mediator protein 4a (CRMP4a) is upregulated in motoneurons of mutant SOD1 mice and can trigger motoneuron axonal degeneration and cell death*. J Neurosci, 2010. **30**(2): p. 785-96.
228. Maimon, R., et al., *A CRMP4-dependent retrograde axon-to-soma death signal in amyotrophic lateral sclerosis*. EMBO J, 2021. **40**(17): p. e107586.
229. Nagai, J., et al., *Crmp4 deletion promotes recovery from spinal cord injury by neuroprotection and limited scar formation*. Sci Rep, 2015. **5**: p. 8269.
230. Jang, S.Y., et al., *Injury-induced CRMP4 expression in adult sensory neurons; a possible target gene for ciliary neurotrophic factor*. Neurosci Lett, 2010. **485**(1): p. 37-42.

231. Girouard, M.P., et al., *Collapsin Response Mediator Protein 4 (CRMP4) Facilitates Wallerian Degeneration and Axon Regeneration following Sciatic Nerve Injury*. eNeuro, 2020. **7**(2).
232. Sun, M.-Y., et al., *Specificity and efficiency of reporter expression in adult neural progenitors vary substantially among nestin-CreERT2 lines*. Journal of Comparative Neurology, 2014. **522**(5): p. 1191-1208.
233. Berg, D.A., et al., *A Common Embryonic Origin of Stem Cells Drives Developmental and Adult Neurogenesis*. Cell, 2019. **177**(3): p. 654-668 e15.
234. Vukovic, J., et al., *Immature doublecortin-positive hippocampal neurons are important for learning but not for remembering*. J Neurosci, 2013. **33**(15): p. 6603-13.
235. Tan, Q. and H.Y. Zoghbi, *Mouse models as a tool for discovering new neurological diseases*. Neurobiology of Learning and Memory, 2019. **165**: p. 106902.
236. Babcock, K.R., et al., *Adult hippocampal neurogenesis in aging and Alzheimer's disease*. Stem Cell Reports, 2021.
237. Martinowich, K. and R.J. Schloesser, *Chapter 3 - Adult Neurogenesis and Cognitive Function: Relevance for Disorders Associated with Human Aging*, in *Genes, Environment and Alzheimer's Disease*, O. Lazarov and G. Tesco, Editors. 2016, Academic Press: San Diego. p. 51-94.
238. Kempermann, G., *Activity Dependency and Aging in the Regulation of Adult Neurogenesis*. Cold Spring Harb Perspect Biol, 2015. **7**(11).
239. Morgenstern, N.A., G. Lombardi, and A.F. Schinder, *Newborn granule cells in the ageing dentate gyrus*. J Physiol, 2008. **586**(16): p. 3751-7.
240. Kempermann, G., H.G. Kuhn, and F.H. Gage, *Experience-induced neurogenesis in the senescent dentate gyrus*. J Neurosci, 1998. **18**(9): p. 3206-12.
241. Trincherro, M.F., et al., *High Plasticity of New Granule Cells in the Aging Hippocampus*. Cell Rep, 2017. **21**(5): p. 1129-1139.